

# **Heterotic Particle Models from various Perspectives**

Dissertation

zur

Erlangung des Doktorgrades (Dr. rer. nat.)

der

Mathematisch-Naturwissenschaftlichen Fakultät

der

Rheinischen Friedrich-Wilhelms-Universität Bonn

vorgelegt von

Michael Ireneus Blaszczyk

aus

Deutsch-Piekar (Polen)

Bonn 2012

Angefertigt mit Genehmigung der Mathematisch-Naturwissenschaftlichen  
Fakultät der Rheinischen Friedrich-Wilhelms-Universität Bonn

1. Gutachter: Prof. Dr. Hans Peter Nilles
2. Gutachter: Priv. Doz. Dr. Stefan Förste

Tag der Promotion: 25.09.2012  
Erscheinungsjahr: 2012

## **Acknowledgements**

First of all I would like to thank Prof. Dr. Hans Peter Nilles for taking me into his group and supervising my thesis, thereby giving me the opportunity to work in this very interesting area of theoretical physics. Great thanks also go to Priv. Doz. Dr. Stefan Förste for taking the job of the coreferee of this thesis. I am very grateful to Prof. Dr. Stefan Groot Nibbelink for the many interesting discussions and fruitful collaborations.

I enjoyed very much the nice atmosphere in the research group through all the years, so I thank everyone for providing a pleasant and motivating environment. In particular I profited from discussions with Nana Cabo Bizet, Dr. Christoph Lüdeling, Damian Mayorga Peña, Paul Oehlmann, Fabian Rühle, Matthias Schmitz, Dr. Michele Trapletti and many more.

Thanks for proofreading go to Dr. Christoph Lüdeling, Paul Oehlmann and Fabian Rühle.

For organizational and technical support I would like to thank Patrizia Zündorf, Dagmar Fassbender and Dr. Andreas Wisskirchen.

Finally I would like to thank my parents and my siblings and all of my friends in Bonn for a memorable time outside of physics.



# Contents

<b>1</b>	<b>Introduction</b>	<b>1</b>
<b>2</b>	<b>Heterotic Strings on Orbifolds</b>	<b>9</b>
2.1	The Heterotic String . . . . .	9
2.2	Orbifold Geometries . . . . .	12
2.3	Strings on Orbifolds . . . . .	15
2.3.1	Examples . . . . .	19
<b>3</b>	<b>GLSM description of Resolved Toroidal Orbifolds</b>	<b>23</b>
3.1	Some Algebraic Geometry . . . . .	23
3.1.1	Local Singularity Resolutions . . . . .	29
3.1.2	Elliptic Curves and their Symmetries . . . . .	31
3.2	Gauged Linear Sigma Models . . . . .	37
3.2.1	(2,2) SUSY in two dimensions . . . . .	38
3.2.2	(2,0) SUSY in two dimensions . . . . .	41
3.3	(2,2) Models of Resolved Toroidal Orbifolds . . . . .	46
3.3.1	Example: Resolution of $T^6/\mathbb{Z}_3$ . . . . .	49
3.3.2	Moduli Spaces . . . . .	59
3.3.3	Example: Resolution of $T^6/\mathbb{Z}_4$ . . . . .	64
3.4	(2,0) Models . . . . .	72
3.4.1	Line and Vector Bundles . . . . .	73
3.4.2	Freely Acting Discrete Symmetries . . . . .	81
<b>4</b>	<b>Phenomenology on Orbifold Resolutions</b>	<b>85</b>
4.1	Effective SUGRA . . . . .	85
4.2	Stringy Effects . . . . .	93
<b>5</b>	<b>Conclusions and Outlook</b>	<b>99</b>
<b>A</b>	<b>Discrete Actions on elliptic Curves and Tori</b>	<b>101</b>
<b>B</b>	<b>Compactification lattice analyses</b>	<b>105</b>
<b>C</b>	<b>Flux Quantization</b>	<b>111</b>
	<b>Bibliography</b>	<b>113</b>

## *Contents*

# 1 Introduction

## Motivation

Today, almost all physical observations can be explained within two physical theories. Gravitational effects, which are dominant at large length scales up to cosmic scales, are described by general relativity, which is a classical theory of the dynamics of spacetime as a Riemannian manifold. Observations at short scales or high energies are governed by the standard model of particle physics, which is a quantum theory of fields in Minkowski space. The detection of a new boson with mass around 125 GeV [1] at the large hadron collider (LHC) is presumably the discovery of the Higgs boson, the last missing piece of the standard model. Thus, within the range of our observation, general relativity and the standard model can be considered as the most fundamental, experimentally confirmed theories.

However, we know that these theories cannot be the full story. On the one hand, there are observations that require extensions of the theories, like neutrino oscillations or the hints for the existence of dark matter. On the other hand, the range of the theories themselves is limited and beyond this range one finds the need for a new underlying theory. From the standard model point of view, problems appear when going to higher energies. Then radiative corrections give quadratic contributions to the Higgs boson mass, resulting in an enormous fine tuning at higher energy scales, known as the hierarchy problem. Another problem is the Landau pole of the running hypercharge gauge coupling which puts an upper bound on the validity range of the theory itself. Besides that, the standard model has a complicated structure with an underlying gauge group  $SU(3)_C \times SU(2)_L \times U(1)_Y$  and chiral matter fields in specific representations. One could ask if this structure and also the values of the theory parameters can be explained in an underlying framework.

Even more problems occur when going to situations when gravitational interactions become comparably strong to the standard model gauge interactions, like black holes or the big bang. Then the quantum nature of gravity must show up and be able to explain e.g. the black hole entropy and Hawking radiation. Here the problem is that simply quantizing general relativity leads to a non-renormalizable theory. So it is desirable to find a consistent theory of quantum gravity which also explains what happens inside a black hole.

Taking the data of the standard model at hand, we see many hints for theoretical concepts that could address these questions and problems. These include

## 1 Introduction

field	SM rep	$SU(5)$ rep	$SO(10)$ rep
$Q$	$(\mathbf{3}, \mathbf{2})_1$	$\mathbf{10}$	$\mathbf{16}$
$\bar{u}$	$(\bar{\mathbf{3}}, \mathbf{1})_{-4}$		
$\bar{e}$	$(\mathbf{1}, \mathbf{1})_6$		
$\bar{d}$	$(\bar{\mathbf{3}}, \mathbf{1})_2$	$\bar{\mathbf{5}}$	
$L$	$(\mathbf{1}, \mathbf{2})_{-3}$		
$\bar{\nu}$	$(\mathbf{1}, \mathbf{1})_0$	$\mathbf{1}$	

Table 1.1: Standard Model fields and their representations under the SM gauge group and common GUT groups. The right handed neutrino  $\bar{\nu}$  is not part of the SM, but is required for neutrino oscillations and for  $SO(10)$  completion.

supersymmetry, supergravity, grand unification, discrete symmetries and extra dimensions. All of these ideas can found in the framework of string theory.

*Supersymmetry* (SUSY) is, by itself, an extension of the Poincaré group by fermionic generators  $Q, \bar{Q}$ , the so-called supercharges. The fermionic nature of the supercharges means that they transform bosonic states into fermionic states and vice versa. In four dimensions we can have supersymmetric extensions ranging from  $N = 1$ , the minimal amount of SUSY, and  $N = 8$ , the maximal amount for a physically meaningful theory. We focus on  $N = 1$  SUSY since  $N > 10$  would lead to non-chiral theories. Then in the minimal supersymmetric standard model (MSSM), each particle gets a superpartner with same quantum numbers but opposite statistics, which has some nice consequences. The quadratic contributions to the Higgs mass cancel between each particle and its superpartner, thus SUSY stabilizes the Higgs mass against high energy physics. The lightest superpartner is stable due to  $R$ -symmetry so it provides a candidate for a cold dark matter particle. Furthermore, the superpartners modify the running of the three gauge couplings such that they meet at a scale  $M_{\text{GUT}} \approx 10^{16}\text{GeV}$ . However, the MSSM has drawbacks. First of all, no superpartners have been observed so far, thus SUSY must be broken. Since the breaking mechanism is not known, one introduces soft breaking terms which increase the amount of parameters from 17 in the standard model to more than 100 in the MSSM. In specific breaking schemes, the amount of parameters is reduced, however, one can only speculate on how SUSY is precisely broken. Promoting SUSY to a local symmetry, one at the same time obtains invariance under general coordinate transformations which results in general relativity. Thus a theory with local supersymmetry is called *supergravity* (SUGRA) [2].

The representation of the standard model chiral spectrum on its own, see table 1.1, may seem unsystematic, apart from the fact that it exactly cancels the gauge anomalies. The idea of *grand unified theories* (GUT's) [3] is to explain



this pattern by embedding the SM gauge group into a bigger group such that the fields join together to representations of the GUT group. The most popular examples are SU(5), where the SM spectrum fits into just two irreducible representations, the **10** and the  $\bar{\mathbf{5}}$ . The next logical step is SO(10) where everything fits into the spinor representation **16** when including a singlet which is a potential right-handed neutrino. The existence of such a GUT theory requires the gauge couplings to be equal. Fortunately, in the MSSM this is realized at the scale  $M_{\text{GUT}} \approx 10^{16}$  GeV. GUT theories also come with some problems that need to be solved for a fully consistent theory. First of all, the breaking mechanism at the GUT scale has to be specified. Then, at the SU(5) level, we also require the unification of the Yukawa couplings for the electrons and down quarks, which is not the case for all three families. In addition, to get full SU(5) multiplets, the Higgs doublet must get a triplet partner, whose absence needs to be explained.

There is one phenomenological problem that occurs in both, the MSSM and in GUT theories, namely the stability of the proton. From experimental observations we know that the lifetime of the proton is greater than  $10^{32}$  years. However, in the MSSM and in GUT theories one can draw graphs which lead to the decay of the proton, so one has to understand the absence or suppression of these processes. A popular solution for this problem is to introduce *discrete symmetries*. Further applications of discrete symmetries can be the explanation of a small  $\mu$  term, which is supposed to be at the electroweak scale  $M_{\text{EW}} \approx 100$  GeV, or the hierarchies between the masses of the three families.

Already Kaluza and Klein realized that theories in lower dimensions can be traced back to simpler theories in higher dimensions by the properties of the compactification space. Many of the aforementioned problems tend to have simple solutions when extending the four observed spacetime dimensions by *extra spatial dimensions* wrapped up at some small scale. Localization of fields in the internal space can divide the 4d theory in various sectors and explain the suppression of their interactions. This way a SUSY breaking sector can be modelled which does not interact directly with the standard model sector. The breaking of GUT symmetries can easily be explained by non-trivial backgrounds of the internal components of the gauge fields, like Wilson lines or fluxes. Also the origin of discrete symmetries can be found in the symmetries of the compactification space.

*String theory* [4–8] is a framework which offers vast possibilities to address all of the forecited issues. First of all, every string theory automatically incorporates a quantum theory of gravity. Due to the regularizing role of the string scale, this theory is fully consistent to all scales. The most fundamental string theories live in ten spacetime dimensions and are necessarily supersymmetric. Thus they can be viewed as starting points for four-dimensional particle theories by compactifying on a six-dimensional manifold. In order to preserve  $N = 1$  SUSY in four dimensions, this space has to be Calabi–Yau (CY). Here we will work with the  $E_8 \times E_8$  heterotic string theory, since, as a ten-dimensional theory, it comes

## 1 Introduction

with a  $E_8 \times E_8$  gauge symmetry, which contains many favoured GUT groups in a chain of subgroups

$$E_8 \supset E_6 \supset SO(10) \supset SU(5) \supset SU(3)_C \times SU(2)_L \times U(1)_Y .$$

The second  $E_8$  factor is usually seen as a hidden sector e.g. for SUSY breaking dynamics.

The big challenge is to find a reduction of the theory to four dimensions such that one recovers the properties of the standard model. Here the compactification on Calabi–Yau manifolds [9] is just one possibility. Its advantage is that many different CYs are known and thus offer a huge playground. The disadvantages lie in the complicated nature of these spaces. In particular, for no compact Calabi–Yau the metric is explicitly known which limits the possibilities for direct string computations. Instead one has to rely on approximation in the string length, which can be seen as compactification of 10d heterotic supergravity. However, in perturbative heterotic SUGRA one finds that the volume of the compactification space is related to the gauge coupling and hence is limited from above. Therefore the validity of the SUGRA approximation in realistic theories is problematic.

More trustworthy approaches are to start with a worldsheet theory with four extended dimensions which one has under control. Then the internal degrees of freedom may or may not have a geometric interpretation. Here the compactification on toroidal *orbifolds* [14, 15] is of great significance since it at the same time offers full calculability due to the flat metric and a geometric picture. Also the concept of local grand unification [33] emerges where different sectors of the theory come in representations of different GUT groups. However, toroidal orbifolds are rather rare so the possibilities for model building are restricted, although not fully explored. Furthermore, orbifold theories sit at very special points in a much bigger moduli space and it turns out that for a fully realistic model one has to leave the orbifold point to a more generic theory. The reasons are, on the one hand, the need to get rid of many of the massless fields which one observes at the orbifold point but not in reality and, on the other hand, the radiative dynamics of the effective theory which destabilize the orbifold point. This can result in a blow-up of the orbifold singularities, so in certain cases the theory can be approximated by a SUGRA theory compactified on the smooth resolved space.

This leads to the question how one can understand the resolution process. From the orbifold point of view one can study the four-dimensional low energy theory and do perturbations around the orbifold point. This way one can understand the spontaneous breaking of symmetries and the decoupling of states by generating masses. But like every perturbation theory it has a limited range of validity and is blind to non-perturbative effects. Another approach is to study the theory from the other side, which is the large volume region of the smooth resolution. Here the SUGRA is a good approximation and corrections appear in

the string length. In fact, the expansion parameters of these two theories can be viewed as inverses of each other. However, since the SUGRA is fully valid in the infinite volume limit, it does not describe true string compactifications. By comparing and matching the orbifold and the resolution theories one can get more insights in the resolution process, but none of these frameworks is able to see exactly what happens in between.

In order to describe a smooth interpolation between orbifold and resolution theories, *gauged linear sigma models* (GLSM) turn out to be the right tool. These are two-dimensional supersymmetric theories in which the moduli can be controlled in an easy way. Having such a GLSM for a toroidal orbifold resolution at hand could show how transition between the theories can be realized. The drawback of GLSM's is that they do not describe string theories by themselves but instead one has to perform the infrared limit where they flow to a conformal non-linear theory. Because of this, fully reliable exact string computations are very difficult and also the quantization of the theory is not straight forward. But still from GLSMs one can infer properties of the string theories and relations among them.

## Outline

In chapter 2 we discuss heterotic string theories on toroidal orbifolds. We first review the construction of the heterotic string and focus on how low energy spectra can be obtained. As a next step we introduce toroidal orbifolds and discuss their geometry, in particular the fixed point structure. Consequently we show how heterotic compactifications on orbifolds are described as free conformal field theories. We argue that many properties can be read off from the Abelianization of the space group. The four-dimensional low energy spectra are determined, with the distinction between twisted and untwisted string, leading to different sectors which play different roles. This will be illustrated with two examples. One is the standard embedding of the  $\mathbb{Z}_3$  orbifold, which is the standard pedagogical example. The other one is a more complicated MSSM-like model on a  $\mathbb{Z}_2 \times \mathbb{Z}_2$  orbifold. Here the relation of freely acting symmetries to non-factorizable lattices is being illuminated.

Chapter 3 deals with how resolutions of toroidal orbifolds can be realized as target spaces of two-dimensional theories. Since the simplicity of the flat but singular orbifolds is lost, one has to use more involved methods. We begin with a brief recap of toric geometry with a focus on the ingredients which one needs for toroidal orbifold resolutions. These are on the one hand the two-tori or elliptic curves, which contain the global information on the resolution geometry, and on the other hand the resolution of local Calabi–Yau singularities, which describe the local properties. We introduce the framework of gauged linear sigma models, which are two-dimensional supersymmetric theories whose target spaces are complete intersections in ambient toric spaces. One distinguishes between

## 1 Introduction

$N = (2, 2)$  models, which are easier to control but leave no freedom in the compactification of the gauge sector, and  $N = (2, 0)$  models, which potentially can describe many different gauge bundles but are very stringent due to the required absence of gauge anomalies. A Green–Schwarz like mechanism to cancel the  $(2, 0)$  anomalies is presented. In the following, we explain how resolutions of toroidal orbifolds are realized as complete intersections in toric ambient spaces and thus as target spaces of GLSMs. We find that all factorizable orbifolds plus some non-factorizable ones can be constructed. We find that there are many different possible models for one orbifold geometry. The minimal models are the simplest ones, but do not allow for Wilson lines. The maximal models offer the most possibilities but this comes at the cost of their complexity. As a first example we choose  $(2, 2)$  models of the  $\mathbb{Z}_3$  orbifold and show how the geometry emerges and how topological properties are deduced. Due to the GLSM we are able to explore many regions of the moduli space which go beyond orbifold and resolution phases. We identify many different phases, among them a non-geometric Landau–Ginzburg like phase and half-geometric hybrid phases. In the cases  $\mathbb{Z}_3$  and  $\mathbb{Z}_4$  we show how non-factorizable orbifolds can be achieved. Here one has to distinguish between non-factorized orbifolds, which are deformations of factorizable ones, and truly non-factorizable orbifolds with different topologies. Finally we discuss properties of  $(2, 0)$  models with the focus on line bundles and their relation to the orbifold CFTs.

In chapter 4 we want to find out what happens as one moves around in the moduli space. For this we first discuss how heterotic SUGRA theories with line bundles are constructed at the large volume region in moduli space and how low energy spectra are obtained. One particular issue is the flux quantization for which we show that it forces the gauge bundle to be related to orbifold data in terms of shift vectors and Wilson lines. As an example we study a simple example on the  $\mathbb{Z}_2 \times \mathbb{Z}_2$  orbifold, where we compare the spectra between the orbifold theory and the smooth resolution theory in four different phases. One finding is that the multiplicity of some states jumps between the different phases which can be explained by the inclusion of non-perturbative string instanton corrections.

## Publications

Parts of this work have been published in scientific journals:

- M. Blaszczyk, S. Groot Nibbelink, M. Ratz, F. Ruehle, M. Trapletti and P. K. S. Vaudrevange,  
“A  $Z_2 \times Z_2$  standard model,”  
Phys. Lett. B **683** (2010) 340 [arXiv:0911.4905 [hep-th]].
- M. Blaszczyk, S. Groot Nibbelink, F. Ruehle, M. Trapletti and P. K. S. Vaudrevange,  
“Heterotic MSSM on a Resolved Orbifold,”  
JHEP **1009** (2010) 065 [arXiv:1007.0203 [hep-th]].
- M. Blaszczyk, S. Groot Nibbelink and F. Ruehle,  
“Green-Schwarz Mechanism in Heterotic (2,0) Gauged Linear Sigma Models: Torsion and NS5 Branes,”  
JHEP **1108** (2011) 083 [arXiv:1107.0320 [hep-th]].
- M. Blaszczyk, N. G. Cabo Bizet, H. P. Nilles and F. Ruehle,  
“A perfect match of MSSM-like orbifold and resolution models via anomalies,”  
JHEP **1110** (2011) 117 [arXiv:1108.0667 [hep-th]].
- M. Blaszczyk, S. Groot Nibbelink and F. Ruehle,  
“Gauged Linear Sigma Models for toroidal orbifold resolutions,”  
JHEP **1205** (2012) 053 [arXiv:1111.5852 [hep-th]].

## *1 Introduction*

## 2 Heterotic Strings on Orbifolds

In this chapter we demonstrate how heterotic string models on orbifolds are constructed. In section 2.1 we review the basics of the heterotic string and how its spectrum is obtained. In section 2.2 we discuss the geometrical and topological properties of toroidal orbifolds. Finally, in section 2.3 we compactify the heterotic string on toroidal orbifolds and determine the low energy spectrum. This is worked out on two examples, the  $\mathbb{Z}_3$  standard embedding and a  $\mathbb{Z}_2 \times \mathbb{Z}_2$  standard model candidate.

### 2.1 The Heterotic String

Perturbative string theories are best described as conformal field theories (CFT) on a two-dimensional worldsheet with Lorentzian signature. If the worldsheet has no boundary, i.e. it is a closed Riemann surface, massless modes strictly split into left- and right-moving parts and so do the supersymmetry generators. The target space, i.e. the space of ground states of the bosonic coordinates, must contain four dimensions to describe our observable universe which is approximated by Minkowski space  $M_4$ . But the worldsheet theory requires more degrees of freedom in order to cancel the conformal anomaly. They can describe a compact space at yet unobservable length scales, or they can be non-geometric or hybrid. The amount of required dofs is dictated by the amount of SUSY.

Theories with  $(0, 0)$  SUSY are pure bosonic string theories, and as such phenomenologically not viable. Theories with gauged  $(1, 1)$  SUSY are referred to as type II theories. By including open strings and their coupling to D-branes, they are able to describe four-dimensional  $N = 1$  theories with a gauge sector and chiral matter. Furthermore, non-perturbative physics of the type II theories can be reflected in M-theory [10] or F-theory [11] which, however, do not capture the full string dynamics of the theories.

The two-dimensional splitting between left- and right-moving dofs allows to have a different amount of SUSY in these two sectors. This enables theories with gauged  $(1, 0)$  SUSY which are referred to as heterotic string theories [12,13]. One can think of them as hybrid theories that are mixed bosonic and superstring theories. When one considers a geometric theory, one chooses the bosons to take values in a target space manifold and the fermions live in the tangent bundle. Then, the consistency of the theory requires the bosonic left-movers to live in a 26-dimensional space whereas the right-moving superstring target space must be

## 2 Heterotic Strings on Orbifolds

ten-dimensional. But this means that in heterotic string theory there are 16 more right-moving bosonic degrees of freedom than left-moving ones. Consistency of the theory highly constrains these dofs.

In the bosonic formulation one describes them as 16 real bosonic fields which must be compactified on a torus which has an underlying even, self-dual lattice. Thus such a torus is rigid and has no dynamics. There are two choices for such a lattice in 16 dimensions, namely the Lie algebra lattice of  $E_8 \times E_8$  or the lattice of  $Spin(32)$  combined with its spinor weight lattice. The advantage of this construction is that it is geometrical, for example group actions on the dofs can be seen as actions on the underlying torus, or we can interpret string states as winding modes along the torus cycles. We will use this construction for the heterotic orbifolds since it nicely visualizes the shifts and Wilson lines. The disadvantage is that a sole right-moving boson does not have a Lagrangian description and thus is less natural to handle.

Equivalently, one can use the fermionic construction where each bosonic dof is replaced by two fermionic ones. Roughly speaking, a boson corresponds to the phase of two fermions combined to a complex one. In this case the two consistent theories correspond to different choices of boundary conditions. A right-moving fermion in two dimensions can be seen as a right-chiral fermion and thus naturally possesses a Lagrangian description. This will be useful e.g. in GLSM constructions in section 3.2.2 where a complex right-moving fermion forms the dynamical dof of an  $N = (2, 0)$  multiplet. In the following we will work with the  $E_8 \times E_8$  heterotic string.

### Low Energy Spectrum

Since string theories are conformal field theories there is huge freedom to choose coordinates while keeping the worldsheet metric constant. For analyzing asymptotic states in the heterotic string one must consider a worldsheet with an infinite timelike direction and a close spatial direction, i.e. an annulus. It is usually parameterized by coordinates  $(\tau, \sigma)$  with identifications  $\sigma \sim \sigma + \pi$ . Alternatively one defines a complex coordinate  $z = e^{2(\tau+i\sigma)}$  where the identification is automatically built in. However, in constructions where the target space is described as a coset by a discrete group,  $\mathcal{M} = \mathcal{A}/G$ , it is more convenient to write closed string by identifying endpoints of the  $\sigma$  coordinate up to a  $G$  action, i.e.  $X(\sigma = \pi) = gX(\sigma = 0)$  with  $g \in G$ .

The simplest theory is the uncompactified ten-dimensional one. For our purposes it will be useful in two different ways. On the one hand, we can deduce from it the ten-dimensional low energy spectrum and its effective action which can be seen as the limit in which the string length goes to zero. This result is ten-dimensional heterotic supergravity which is used as a starting point for CY compactifications. On the other hand it is useful when we study orbifold compactifications. Since toroidal orbifolds are flat spaces, up to fixed points of



## 2.1 The Heterotic String

a discrete group action, the string quantization on them is very similar to the ten-dimensional case.

To be more precisely, the bosonic formulation of the heterotic string consists of the fields  $X^\mu$ ,  $\mu = 1, \dots, 10$  which describe the ten-dimensional target space, their right-moving superpartners  $\psi^\mu$  and 16 left-moving bosons  $X^A$ . The bosons are subject to a compactification on a torus with underlying Lie algebra lattice of  $E_8 \times E_8$  or  $\text{Spin}(32)$ , i.e.

$$X^A(\sigma + \pi) = X^A(\sigma) + P^A, \quad \text{with} \quad P^A \in \Lambda_{E_8 \times E_8} \text{ or } \Lambda_{\text{Spin}(32)}. \quad (2.1)$$

Since in ten dimensions we have a flat metric and no additional background fields, the theory of those fields is a free theory and can thus be canonically quantized in a well known fashion. One first defines a ground state which is the direct product of a left- and a right-moving ground state. The left-moving one is determined by the boundary condition of the bosons  $X^A$ , i.e. it is labeled by  $|P\rangle$  with the winding number  $P$  explained in (2.1). For the right-moving ground state we have to specify boundary conditions for the fermions, which can be periodic or anti-periodic,  $\Psi(\sigma + \pi) = \pm\Psi(\pi)$  giving rise to the Ramond (R) or Neveu–Schwarz (NS) sectors. Whereas the R sector leads to space time fermions, in the NS sector we find bosonic states. From the worldsheet energy momentum tensor we get the expressions for the target space mass of the states. In particular, for massless states we find that the right-moving state necessarily must form a vector (NS) or Majorana–Weyl spinor (R) representation of the ten-dimensional Lorentz group  $SO(9, 1)$ . In the left-moving sector we have more freedom. The masslessness condition can be stated as

$$1 = \frac{P^2}{2} + N, \quad (2.2)$$

in terms of the winding number  $P$  and the oscillator number  $N$ . Thus we can build massless states by either having  $P^2 = 2$  which corresponds to the roots of  $E_8 \times E_8$  or by switching on an oscillator excitation. This leads to the following massless spectrum,

$$|q\rangle \otimes \alpha_{-1}^\mu |0\rangle \rightarrow \begin{cases} g_{\mu\nu} & \text{graviton,} \\ B_{\mu\nu} & \text{2-form,} \\ \phi & \text{dilaton,} \\ \psi_\mu & \text{gravitino,} \\ \psi & \text{dilatino,} \end{cases} \quad (2.3)$$

building up an  $N = 1$  SUGRA multiplet and

$$\left. \begin{array}{l} |q\rangle \otimes \alpha_{-1}^I |0\rangle \\ |q\rangle \otimes |P\rangle \end{array} \right\} \rightarrow \begin{cases} A_\mu^a & \text{gauge bosons,} \\ \lambda^a & \text{gauginos,} \end{cases} \quad (2.4)$$

which is a  $N = 1$  vector multiplet transforming in the adjoint of  $E_8 \times E_8$ .

## 2.2 Orbifold Geometries

In this section we discuss the construction and properties of toroidal orbifolds. Since we want to have a canonically quantizable string theory, we need a compactification space with a flat metric. Such spaces can be described as quotients of flat Euclidean space by a discrete symmetry group  $S$  which is called space group. For convenience, the Euclidean space  $\mathbb{C}^3$  will be parameterized by three complex coordinates  $z^i$  rather than six real ones. To make sure that the compactification space is compact, the space group will contain a six-dimensional lattice as a subgroup,  $S \supset \Lambda_6 \cong \mathbb{Z}^6$ . If the space group would only be the lattice, the resulting space would be a six torus, which is nice to study for compactifications, but leaves too much supersymmetry since it acts trivially on the internal spinors. This can be changed by having a space group which also acts rotationally and thus is able to project out some of the internal spinors, which immediately leads to the space group of an orbifold. It contains lattice shifts in all six directions and in addition rotational generators which must be compatible with the lattice. Thus it can be written as a semi direct product of the lattice  $\Lambda_6$  with a so-called point group  $P$  which contains just the rotations. Then any element of  $S$  can be written as

$$S \ni (\theta, n_\alpha e_\alpha) : z^i \longmapsto \theta_i z^i + n_\alpha e_\alpha^i, \quad (2.5)$$

where  $e_\alpha$  span the lattice  $\Lambda_6$ ,  $n_\alpha$  are integers and  $\theta_i = e^{2\pi i v_i}$ , where  $N v_i \in \mathbb{Z}$ ,  $N$  being the order of the element. For convention we choose  $0 \leq v_i < 1$ . The vector  $v = (v_1, v_2, v_3)$  is called twist vector. The requirement to preserve  $N = 1$  SUSY in  $d = 4$  reads  $v_1 + v_2 + v_3 = 0$  modulo 1, which restricts the choices for  $P$  to be either of the form  $\mathbb{Z}_N$  or  $\mathbb{Z}_N \times \mathbb{Z}_M$ . In principle one could consider more exotic space groups which have generators that simultaneously shift and rotate in different complex planes, or which contain rotations around different centers.

To specify an orbifold, one first specifies the point group and then the lattice which is compatible with the point group. The list of point groups, for which there exist six-dimensional compatible lattices is not very long, see table 2.1. Concerning the lattices, one distinguishes between two cases, factorizable and non-factorizable lattices. Here a lattice is called factorizable if, once the point group action is diagonal in the complex coordinates, the lattice can be written as a direct sum of three two-dimensional lattices, where each of them lies in one of the complex planes. In these cases the geometry is easy to understand. One can first mod out the lattice to obtain a direct product of three two-tori. Then the point groups rotates each two-torus into itself, however since it always rotates multiple tori simultaneously, the direct product structure is lost. Instead one obtains a ‘‘semi-direct product’’ structure, where one can understand the geometry as torus fibration with degenerating fibers over some points. Then each two-torus is geometrically specified by a Kähler modulus  $a_i$ , which measures the volume of the torus, and a complex structure modulus  $\tau_i$ , which is the ratio

Point group	Twist vector(s)	Lattice(s)
$\mathbb{Z}_3$	$\frac{1}{3}(1, 1, 1)$	$\mathbf{A}_2^3$
$\mathbb{Z}_4$	$\frac{1}{4}(1, 1, 2)$	$\mathbf{D}_2^2 \times \mathbf{A}_1^2, D_2 \times A_1 \times A_3, A_3^3$
$\mathbb{Z}_{6-I}$	$\frac{1}{6}(1, 1, 4)$	$\mathbf{G}_2^2 \times \mathbf{A}_2$
$\mathbb{Z}_{6-II}$	$\frac{1}{6}(1, 2, 3)$	$\mathbf{G}_2 \times \mathbf{A}_2 \times \mathbf{A}_1^2, A_5 \times A_1, A_2 \times D_4, A_2 \times B_3 \times A_1$
$\mathbb{Z}_7$	$\frac{1}{7}(1, 2, 4)$	$A_6$
$\mathbb{Z}_{8-I}$	$\frac{1}{8}(1, 2, 5)$	$B_4 \times B_2$
$\mathbb{Z}_{8-II}$	$\frac{1}{8}(1, 3, 4)$	$B_4 \times B_2, D_5 \times A_1$
$\mathbb{Z}_{12-I}$	$\frac{1}{12}(1, 4, 7)$	$E_6, A_2 \times F_4$
$\mathbb{Z}_{12-II}$	$\frac{1}{12}(1, 5, 6)$	$D_2 \times F_4$
$\mathbb{Z}_2 \times \mathbb{Z}_2$	$\frac{1}{2}(0, 1, 1), \frac{1}{2}(1, 0, 1)$	$\mathbf{A}_1^6, \mathbf{A}_1^3 \times \mathbf{A}_3, A_3^2$
$\mathbb{Z}_2 \times \mathbb{Z}_4$	$\frac{1}{2}(0, 1, 1), \frac{1}{4}(1, 3, 0)$	$\mathbf{D}_2^2 \times \mathbf{A}_1^2$
$\mathbb{Z}_2 \times \mathbb{Z}_{6-I}$	$\frac{1}{2}(0, 1, 1), \frac{1}{6}(1, 1, 4)$	$\mathbf{G}_2^3$
$\mathbb{Z}_2 \times \mathbb{Z}_{6-II}$	$\frac{1}{2}(0, 1, 1), \frac{1}{6}(1, 5, 0)$	$\mathbf{G}_2^2 \times \mathbf{A}_1^2$
$\mathbb{Z}_3 \times \mathbb{Z}_3$	$\frac{1}{3}(0, 1, 2), \frac{1}{3}(1, 2, 0)$	$\mathbf{A}_2^3$
$\mathbb{Z}_3 \times \mathbb{Z}_6$	$\frac{1}{3}(0, 1, 2), \frac{1}{6}(1, 5, 0)$	$\mathbf{G}_2^2 \times \mathbf{A}_3$
$\mathbb{Z}_4 \times \mathbb{Z}_4$	$\frac{1}{4}(0, 1, 3), \frac{1}{4}(1, 3, 0)$	$\mathbf{D}_2^3$
$\mathbb{Z}_6 \times \mathbb{Z}_6$	$\frac{1}{6}(0, 1, 5), \frac{1}{6}(1, 5, 0)$	$\mathbf{G}_2^3$

Table 2.1: Points groups, generating twist vectors and possible lattices for three-dimensional orbifolds. Factorizable lattices are written boldface.

## 2 Heterotic Strings on Orbifolds

of the two basis lattice vectors as complex numbers. From this we see that the point group  $P$  must be compatible with the symmetries of each two-torus, which boils the order of the elements of  $P$  down to four choices:

- $\mathbb{Z}_2$  with the complex structure being unconstrained,
- $\mathbb{Z}_3$  where  $\tau$  is fixed to  $\xi := e^{2\pi i/3}$ ,
- $\mathbb{Z}_4$  with  $\tau = i$ ,
- $\mathbb{Z}_6$  where again  $\tau = \xi$ .

The lattices are only defined up to continuous deformations which in general destroy the property that they can be written as root lattices of some Lie algebras. More precisely, to describe these deformations, we look at differential forms on a torus and see which of those are invariant under the point group. On the six-torus, written in complex coordinates  $z^i$ , we define the one-forms  $dz^i$  and  $d\bar{z}^i$  which are a basis of the cohomology groups  $H^{(1,0)}$  and  $H^{(0,1)}$ , respectively. These one-forms can be taken as generators of the whole torus cohomology, i.e. every  $(p, q)$  form can be written as

$$\omega^{(p,q)} = dz^{i_1} \wedge \dots \wedge dz^{i_p} \wedge d\bar{z}^{j_1} \wedge \dots \wedge d\bar{z}^{j_q}. \quad (2.6)$$

These forms transform under the point group and only the invariant ones correspond to differential forms on the orbifold. A closer look reveals that the one-forms always get projected out<sup>1</sup>. Next, we observe that there is always a holomorphic  $(3, 0)$  form  $\Omega = dz^1 \wedge dz^2 \wedge dz^3$ , and its conjugate  $(0, 3)$  form, which is left invariant due to the  $N = 1$  SUSY condition. This implies that also the  $(2, 0)$  forms get projected out. Thus we are left with two independent types of forms which can be present on orbifolds. These two classes correspond to the allowed deformations of the orbifold lattices, the so called untwisted moduli:

- The  $(1, 1)$  forms correspond to Kähler deformations of the geometry. On orbifolds there are always at least three such forms, namely,  $R_i = dz^i \wedge d\bar{z}^i$  which in the factorizable case scale the size of the three two-tori. There can be more  $(1, 1)$  forms,  $R_{ij} = dz^i \wedge d\bar{z}^j$  if  $v^i = v^j$  for all point group elements. In this case, switching on these moduli makes the lattice non-factorizable by tilting the two-tori into one another.
- If the point group acts on the  $i$ th plane only to second order, then the  $(2, 1)$  form  $dz^j \wedge dz^k \wedge d\bar{z}^i$  with  $i \neq j \neq k \neq i$  is invariant. For factorizable orbifolds it corresponds to the complex structure modulus  $\tau_i$  which, as we discussed, is only free in the  $\mathbb{Z}_2$  case.

---

<sup>1</sup>One might construct orbifolds where the point group acts non-trivially in just two complex planes where this is not true. However, such orbifolds can always be written as a product of a two-torus and a two-dimensional orbifold and leave  $N = 2$  SUSY unbroken in four dimensions. Thus they will not be considered here.

To sum up, the amount of untwisted  $(p, q)$  forms is specified by the two numbers  $h_{\text{untw.}}^{1,1}$  and  $h_{\text{untw.}}^{2,1}$ , the rest follows from Hodge duality and symmetry under complex conjugation<sup>2</sup>.

### Fixed points

Since the space group contains rotational elements, its action on  $\mathbb{C}^3$  is not free but rather has fixed points. For example one easily sees that the point group elements always have the origin as fixed point. In general, if an element rotates in all three planes, it has exactly one fixed point which is the center of rotation. If the element rotates in two planes and acts trivially in the third plane, one has a so called fixed line. Depending on the remaining space group action, the fixed line may have the topology of a  $T^2$ , or, if there are more twisting elements, an orbifolded torus  $T^2/\mathbb{Z}_N$ . When discussing strings on orbifolds, we will see that the fixed points correspond to conjugacy classes of the space group.

Now away from the fixed points, the orbifold is a flat space, i.e. it can be endowed with a flat metric. To see this, note that every point which is not a fixed point has a neighborhood such that all the images of the neighborhood under the space group are disjoint. For a fixed point we cannot find such a neighborhood. Instead, imagine a ball around the fixed point. After modding out the space group, the ratio of surface area to radius does not correspond to the flat space value, thus indicating non-vanishing curvature inside the ball. But all points except the fixed point are flat, the curvature must be concentrated in a delta-peak at the fixed point. Thus the orbifold is no longer a manifold, which by definition must be smooth. Understanding toroidal orbifolds as limits of smooth Calabi–Yau manifolds will be discussed in chapter 3. For factorizable orbifolds the fixed point structure can always be understood in terms of the fixed points on the two tori, which is rather simple. They will be discussed in section 3.1 when discussed in the context of elliptic curves.

## 2.3 Strings on Orbifolds

To put strings on an orbifold we use the property that the orbifold is written as flat space modulo the space group. For convenience, we define the complex coordinate fields on the worldsheet  $Z^i = X^{2i+2} + iX^{2i+3}$ ,  $i = 1, 2, 3$  and sum over all closed string boundary conditions of the form  $Z^i(\sigma + \pi) = gZ^i(\sigma)$  where  $g$  runs over the whole space group. The uncompactified dimensions must stay untouched. Then, supersymmetry dictates how the fermionic superpartners on the worldsheet have to transform, again up to a sign ambiguity to distinguish the NS and R sectors. Finally, in heterotic string theory the action of  $S$  sixteen extra

---

<sup>2</sup>Or alternatively from Serre duality.

## 2 Heterotic Strings on Orbifolds

left-moving degrees has to be specified and will necessarily be non trivial<sup>3</sup> due to the invariance of the one loop partition function under modular transformations. We will only consider Abelian embeddings of the space group, so we must only specify its action on the Abelianization of  $S$ . The Abelianization is defined as the quotient of  $S$  by the subgroup which is generated by all commutators inside  $S$ ,  $\text{Ab}(S) = S/[S, S]$ . One finds that the Abelianization of an orbifold space group is a finite Abelian group, and thus can be written as a direct product of cyclic groups  $\mathbb{Z}_M$ . In fact it can always be written as a direct product of the point group  $P$  with some other cyclic factors,  $\text{Ab}(S) = P \times \prod_{\alpha} \mathbb{Z}_{N_{\alpha}}$ , where the elements in the  $\mathbb{Z}_{N_{\alpha}}$  can be represented by non-twisting elements, i.e. by lattice vectors. In the bosonic formulation, the action of  $\text{Ab}(S)$  on the sixteen extra left-movers is given by a shift. More precisely, it is given by

$$g : X^I \mapsto X^I + kV^I + mV'^I + \sum_{\alpha} n_{\alpha} W_{\alpha}^I, \quad \text{for } g = (\theta^k \theta^m, n_{\alpha} e_{\alpha}) \in S, \quad (2.7)$$

where  $\theta'$  and  $V'$  are trivial for  $P = \mathbb{Z}_N$ . The vectors  $V, V'$  are called shift vectors, and the  $W_{\alpha}$  are discrete Wilson lines, where the name is inherited from the continuous Wilson lines on the torus. Since  $\text{Ab}(S)$  is finite, the shift vectors and Wilson lines underly quantization conditions. For  $P = \mathbb{Z}_N \times \mathbb{Z}_M$  we find

$$NV \in \Lambda_{E_8 \times E_8}, \quad MV' \in \Lambda_{E_8 \times E_8}, \quad N_{\alpha} W_{\alpha} \in \Lambda_{E_8 \times E_8}. \quad (2.8)$$

In the fermionic construction the action of  $\text{Ab}(S)$  is by phase rotations of the 16 complex fermions, thus showing that they correspond to linear representations. Having fixed  $V, V'$  and  $W_{\alpha}$  we have specified a particular string theory at the orbifold point and can start quantizing it. For this one finds that the different sectors in the partition function correspond to the conjugacy classes of the space group. Indeed, if two elements are conjugate,  $g' = hgh^{-1}$ , the strings closed under  $g$  and  $g'$  are mapped onto each other by  $h$ , or more precisely, will correspond to sums over all elements in the conjugacy class in order for the state to be invariant under  $S$ . The conjugacy classes of  $S$  fall into three categories. In the trivial class one finds the untwisted strings. Then, there is a finite number of classes which contain all element with non-trivial twists. Strings in these classes are called twisted strings. Finally, there are infinitely many classes containing the non-trivial elements of  $\Lambda$ . Strings in these classes are pure winding string and are in general massive and will thus not be considered here.

Note that in the case of factorizable orbifolds, the additional factors in the Abelianization of the space group can be read off from the restriction of  $S$  to the two-tori. Since there are only four different orbifolds of two-tori,  $\text{Ab}(S)$  can quickly be classified for them and be used for the higher dimensional cases. For

---

<sup>3</sup>There are two exceptions,  $\mathbb{Z}_3$  and  $\mathbb{Z}_7$  where it can be trivial.

this we first look at the commutator subgroups. Due to the semidirect product structure of  $S = P \ltimes \Lambda$ , it follows that each commutator has a trivial twist and thus is a lattice vector. Therefore  $[S, S]$  is a sublattice of  $\Lambda$  which we will denote by  $\Lambda_{\text{coarse}}$ . Then we find  $\text{Ab}(S) = P \times \Lambda / \Lambda_{\text{coarse}}$  where the lattice quotient is indeed a finite Abelian group. For the two-dimensional lattices it is

- $\mathbb{Z}_2 \times \mathbb{Z}_2$  for the  $\mathbb{Z}_2$  orbifold,
- $\mathbb{Z}_3$  for the  $\mathbb{Z}_3$  orbifold,
- $\mathbb{Z}_2$  for the  $\mathbb{Z}_4$  orbifold,
- trivial for the  $\mathbb{Z}_6$  orbifold.

### Untwisted sector

The quantization in the untwisted sector is almost as in the ten-dimensional case. In particular, as a starting point one can take the ten-dimensional spectrum which, however, will be subject to projections. For each space group element one can divide the space group into its stabilizer, which is normal in  $S$ , and the quotient. To create  $S$  invariant states, these two groups play different roles. The quotient is used to construct linear combinations over the whole conjugacy class. The stabilizer, on the other hand, will lead to projections of the states. In the case of the identity class, the whole group is the stabilizer so all elements will act by projections. It is sufficient to take a generating set of the stabilizer to find all the projections. A massless string state is made of a right-moving ground state  $|q\rangle_{NS/R}$ , a left-moving states with winding  $|P\rangle$  and left-moving oscillators  $\alpha^\mu$ . These elements transform as

$$|q\rangle \rightarrow e^{-2\pi i q \cdot v} |q\rangle, \quad (2.9a)$$

$$\tilde{\alpha}_n^a \rightarrow e^{2\pi i v_a} \tilde{\alpha}_n^a, \quad (2.9b)$$

$$|P\rangle \rightarrow e^{2\pi i P \cdot V_\theta} |P\rangle. \quad (2.9c)$$

From this we find the following states surviving the orbifold projection. We show only the bosons since the corresponding fermions can always be obtained by applying the supersymmetry generator which lowers  $q$  by  $(1/2, 1/2, 1/2, 1/2)$ .

- $|q_V\rangle \otimes \alpha^{\mu=1,2}|0\rangle$  where  $q_V = (1, 0, 0, 0)$  are the four dimensional graviton, dilaton and universal axion
- $|q_V\rangle \otimes \alpha^I|0\rangle$  are  $U(1)^{16}$  gauge bosons
- $|q_V\rangle \otimes |P\rangle$  are non-Abelian gauge bosons if  $P \cdot V \equiv P \cdot W_\alpha \equiv 0$ , where  $\equiv$  means equal modulo one. They enhance the  $U(1)^{16}$  to a non-Abelian group  $G$ .

## 2 Heterotic Strings on Orbifolds

- $|q_S\rangle \otimes |P\rangle$ , where  $q_S = (0, \underline{1}, 0, 0)$ , are charged chiral field if  $q_S \cdot v \equiv P \cdot V$  and  $P \cdot W_\alpha \equiv 0$ . They transform in representations of  $G$  according to the decomposition of the breaking  $E_8 \times E_8 \rightarrow G$ .
- $|q_S\rangle \otimes \alpha^a |0\rangle$  are the untwisted moduli corresponding to untwisted  $(1, 1)$  and  $(2, 1)$  forms.

### Twisted Sectors

Obtaining the spectrum in the twisted sectors is a little more involved, however still straight forward. First one has to notice that the twisting boundary conditions lead to changes in the mode expansion of the coordinate fields. Instead of going into the details we recite the results and their implications for the spectrum. First of all, one finds that the center of mass of twisted strings necessarily lies on the fixed point of the space group element and that the momentum has to vanish. Thus these string states are localized in the internal space. At the same time the oscillators get fractional in the internal space, which for the description of the right-mover leads to a shift in the momentum vector. The masslessness condition then implies that the shifted weight of the boson is equal to the twist vector up to integers such that all entries are non negative,  $q_{\text{sh}} \equiv v$ . Next we focus on the changes in the left-moving sector. Here the 16 extra dofs also get shifted boundary condition,

$$X^I(\sigma + \pi) = X^I(\sigma) + P_{\text{sh}}^I, \quad \text{where } P_{\text{sh}} = P + V_g, \quad P \in \Lambda_{E_8 \times E_8}, \quad (2.10)$$

$$V_g = kV + mV' + n_\alpha W_\alpha, \quad \text{for } g = (\theta^k \theta'^m, n_\alpha e_\alpha).$$

$V_g$  is called the local shift. Thus the twisted states are of the form  $|q_{\text{sh}}\rangle \otimes |P_{\text{sh}}\rangle$  with possible fractional oscillators acting on them. To be a physical state in the low energy theory, they must fulfill the masslessness condition

$$P_{\text{sh}}^2 + 2N = \sum_i v_i^2 + 1, \quad (2.11)$$

$N$  being the sum of oscillator numbers. Furthermore, they must survive the projections (2.9) by the centralizer of  $g$ .

### Anomalous U(1)

The breaking of the gauge symmetry from  $E_8 \times E_8$  to the four-dimensional gauge group due to the shifts and Wilson lines works in an Abelian fashion. This means it can be thought of an internal background value of the gauge fields in the Cartan subgroup. Thus, the four-dimensional gauge group should naively be of the same rank as  $E_8 \times E_8$  which is 16. However, in general models one finds that one U(1) factor in four dimensions appears anomalous from the chiral spectrum point of view. This anomaly is cancelled in a Green–Schwarz fashion [22] by



the unique orbifold axion  $a_{\text{orbi}}$  which is dual to the four-dimensional components of the Kalb–Ramond field. This in turn generates a Stückelberg mass term for the associated gauge boson. In addition one finds a non-vanishing Fayet–Illiopolous term [53], which reveals that the orbifold point is not a stable point in moduli space. Instead, for a stable SUSY vacuum, some of the chiral fields must have non-trivial vevs [23]. This can result in a backreaction on the orbifold geometry, like the resolution of the orbifold singularities. Going away from the orbifold point can lead to further breaking of the gauge symmetries and decoupling of states, but also the appearance of unexpected novel states, which will be discussed in section 4.2. The relation between anomalies on orbifold and resolution is addressed in [36, 45].

### 2.3.1 Examples

We want to demonstrate heterotic orbifold models with two examples, the standard embedding on the  $\mathbb{Z}_3$  orbifold and a more complicated semi-realistic model on  $\mathbb{Z}_2 \times \mathbb{Z}_2$ .

#### Standard Embedding on $T^6/\mathbb{Z}_3$

The first and best studied example of a heterotic orbifold compactification is the standard embedding on the  $\mathbb{Z}_3$  orbifold on the lattice  $A_2^3$ . After rescalings the lattice basis vectors are

$$\begin{aligned} e_1 &= \begin{pmatrix} 1 \\ 0 \\ 0 \end{pmatrix}, & e_2 &= \begin{pmatrix} \xi \\ 0 \\ 0 \end{pmatrix}, & e_3 &= \begin{pmatrix} 0 \\ 1 \\ 0 \end{pmatrix}, \\ e_4 &= \begin{pmatrix} 0 \\ \xi \\ 0 \end{pmatrix}, & e_5 &= \begin{pmatrix} 0 \\ 0 \\ 1 \end{pmatrix}, & e_6 &= \begin{pmatrix} 0 \\ 0 \\ \xi \end{pmatrix}. \end{aligned} \quad (2.12)$$

The point group acts as  $\theta e_{2i-1} = e_{2i}$ ,  $\theta e_{2i} = -e_{2i-1} - e_{2i}$ . This action has 27 fixed points which we label by  $F_{\alpha\beta\gamma} = \{z^1 = z_\alpha^{\text{fixed}}, z^2 = z_\beta^{\text{fixed}}, z^3 = z_\gamma^{\text{fixed}}\}$  where  $z_1^{\text{fixed}} = 0$ ,  $z_2^{\text{fixed}} = (2 + \xi)/3$  and  $z_3^{\text{fixed}} = (1 + 2\xi)/3$ . Since the lattice is factorizable, we immediately find that  $\text{Ab}(S)$  contains, besides the point group, three factors of  $\mathbb{Z}_3$ , so we have to specify a third order shift vector  $V$  and three Wilson lines  $W_{2i}$ , also of order three. In the standard embedding, the shift vector is in its first components equal to the twist, up to integers, and the Wilson lines are trivial,

$$V_{\text{std.emb.}} = \frac{1}{3}(1, 1, -2, 0^{13}), \quad W_\alpha = (0^{16}). \quad (2.13)$$

The resulting gauge group is  $SU(3) \times E_6 \times E_8$ . Concerning chiral matter, the untwisted sector contains three copies of  $(\mathbf{27}, \mathbf{3})$ , and nine singlets which are

## 2 Heterotic Strings on Orbifolds

the complexified Kähler moduli inherited from the torus. Due to the absence of Wilson lines, the 27 twisted sectors are all the same. They contain one multiplet in the  $(\mathbf{27}, \mathbf{1})$  and three transforming as  $(\mathbf{1}, \overline{\mathbf{3}})$ . Due to its simplicity this model is frequently used, e.g. for the study of interactions [49], T-duality [50] or, more recently, elusive moduli [51], just to name a few.

### A Standard Model candidate on $\mathbb{Z}_2 \times \mathbb{Z}_2$

The next example is a standard model candidate constructed in [40, 41]. In the heterotic orbifold framework there have been many attempts to build more or less realistic models with standard model gauge group and three families of chiral matter. There are standard-like models on the  $\mathbb{Z}_3$  orbifold [25, 26], the  $\mathbb{Z}_7$  orbifold [27], and more recently on the  $\mathbb{Z}_{12-I}$  orbifold [28] and the  $\mathbb{Z}_{6-II}$  [29–32] which goes under the name “Mini-Landscape”.

For the  $\mathbb{Z}_2 \times \mathbb{Z}_2$  model presented here, there are two equivalent ways to think of its construction. One way is to start with a factorizable  $\mathbb{Z}_2 \times \mathbb{Z}_2$  orbifold model, with low energy gauge group containing an  $SU(5)_{\text{GUT}}$  factor and six chiral families in the  $\mathbf{10} \oplus \overline{\mathbf{5}}$ . Then one divides out a  $\mathbb{Z}_{2,\text{free}}$  which is freely acting on the orbifold. This will divide the chiral spectrum by two and at the same time, by an associated Wilson line, break  $SU(5)$  down to the standard model. An equivalent way to think of it is to start with a factorizable six-torus and first mod out the  $\mathbb{Z}_{2,\text{free}}$  to obtain a non-factorizable torus, based on the root lattice of  $A_3 \times A_1^3$ . The  $\mathbb{Z}_2 \times \mathbb{Z}_2$  orbifold of this will reproduce the same model, just that  $\mathbb{Z}_{2,\text{free}}$  is already included as part of the spacegroup. Here we will use the approach with the non-factorizable lattice.

Imagine a factorizable lattice, spanned by vectors  $e_\alpha$  which has only non-zero components in the  $[\alpha/2]^{\text{th}}$  complex plane. The  $\mathbb{Z}_{2,\text{free}}$  acts on it as a shift by  $(e_2 + e_4 + e_6)/2$ . Since this is a half lattice vector, we obtain a new lattice whose fundamental cell is one half of the one of the factorizable lattice. To see that this lattice corresponds to  $A_3 \times A_1^3$ , choose the basis

$$\tilde{e}_2 = \frac{e_2 + e_4 + e_6}{2}, \quad \tilde{e}_4 = \frac{-e_2 - e_4 + e_6}{2}, \quad \tilde{e}_6 = \frac{-e_2 + e_4 - e_6}{2}, \quad (2.14)$$

and  $\tilde{e}_\alpha = e_\alpha$  for  $\alpha = 1, 3, 5$ . For an appropriate choice of lengths of the lattice basis, the inner product of the even  $e_\alpha$  becomes the Cartan matrix for  $A_3$ . The  $\mathbb{Z}_2 \times \mathbb{Z}_2$  acts by rotations by 180 degrees in two complex planes simultaneously,

$$\theta_a : z_b \longmapsto -(-1)^{\delta_{ab}} z_b, \quad a, b = 1, 2, 3. \quad (2.15)$$

This action extends to the basis vectors as

$$\theta_1 : \begin{pmatrix} \tilde{e}_1 \\ \tilde{e}_2 \\ \tilde{e}_3 \\ \tilde{e}_4 \\ \tilde{e}_5 \\ \tilde{e}_6 \end{pmatrix} \mapsto \begin{pmatrix} \tilde{e}_1 \\ -\tilde{e}_2 - \tilde{e}_4 - \tilde{e}_6 \\ -\tilde{e}_3 \\ \tilde{e}_6 \\ -\tilde{e}_5 \\ \tilde{e}_4 \end{pmatrix}, \quad \theta_2 : \begin{pmatrix} \tilde{e}_1 \\ \tilde{e}_2 \\ \tilde{e}_3 \\ \tilde{e}_4 \\ \tilde{e}_5 \\ \tilde{e}_6 \end{pmatrix} \mapsto \begin{pmatrix} -\tilde{e}_1 \\ \tilde{e}_6 \\ \tilde{e}_3 \\ -\tilde{e}_2 - \tilde{e}_4 - \tilde{e}_6 \\ -\tilde{e}_5 \\ \tilde{e}_2 \end{pmatrix}, \quad (2.16)$$

and  $\theta_3 = \theta_1\theta_2$ , which specifies the space group multiplication rules. From this we can determine its Abelianization. It is isomorphic to  $\mathbb{Z}_2^2 \times \mathbb{Z}_2^3 \times \mathbb{Z}_4$ , where the first two  $\mathbb{Z}_2$  factors correspond to the point group whereas the next three  $\mathbb{Z}_2$  factors represent the lattice vectors  $\tilde{e}_\alpha$ ,  $\alpha = 1, 3, 5$ . The  $\mathbb{Z}_4$  factor in turn is generated by any of the  $\tilde{e}_\alpha$  for  $\alpha$  even. Thus in the heterotic model we can assign three Wilson lines  $W_\alpha$ ,  $\alpha = 1, 3, 5$  of order two, and one Wilson line  $W_0$  of fourth order. In the free quotient construction [40, 41]  $W_0$  corresponds to the freely acting Wilson line  $W_{\text{free}}$ . Here the Abelianization of the non-factorizable space group answers the question why a freely acting  $\mathbb{Z}_2$  is associated to a fourth order Wilson line.

Next, we inspect the fixed point structure. In the  $\theta_1$  sector, there are eight fixed lines which can be represented by the space group elements

$$(\theta_1, n_3\tilde{e}_3 + n_5\tilde{e}_5 + n_0(\tilde{e}_2 + \tilde{e}_4)), \quad n_i = 0, 1. \quad (2.17)$$

Similarly the  $\theta_2$  and  $\theta_3$  sectors have eight fixed planes each, corresponding to the elements

$$(\theta_2, n_1\tilde{e}_1 + n_5\tilde{e}_5 + n_0(\tilde{e}_4 + \tilde{e}_6)), \quad n_i = 0, 1, \quad \text{and} \quad (2.18)$$

$$(\theta_3, n_1\tilde{e}_1 + n_3\tilde{e}_3 + n_0(\tilde{e}_2 + \tilde{e}_6)), \quad n_i = 0, 1. \quad (2.19)$$

Note that the  $\tilde{e}_i$  with even  $i$  only appear in even multiples. This implies that the twisted sectors only feel twice the Wilson line  $W_0$ , which has the nice feature that we can choose  $W_0$  such that  $2W_0$  preserves an  $SU(5)$  GUT symmetry, whereas  $W_0$  breaks it down to the standard model gauge group. In such a case, all twisted sectors come in representations of  $SU(5)$  which favors the appearance of complete families. The untwisted sector, however, is affected by  $W_0$  so one can realize a pair of Higgs doublets without their triplet partners. The space group elements with an odd multiple of the even  $\tilde{e}_i$  do not have fixed points, which reflects the non-trivial fundamental group of the orbifold,  $\pi_1(T_{A_3 \times A_1}^6 / \mathbb{Z}_2 \times \mathbb{Z}_2) \cong \mathbb{Z}_2$ .

A concrete model is given by the two shift vectors

$$V_1 = \left( \frac{5}{4}, -\frac{3}{4}, -\frac{7}{4}, \frac{1}{4}, \frac{1}{4}, -\frac{3}{4}, -\frac{3}{4}, \frac{1}{4} \right) (0, 1, 1, 0, 1, 0, 0, -1), \quad (2.20a)$$

$$V_2 = \left( -\frac{1}{2}, -\frac{1}{2}, -\frac{1}{2}, \frac{1}{2}, -\frac{1}{2}, -\frac{1}{2}, -\frac{1}{2}, -\frac{1}{2} \right) \left( \frac{1}{2}, \frac{1}{2}, 0, 0, 0, 0, 0, 4 \right), \quad (2.20b)$$

## 2 Heterotic Strings on Orbifolds

multiplicity	representation	label	multiplicity	representation	label
3	$(\bar{\mathbf{3}}, \mathbf{2}; \mathbf{1}, \mathbf{1}, \mathbf{1})_{\frac{1}{6}}$	$q$	3	$(\mathbf{3}, \mathbf{1}; \mathbf{1}, \mathbf{1}, \mathbf{1})_{-\frac{2}{3}}$	$\bar{u}$
3	$(\mathbf{3}, \mathbf{1}; \mathbf{1}, \mathbf{1}, \mathbf{1})_{\frac{1}{3}}$	$\bar{d}$	3	$(\mathbf{1}, \mathbf{2}; \mathbf{1}, \mathbf{1}, \mathbf{1})_{-\frac{1}{2}}$	$\ell$
3	$(\mathbf{1}, \mathbf{1}; \mathbf{1}, \mathbf{1}, \mathbf{1})_1$	$\bar{e}$	33	$(\mathbf{1}, \mathbf{1}; \mathbf{1}, \mathbf{1}, \mathbf{1})_0$	$s$
4	$(\mathbf{1}, \mathbf{2}; \mathbf{1}, \mathbf{1}, \mathbf{1})_{-\frac{1}{2}}$	$h$	4	$(\mathbf{1}, \mathbf{2}; \mathbf{1}, \mathbf{1}, \mathbf{1})_{\frac{1}{2}}$	$\bar{h}$
5	$(\mathbf{3}, \mathbf{1}; \mathbf{1}, \mathbf{1}, \mathbf{1})_{\frac{1}{3}}$	$\bar{\delta}$	5	$(\bar{\mathbf{3}}, \mathbf{1}; \mathbf{1}, \mathbf{1}, \mathbf{1})_{-\frac{1}{3}}$	$\delta$
5	$(\mathbf{1}, \mathbf{1}; \mathbf{3}, \mathbf{1}, \mathbf{1})_0$	$x$	5	$(\mathbf{1}, \mathbf{1}; \bar{\mathbf{3}}, \mathbf{1}, \mathbf{1})_0$	$\bar{x}$
6	$(\mathbf{1}, \mathbf{1}; \mathbf{1}, \mathbf{1}, \mathbf{2})_0$	$y$	6	$(\mathbf{1}, \mathbf{1}; \mathbf{1}, \mathbf{2}, \mathbf{1})_0$	$z$

Table 2.2: Spectrum at the orbifold point. We show the representations w.r.t.  $SU(3)_C \times SU(2)_L \times U(1)_Y \times [SU(3) \times SU(2) \times SU(2)]_{\text{hid}}$  and their multiplicities and labels. The  $[\dots]_{\text{hid}}$  groups stem from the second  $E_8$ .

and the Wilson lines

$$W_3 = \left( -\frac{3}{4}, -\frac{1}{4}, \frac{1}{4}, \frac{7}{4}, -\frac{1}{4}, -\frac{1}{4}, -\frac{1}{4}, -\frac{1}{4} \right) \left( \frac{1}{4}, \frac{1}{4}, \frac{1}{4}, \frac{5}{4}, -\frac{3}{4}, \frac{1}{4}, -\frac{3}{4}, \frac{1}{4} \right), \quad (2.21a)$$

$$W_5 = \left( -\frac{1}{2}, -\frac{1}{2}, \frac{1}{2}, -\frac{1}{2}, \frac{1}{2}, -\frac{1}{2}, \frac{1}{2}, \frac{1}{2} \right) \left( \frac{1}{2}, \frac{1}{2}, 0, 0, 0, 0, -\frac{1}{2}, -\frac{1}{2} \right), \quad (2.21b)$$

$$W_0 = \left( \frac{5}{8}, \frac{1}{8}, \frac{3}{8}, -\frac{1}{8}, -\frac{1}{8}, \frac{3}{8}, \frac{3}{8}, \frac{3}{8} \right) \left( -\frac{1}{8}, \frac{3}{8}, \frac{5}{8}, \frac{5}{8}, \frac{1}{8}, \frac{1}{8}, \frac{1}{8}, \frac{1}{8} \right), \quad (2.21c)$$

and  $W_1$  trivial. The resulting four-dimensional gauge symmetry is  $SU(3)_C \times SU(2)_L \times U(1)_Y \times [SU(3) \times SU(2) \times SU(2)]_{\text{hid}}$  together with some  $U(1)$  factors, one of which is anomalous. The massless spectrum was computed using [34]. It is summarized in table 2.2. More details on the spectrum and possible semi-realistic vacua can be found in [40].

# 3 GLSM description of Resolved Toroidal Orbifolds

This chapter is dedicated to the construction of resolutions of toroidal orbifolds in the context of two-dimensional theories. In section 3.1 we first review aspects of algebraic geometry, in particular toric geometry, which is required to understand the geometry and topology of the emergent target spaces. This includes the description of two-tori as elliptic curves and the resolution of local singularities, which are the basic ingredients for global resolutions. Then, in section 3.2 we introduce Gauged Linear Sigma Models (GLSMs) which are two-dimensional supersymmetric theories whose target spaces naturally are complete intersections in toric varieties with vector bundles. In section 3.3 we show how resolved toroidal orbifolds can be realized in the GLSM by two examples, the  $\mathbb{Z}_3$  and  $\mathbb{Z}_4$  orbifold, each of which has realizations on different lattices. We take simple examples to study the  $(2, 2)$  moduli spaces and identify the phase structure. Finally, in section 3.4 we discuss issues of  $(2, 0)$  models with the example  $\mathbb{Z}_2 \times \mathbb{Z}_2$ .

## 3.1 Some Algebraic Geometry

A huge class of complex geometries is best described by the means of toric geometry. Therefore we will review briefly the construction of toric varieties and discuss their basic properties. As an application we will construct the resolution of local  $\mathbb{C}^3/P$  singularities, with an Abelian finite point group  $P$ , and of elliptic curves. These are at the same time the basic ingredients which are required for the construction of resolved toroidal orbifolds.

### Toric Geometry

There are many ways in which one can understand the construction of toric varieties. The underlying feature of all these is that properties of a complicated complex geometry are reflected in the combinatorics of a fan, i.e. a collection of rational convex polyhedral cones. For a proper introduction, see [17, 18].

### Holomorphic Quotient

The maybe most intuitive way to think of a toric variety is the holomorphic quotient construction. For this we start with a  $d$ -dimensional lattice  $N \cong \mathbb{Z}^d$ ,

### 3 GLSM description of Resolved Toroidal Orbifolds

where  $d$  is supposed to be the complex dimension of the variety. In this lattice we choose  $r$  vectors  $v_1, \dots, v_r \in N$  where  $r \geq d$ . Out of these vectors we now construct the fan. For this we start with the definition of a convex rational polyhedral cone. These are subsets  $\sigma$  of  $N \otimes_{\mathbb{Z}} \mathbb{R} \cong \mathbb{R}^N$  which can be written as

$$\sigma = \langle v_{i_1}, \dots, v_{i_k} \rangle := \left\{ \sum_j a_j v_{i_j} \mid a_j \in \mathbb{R}_0^+ \right\}. \quad (3.1)$$

The convexity condition restricts the cone to lie in a half-space, in other words,  $x, -x \in \sigma \Rightarrow x = 0$ . Now a fan  $\Sigma$  is defined as a collection of convex rational polyhedral cones together with two criteria. First, for each cone  $\sigma \in \Sigma$ , the faces of  $\sigma$ , i.e. cones which are generated by subsets of the generators of  $\sigma$  are also in  $\Sigma$ . Second, the intersection of two cones in  $\Sigma$  must also be a cone in  $\Sigma$  of lower dimension. If these criteria are met, one can proceed to define the toric variety. For this, we associate to each vector  $v_i$  a coordinate  $z_i$ , which from now on will be called homogeneous coordinate. Since we assumed  $r \geq d$ , the vectors  $v_i$  are subject to linear equivalence relations of the form

$$\sum_i q_i^I v_i = 0, \quad I = 1, \dots, r - d. \quad (3.2)$$

We use these relations to define a  $(\mathbb{C}^*)^{r-d}$  action on the coordinates,

$$\mu_a z_i \longmapsto \mu^{q_i^a} z_i. \quad (3.3)$$

One last ingredient we need is the exclusion set  $F$  which is defined as,

$$F = \bigcup_{\substack{\{i_1, \dots, i_k\} \subset [1, r] \cap \mathbb{Z} \\ \langle v_{i_1}, \dots, v_{i_k} \rangle \notin \Sigma}} \{z_{i_1} = \dots = z_{i_k} = 0\} \quad (3.4)$$

We have all together in order to define the toric variety. For this we take the vector space spanned by all homogeneous coordinates, remove the exclusion set and divide out the  $(\mathbb{C}^*)^{r-d}$  action,

$$\mathcal{V} = \frac{\mathbb{C}^r - F}{(\mathbb{C}^*)^{r-d}}. \quad (3.5)$$

The holomorphic quotient as presented here only works properly if the vectors  $v_i$  span the full lattice  $N$ . In that case the resulting variety is smooth. Otherwise, a further finite discrete symmetry, isomorphic to the quotient of  $N$  by the span of the  $v_i$ , has to be divided out and gives rise to orbifold singularities. Later we will see that it is also possible to induce these symmetries as remnants of some  $(\mathbb{C}^*)^l$  action.

### Symplectic Quotient

Another way to understand a toric variety is the symplectic quotient construction. For this, the basic observation is that the multiplicative group  $\mathbb{C}^*$  can be written as a direct product,  $\mathbb{C}^* = U(1) \times \mathbb{R}_+$ , which corresponds to writing complex numbers in polar coordinates  $z = re^{i\phi}$ . Then, we start with a set of homogeneous coordinates  $z_i$  with  $U(1)^{r-d}$  charges  $q_i^I$ . The  $U(1)^{r-d}$  action will be divided out as before, but instead of also dividing out  $\mathbb{R}_+^{r-d}$ , we impose a set of  $r - d$  real equations,

$$\sum_i q_i^I |z_i|^2 = a^I, \quad I = 1, \dots, r - d, \quad (3.6)$$

where  $a^I$  are real parameters. The toric variety is then the solution set of these equations, divided by  $U(1)^{r-d}$ . This way the exclusion set  $F$  is automatically determined as the union of simultaneous zero loci of coordinates for which the equations (3.6) have no solution. This set is highly dependent on the values of the  $a^I$ , but at generic points it corresponds to the exclusion set as determined by a fan as in the holomorphic quotient. These parameters  $a^I$  correspond to the Kähler moduli of the space, i.e. they control the volumes of the variety and its subspaces and can lead to geometric transitions.

Both constructions, the symplectic and the holomorphic quotient have their pros and cons. The advantage of the holomorphic quotient is clearly its holomorphicity, which allows to use the techniques of complex geometry. Furthermore, since one can mod out a whole  $\mathbb{C}^*$  action, one can always set certain coordinates to arbitrary values (usually to one) in exchange for the  $\mathbb{C}^*$  scalings, and simply use the remaining ones as coordinates. The disadvantage is that, to determine the exclusion set, one has to start from a fan, which particularly in higher dimensions can be quite tedious. Here lies the advantage of the symplectic quotient, since one immediately start with the coordinates and their charges. The precise topology of the space is determined by a set of equations, which can be viewed as linear in the absolute values squares of the coordinates. Furthermore, by varying the parameters  $a^I$  one can explore various phases of the variety, even singular ones, which would correspond to different fans. For our convenience, we will use the advantages of both of those constructions.

### Divisors, Intersections

The topology of a manifold can be described in terms of its homology classes and their intersection ring. Since we are working with complex coordinates, most even homology classes can easily be described. In terms of algebraic geometry, a hypersurface is described as a zero locus of a holomorphic equation. A divisor is then defined as a formal linear combination of such hypersurfaces. In order for such an equation to be well-defined, it must only contain terms of a fixed degree

### 3 GLSM description of Resolved Toroidal Orbifolds

(i.e. charge under the  $(\mathbb{C}^*)^{r-d}$ ). For many purposes, e.g. the computation of the intersection numbers, the divisor is sufficiently specified by this degree. If, for given degree, there exists only one monomial, the associated divisor is rigid. If, however, there are more monomials of the same degree, the divisor can be moved around and the coefficients encode its locus.

There are linear equivalences between the divisors that arise by factorization of the polynomials. If a polynomial, or in the simplest case a monomial, is a product of some pieces, the associated divisor is equivalent to the sum of the divisors of the factors. Thus as a generating set of divisors one can use the zero loci of the homogeneous coordinates  $D_i := \{z_i = 0\}$ . However, they are not linearly independent, but fulfill  $d$  linear dependence conditions

$$\sum_i v_i^a D_i \sim 0, \quad (3.7)$$

where  $v_i^a$  is the  $a^{\text{th}}$  component of the vector  $v_i \in N$ . If, however, one wants a basis of divisors, one can try to find polynomials  $p_I(z_i)$  with charge  $q_J(p_I) \propto \delta_{IJ}$  and associate divisors  $\tilde{D}_I := \{p_I = 0\}$ . In all our examples we will be able to find such a basis, thus in the following we will assume its existence.

Elements of the even homology classes can then be realized as intersections of divisors. In particular, the intersections of  $d$  divisors, which are points, characterize the topology. Since the intersection numbers only depend on the divisor class (i.e. the degree of the polynomial), one can use linear equivalences among the divisors to determine all intersection numbers including self-intersections. Knowing all the intersection numbers, one can use them to compute topological integrals on the variety of the Poincaré-dual  $(1,1)$ -forms. We will use the same symbols for divisors and their Poincaré-dual forms. It will be clear from the context which one is meant. The intersections or wedge products will thus simply be written as products, where for intersection numbers the integral will be implicit.

#### Kähler Form, Characteristic Classes

Toric varieties, if smooth, are automatically Kähler manifolds which means one can define a closed Kähler form. Then we can expand the Kähler class in our divisor basis,

$$\mathcal{J} = \sum_I a^I \tilde{D}_I. \quad (3.8)$$

The notation  $a^I$  for the Kähler moduli is chosen to be the same as the parameters in the equations (3.6) in the symplectic quotient construction. In the upcoming examples we will indeed see that these two things can be identified. The Kähler form can be used to compute the volumes of the holomorphic submanifolds. Here



we specify to the three-dimensional case and give the formulæ for the volumes of the whole variety  $\mathcal{V}$ , the divisors  $D$  and the curves  $C$ ,

$$\text{Vol}(\mathcal{V}) = \frac{1}{6} \mathcal{J} \mathcal{J} \mathcal{J}, \quad \text{Vol}(D) = \frac{1}{2} \mathcal{J} \mathcal{J} D, \quad \text{Vol}(C) = \mathcal{J} C. \quad (3.9)$$

In the next step we can define the Kähler cone of the variety. The Kähler cone is then defined as the subset of moduli space for which the volumes of all these subvarieties are positive. This set is a cone, since for  $\mathcal{J}$  in it,  $\lambda \mathcal{J}$  is also in it if and only if  $\lambda \in \mathbb{R}_+$ . At the boundary of the Kähler cone, typically the volume of a curve goes to zero and the variety becomes singular. When one crosses such a boundary, flop transitions can occur, in which a curve disappears and another curve, whose class is minus the class of former one, appears. Then one ends up in the Kähler cone of a different variety, whose cones only differ by the flopped cones. Even worse transitions can happen, including the jump of the dimension, which will be demonstrated in section 3.3.2. In the symplectic quotient, these transitions occur automatically as one varies the FI parameters in (3.6). We will show this with an example in section 3.1.1

Another important quantity of a complex manifold is the Chern class. It is formally defined via the determinant of the curvature two-form, but using methods from algebraic geometry there are easier methods to obtain it. In terms of the divisors it is

$$c(\mathcal{V}) = \prod_i (1 + D_i) = 1 + \underbrace{\sum_i D_i}_{c_1(X)} + \underbrace{\sum_{i < j} D_i D_j}_{c_2(X)} + \underbrace{\sum_{i < j < k} D_i D_j D_k}_{c_3(X)}. \quad (3.10)$$

We will need the Chern classes in various contexts. The vanishing of the first Chern class is an indicator for the Calabi–Yau property. The second Chern class appears in the Bianchi identity of the Kalb–Ramond field strength. Last but not least, the integrated third Chern class gives the Euler characteristic of the threefold, which serves as a cross check.

## Vector Bundles, Cohomology

Now we have everything we need to describe the compactification geometry, at least topologically. But for a viable and consistent heterotic compactification we also need to switch on background fluxes of the gauge field. These fluxes are, in the context of algebraic geometry, nicely described in terms of vector bundles, or more precisely, coherent sheaves. Here we will refrain from giving precise mathematical definitions but rather review the relevant properties.

Vector bundles are characterized, though by far not uniquely, by their structure group, which is related to their holonomy group. The simplest vector bundles are line bundles those fibers are one-dimensional and thus their structure group

### 3 GLSM description of Resolved Toroidal Orbifolds

is  $U(1)$  or a subgroup thereof. In order to classify line bundles, we look at the curvature of their connection, which in physical terms can be thought of as a Abelian field strength. For holomorphic line bundles the curvature is a  $(1, 1)$ -form<sup>1</sup> and thus dual to a divisor. Thus by specifying a divisor class  $D$  we at the same time describe a line bundle which we will call  $\mathcal{O}(D)$  or alternatively  $\mathcal{O}(q)$  where  $q$  is the charge vector of the defining polynomial of  $D$ . To close the circle, the divisor  $D$  is cut out as the zero set of a homogeneous polynomial which is a global section of the line bundle  $\mathcal{O}(D)$ ,

$$D = \{p(z) = 0\}, \quad \text{with} \quad p(z) \in \Gamma(\mathcal{O}(D)). \quad (3.11)$$

Vector bundles which are not (sums of) line bundles are more complicated to obtain. One way to define them is as kernels or cokernels of linear maps between line bundles. One such construction, which also appears in  $(2, 0)$  GLSMs is the so called monad complex

$$0 \longrightarrow \mathcal{O}^N \xrightarrow{a} \bigoplus_i \mathcal{O}(q_i) \xrightarrow{b} \bigoplus_l \mathcal{O}(Q_l) \longrightarrow 0, \quad (3.12)$$

where vector bundle is defined as  $\mathcal{V} = \ker b / \text{ima}$ . As an example, the tangent bundle of a (complete intersection in a) toric variety can always be defined in this way.

One important property of a vector bundle are its cohomology groups  $H^p(\mathcal{V})$ . For the physical context it might be appropriate to think of the elements of  $H^p(\mathcal{V})$  as bundle valued  $p$ -forms which are harmonic w.r.t a covariant Laplacian containing the bundle connection.

### Hypersurfaces and Complete Intersections

When looking at the definition of the first Chern class (3.10) together with the set of linear equivalence relations among the divisors (3.7) we find that a toric variety is Calabi–Yau, i.e. has vanishing first Chern class, if and only if the vectors  $v_i$  lie in a plane. In that case, however, the fan does not span the whole vector space  $N \otimes_{\mathbb{Z}} \mathbb{R}$  which reflect the fact that the variety is not compact. We will use such Calabi–Yau constructions when we discuss the resolution of non-compact singularities in section 3.1.1, but for a proper heterotic compactification we need compact Calabi–Yau spaces. For this we look at complete intersections of hypersurfaces in ambient toric varieties. A subvariety  $\mathcal{X}$  is called complete intersection if it can be cut out by a set of holomorphic homogeneous polynomials  $p_{k=1, \dots, s}(z_i)$  with  $s = \text{codim}_{\mathcal{V}} \mathcal{X}$ . For such complete intersections the formula for the Chern classes gets modified,

$$c(\mathcal{X}) = \prod_i (1 + D_i) \prod_{k=1}^s (1 + H_k)^{-1}, \quad (3.13)$$

---

<sup>1</sup>Its Dolbeaut cohomology class is the first Chern class of the bundle.

where  $H_k$  are the divisors cut out by  $p_k$ . Here, and in general, the divisors have to be restricted to  $\mathcal{X}$ . If we denote the charge of  $p_k$  by  $Q_k$ , the Calabi–Yau condition for a complete intersection reads

$$\sum_i q_i = \sum_k Q_k. \quad (3.14)$$

### 3.1.1 Local Singularity Resolutions

Throughout this work we deal with singularities which locally look like  $\mathbb{C}^3/P$  with  $P = \mathbb{Z}_N$  or  $P = \mathbb{Z}_N \times \mathbb{Z}_M$ . These singularities can all be realized as non-compact toric varieties together with the possibility to blow them up. We will describe this process here in the symplectic quotient picture and show the properties of the resolved spaces. The basic idea is to promote the discrete  $P$  action to a continuous  $U(1)$  (or  $\mathbb{C}^*$  in the holomorphic quotient) action. Since modding out a continuous action would reduce the dimension of the space, we at the same time have to introduce new coordinates. The charges are then to be chosen such that the action of  $P$  can get induced.

More concretely, the action of  $P$  is of the form

$$\theta_r : (z_1, z_2, z_3) \mapsto \left( e^{2\pi i \frac{q_1}{N_r}} z_1, e^{2\pi i \frac{q_2}{N_r}} z_2, e^{2\pi i \frac{q_3}{N_r}} z_3 \right), \quad (3.15)$$

with  $q_1 + q_2 + q_3 = 0 \pmod{N_r}$ ,  $0 \leq q_i < N_r$  and  $q_1, q_2, q_3, N_r$  relatively prime. If an element  $\theta_r$  satisfies  $q_1^r + q_2^r + q_3^r = N_r$ , one introduces a homogeneous coordinate  $x_r$  and a  $U(1)_{E_r}$  action with charge assignment

coordinate	$z_1$	$z_2$	$z_3$	$x_r$
charge	$q_1^r$	$q_2^r$	$q_3^r$	$-N_r$

At the same time we impose an equation

$$q_1^r |z_1|^2 + q_2^r |z_2|^2 + q_3^r |z_3|^2 - N_r |x_r|^2 = b_r. \quad (3.16)$$

We observe that since the sum of charges is zero, the resulting space is Calabi–Yau. If  $b_r < 0$ , we find that  $x_r$  cannot vanish and we can fix its phase by a  $U(1)_{E_r}$  rotation, thus breaking it down to a  $\mathbb{Z}_{N_r}$  action that acts on  $z_i$  like (3.15). Thus, for all  $b_r < 0$  we recover the orbifold  $\mathbb{C}^3/P$  with fixed point at  $(0, 0, 0)$ .

Now if  $b_r > 0$ , we see that the fixed point can no longer satisfy (3.16) and thus is removed. Instead one finds the exceptional divisor  $E_r = \{x_r = 0\}$  as a smooth hypersurface replacing the singularity. For the set  $\{x_r \neq 0\}$  the same argument as above applies, thus it look like a  $\mathbb{C}^3/P$  with the singularity removed. In fact, introducing  $U(1)_{E_r}$  actions for a generating set of  $\theta_r \in P$  would be sufficient to induce the  $P$  action on the coordinates  $z_a$ , however, one needs to introduce all of them in order to be able to construct a smooth space. Leaving out some of them would necessarily result in subsingularities.

### 3 GLSM description of Resolved Toroidal Orbifolds

In the holomorphic quotient construction we would have to construct a fan that reproduces the charges. For this we first have to assign the vectors  $v_a$  corresponding to the coordinates  $z_a$ . They must be chosen such that the rationomials  $\prod_a z_a^{v_a^i}$  are an integral basis of invariant monomials. The Calabi–Yau condition implies that  $z_1 z_2 z_3$  can always be chosen as such a basis vector, thus one conveniently fixes  $v_a^1 = 1$  and the vectors lie in a plane. Next, one has to add exceptional divisors, i.e. for each  $\theta_r$  fulfilling the conditions above one adds the vector  $u_r = \sum_a q_a^r / N_r \cdot v_a$ , which also lies in the same plane. This corresponds to adding all vectors which lie in the triangle spanned by the  $v_a$  in this plane. Finally, in order to determine the higher dimensional cones, one has to triangulate the diagram which corresponds to fixing the way in which the exceptional divisors intersect. This triangulation is in many cases not unique, and different triangulations correspond to different topologies.

Already at this stage we are able to describe some different phases of the geometry, which we study in the symplectic quotient construction.

- For all  $b_r < 0$ , we are in the orbifold phase in which the exceptional divisors  $E_r$  do not exist, but which is the only phase for which the fixed point  $(z_1, z_2, z_3) = (0, 0, 0)$  is part of the geometry.
- The full resolution phase is basically given if all  $b_r > 0$ , however, there might be more constraints. First of all, (3.16) only tells that for  $b_r > 0$  the divisor  $E_r = \{x_r = 0\}$  exists. However, there can still be singularities that need to be blown up in higher codimension, like e.g. conifold singularities. In fact, whenever one finds a linear combination of the equations (3.16) which is of the form

$$|y_1|^2 + |y_2|^2 - |y_3|^2 - |y_4|^2 = f(b_r), \quad y_i = x_r, z_a, \quad (3.17)$$

where  $f(b_r)$  is a linear polynomial, one can observe conifold transitions within the resolved singularity. If  $f(b_r) < 0$ , the curve  $\{y_1 = y_2 = 0\}$  exists whereas the curve  $\{y_3 = y_4 = 0\}$  does not, and vice versa for  $f(b_r) > 0$ . The point  $f(b_r) = 0$  is a conifold point with a singularity at  $y_1 = y_2 = y_3 = y_4 = 0$ . Going through such a point is called a flop transition and changes the intersection numbers of the divisors. In the holomorphic quotient this corresponds to a change of the fan.

- In between there usually are intermediate, not fully resolved phases. These are e.g. given if some  $b_r$  are smaller than zero while others are greater. In such a case the orbifold singularity is removed but just partially resolved. It may also happen that if all  $b_r > 0$  there are regions where the singularity is not fully resolved. Then, all divisors exist, but some curves which are necessary to resolve the subsingularities do not.

### 3.1.2 Elliptic Curves and their Symmetries

As we are studying toroidal orbifolds, we need to have an algebraic description for the torus as a starting point. In algebraic geometry we are able to describe two-tori, i.e. elliptic curves, and products thereof. However, it is not possible to describe higher-dimensional tori at an arbitrary point in moduli space which is why a priori we can only deal with factorizable orbifolds. In section 3.3.3 we will see that in some cases we are still able to obtain non-factorizable orbifolds.

Elliptic curves are the only two-dimensional compact spaces which are Calabi–Yau. Thus, we will have to realize them as subvarieties in ambient toric spaces. In fact we will restrict ourselves to weighted projective spaces which are toric varieties with just one  $U(1)$  action. Let’s say we have coordinates  $z_i$ ,  $i = 1, \dots, N$  with charges  $q_i$ , then we need  $N - 2$  hypersurface constraints  $p_k(z_i) = 0$ , with charge  $Q_k$ , to obtain a complex one-dimensional space. This may look like there are many possibilities to construct elliptic curves, but with two additional requirements we will boil it down to just four. First, if  $q_i = Q_k$  for some  $i$  and  $k$ , then  $p_k$  can uniquely be solved for  $z_i$  and both, the equation and the coordinate, can be removed. Thus we require  $q_i \neq Q_k$  for all  $i, k$ . Next, we require all  $Q_k$  to be divisible by all  $q_i$ , since in this case  $p_k$  can be written using only pure monomials, i.e. powers of a single coordinate, which makes the discrete symmetries of the elliptic curve practically tractable. This leaves us with four choices, each of which corresponds to a  $T^2$  with a certain orbifold symmetry,

$$\mathbb{P}_{111}^2[3], \quad \mathbb{P}_{112}^2[4], \quad \mathbb{P}_{123}^2[6], \quad \mathbb{P}_{1111}^3[2, 2]. \quad (3.18)$$

The numbers in the subscript denote the charges of the coordinates and the numbers in the brackets are the charges of the polynomials. We will discuss these cases in detail later, but first we want to connect these elliptic curves to the classical torus  $T^2 = \mathbb{C}/\Lambda$ .

#### The Weierstrass Map

We define the torus as  $T^2 = \mathbb{C}/\Lambda$  where  $\Lambda = e_1\mathbb{Z} \oplus e_2\mathbb{Z}$  and want to map it into a (weighted) projective space. For this we need to define meromorphic, double periodic functions on  $\mathbb{C}$  which is easiest done by an infinite sum over the lattice. In order for it to be convergent, the degrees must be sufficiently negative, and the simplest such example is the Weierstrass elliptic function,

$$\begin{aligned} \wp(u) &= \frac{1}{u^2} + \sum_{v \in \Lambda - 0} \left( \frac{1}{(u-v)^2} - \frac{1}{v^2} \right) \\ &= \frac{1}{u^2} + \sum_{\substack{(n,m) \in \mathbb{Z}^2 \\ (m,n) \neq (0,0)}} \left( \frac{1}{(u - me_1 - ne_2)^2} - \frac{1}{(me_1 + ne_2)^2} \right). \end{aligned} \quad (3.19)$$

### 3 GLSM description of Resolved Toroidal Orbifolds

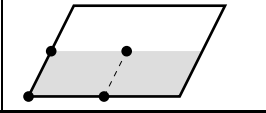
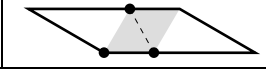
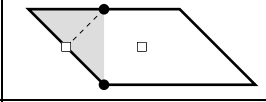
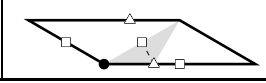
Point Group	Geometry	$n$ -volution	elliptic curve
$\mathbb{Z}_2$		$\mathbb{Z}_2 \times \mathbb{Z}_2$	$\mathbb{P}^3_{(1,1,1,1)}[2, 2]$
$\mathbb{Z}_3$		$\mathbb{Z}_3$	$\mathbb{P}^2_{(1,1,1)}[3]$
$\mathbb{Z}_4$		$\mathbb{Z}_2$	$\mathbb{P}^2_{(1,1,2)}[4]$
$\mathbb{Z}_6$		—	$\mathbb{P}^2_{(1,2,3)}[6]$

Table 3.1: The four elliptic curves corresponding to the four point groups in two dimensions. The the second column shows the geometry where the shaded region is a fundamental domain and the dots are at the fixed point positions. Squared and triangled dots get identified under the point group.

The Weierstrass elliptic function fulfills the Weierstrass differential equation

$$\wp'(u)^2 = 4\wp(u)^3 - f(e_1, e_2)\wp(u) - g(e_1, e_2), \quad (3.20)$$

where  $f$  and  $g$  encode the information on the complex structure modulus  $\tau = e_2/e_1$ . More precisely, the Klein invariant of the coomplex structure is found to be  $j(\tau) = 1728f^3/(f^3 - 27g^2)$ . There are two special values for  $\tau$  corresponding to enhanced symmetry of the torus at  $\tau = i \leftrightarrow g = 0$  and  $\tau = \zeta := e^{2\pi i/3} \leftrightarrow f = 0$ .

Now suppose we have an elliptic curve which is a hypersurface in a two-dimensional ambient space. Then, if we can bring the hypersurface equation to the form

$$y^2 = 4x^3 - fx - g, \quad (3.21)$$

where  $y$  and  $x$  are meromorphic global coordinate functions, we get a holomorphic map between the elliptic curve and the classical two-torus. This will help to identify the required symmetries of our elliptic curves, as we will see in the following examples.

#### Two-torus $T^2_3$ with $\mathbb{Z}_3$ symmetry

In general, if we have coordinates with charges  $q_i$  and equations of order  $Q_k$ , for each coordinate there is a discrete symmetry rotational  $\mathbb{Z}_N$  symmetry, with

### 3.1 Some Algebraic Geometry

$N = \gcd\{Q_k\}/q_i$  if we only allow for pure monomials. Thus in order to realize a  $\mathbb{Z}_3$  symmetry we choose the elliptic curve  $\mathbb{P}_{111}^2[3]$  with defining equation,

$$z_1^3 + z_2^3 + z_3^3 = 0. \quad (3.22)$$

Possible prefactors have been absorbed into the coordinates. This equation has  $\mathbb{Z}_3$  symmetries acting as,

$$\theta_i : z_i \mapsto \zeta z_i, \quad z_{j \neq i} \mapsto z_j, \quad i = 1, 2, 3. \quad (3.23)$$

This actually generates a  $\mathbb{Z}_3^2$  symmetry since  $\theta_1\theta_2\theta_3$  is already an element of the  $U(1)$  action and thus acts trivially on the torus. Thus for a generating set we choose  $\theta := \theta_1$  and  $\alpha := \theta_3\theta_2^2$  and call it  $\mathbb{Z}_{3,\text{orbi}} \times \mathbb{Z}_{3-\text{vol}}$ . Now each  $\theta_i$  has three fixed points at  $z_i = 0$  which lie at  $z_j + \zeta^l z_k = 0$  with  $l = 0, 1, 2$  and  $i \neq j \neq k \neq i$ . On the other hand,  $\alpha$  is freely acting on the torus.

Let us establish the map to the classical torus. For this we do the coordinate transformation,

$$\begin{pmatrix} z_1 \\ z_2 \\ z_3 \end{pmatrix} = 2^{-1/3} \begin{pmatrix} -2 & 0 & 0 \\ 0 & 3^{-1/2} & 1 \\ 0 & -3^{-1/2} & 1 \end{pmatrix} \begin{pmatrix} x \\ y \\ v \end{pmatrix}, \quad (3.24)$$

to bring it to the form,

$$y^2 v = 4x^3 - v^3. \quad (3.25)$$

Using the identifications,

$$\wp(u) = \frac{x}{v}, \quad \wp'(u) = \frac{y}{v}, \quad (3.26)$$

we restore the Weierstrass equation (3.20) with  $(f, g) = (0, 1)$  corresponding to complex structure  $\tau = \zeta$  as expected. The singularity of  $\wp$  at  $u = 0$  is mapped to  $v = 0$ . Now we can translate the discrete symmetries to to classical torus, which is in detail done in appendix A. The result is:

$$\theta : u \mapsto \zeta u, \quad \alpha : u \mapsto u + \frac{\zeta - 1}{3}. \quad (3.27)$$

We find that  $\theta$  is indeed the orbifold symmetry, and  $\alpha$  is a discrete symmetry which acts as a shift on the torus. Since it is freely acting on the torus, we call it 3-volution (or in general  $n$ -volution for a  $\mathbb{Z}_n$  that is freely acting on the torus). This 3-volution maps the three  $\theta_i$  fixed points onto each other for all  $i$ . Thus there are two ways to get a  $T^2/\mathbb{Z}_3$  orbifold: either one simply divides out  $\mathbb{Z}_{3,\text{orbi}}$ , then there are three fixed points at  $z_1 = 0$ , or one divides out the full  $\mathbb{Z}_{3,\text{orbi}} \times \mathbb{Z}_{3-\text{vol}}$ , then there is one fixed point at  $z_i$  for  $i = 1, 2, 3$  each.

### 3 GLSM description of Resolved Toroidal Orbifolds

#### Two-torus $T_4^2$ with $\mathbb{Z}_4$ symmetry

In order to realize a  $\mathbb{Z}_4$  symmetric torus, we choose the elliptic curve  $\mathbb{P}_{1,1,2}^2[4]$  with defining equation

$$z_1^4 + z_2^4 + z_3^2 = 0. \quad (3.28)$$

This has the symmetries,

$$\begin{aligned} \theta_i : z_i &\longmapsto iz_i, & z_{j \neq i} &\longmapsto z_j, & i = 1, 2, \\ \theta_3 : z_3 &\longmapsto -z_3, & z_{j \neq i} &\longmapsto z_j. \end{aligned} \quad (3.29)$$

Again, the combination  $\theta_1\theta_2\theta_3$  is a  $U(1)$  element, thus we are left with a  $\mathbb{Z}_{4,\text{orbi}} \times \mathbb{Z}_{2-\text{vol}}$  symmetry generated by  $\theta = \theta_1$  and the involution (2-volution)  $\alpha = \theta_1\theta_2^3$ . Let us analyze the fixed point structure. We observe that  $\theta_1$  has two fixed points at  $z_1 = 0$  and  $z_2^2 = \pm z_3$ , while  $\theta_1^2$  has two additional  $\mathbb{Z}_2$  fixed points at  $z_2 = 0$ . However, these get identified by  $\theta_1$  as expected from a rotational  $\mathbb{Z}_4$  orbifold action. On the other hand,  $\theta_3$  has four fixed points at  $z_3 = 0$  and  $z_1 = i^l z_2$ ,  $l = 0, 1, 2, 3$ . The involution  $\alpha$  has no fixed points.

As before, we want to map the elliptic curve to the classical torus via the Weierstrass function. For this we perform a coordinate transformation,

$$\begin{pmatrix} z_1 \\ z_2 \\ z_3 \end{pmatrix} = \begin{pmatrix} 1 & 0 & 2^{-1}i \\ i^{1/2} & 0 & -2^{-1}i^{1/2} \\ 0 & i & 0 \end{pmatrix} \begin{pmatrix} x \\ y \\ v \end{pmatrix}, \quad (3.30)$$

to bring it to the form

$$y^2 = 4x^3v - xv^3. \quad (3.31)$$

Using the identifications

$$\wp(u) = x/v, \quad \text{and } \wp'(u) = y/v^2, \quad (3.32)$$

this becomes the Weierstrass equation (3.20) with  $(f, g) = (1, 0)$ , i.e. the torus has complex structure  $\tau = i$ . This map translates the discrete symmetries to

$$\theta : u \mapsto iu, \quad \alpha : u \mapsto u + \frac{1+i}{2}. \quad (3.33)$$

A detail calculation can be found in appendix A. As expected,  $\theta$  is the rotational orbifold symmetry while  $\alpha$  is a discrete shift. In analogy to the  $\mathbb{Z}_3$  case we find two ways to obtain a  $T^2/\mathbb{Z}_4$  orbifold. Either we just divide out  $\mathbb{Z}_{4,\text{orbi}}$ , then the two  $\mathbb{Z}_4$  fixed points are at  $z_1 = 0$  and one  $\mathbb{Z}_2$  fixed point is at  $z_2 = 0$ . Or we divide out the full  $\mathbb{Z}_{4,\text{orbi}} \times \mathbb{Z}_{2-\text{vol}}$ , then there is one  $\mathbb{Z}_4$  fixed point at  $z_1 = 0$  and  $z_2 = 0$  each, and the  $\mathbb{Z}_2$  fixed point lies at  $z_3 = 0$ .



### Two-torus $T_6^2$ with $\mathbb{Z}_6$ symmetry

For a torus with  $\mathbb{Z}_6$  symmetry we have to choose the elliptic curve  $\mathbb{P}_{1,2,3}^2[6]$  with defining equation,

$$z_1^6 + z_2^3 + z_3^2 = 0. \quad (3.34)$$

The symmetries are,

$$\begin{aligned} \theta_1 : z_1 &\longmapsto -\zeta^2 z_1, & z_{j \neq 1} &\longmapsto z_j, \\ \theta_2 : z_2 &\longmapsto \zeta z_2, & z_{j \neq 1} &\longmapsto z_j, \\ \theta_3 : z_3 &\longmapsto -z_3, & z_{j \neq 1} &\longmapsto z_j. \end{aligned} \quad (3.35)$$

As usual, we have  $\theta_1 \theta_2 \theta_3$  being an element of  $U(1)$ , thus we are effectively left with a  $\mathbb{Z}_{6,\text{orbi}}$  action generated by  $\theta = \theta_1$ . It has one fixed point at  $z_1 = 0$ . Furthermore,  $\theta^2$  has two additional fixed points at  $z_2 = 0$  which get identified by  $\theta$ , and  $\theta^3$  has three fixed points  $z_3 = 0$  which are also identified by  $\theta$ . To sum up, we find exactly the fixed point structure of the  $T^2/\mathbb{Z}_6$  orbifold.

Here the defining equation is almost in Weierstrass form with  $(f, g) = (0, 1)$  or  $\tau = \zeta$ , one just has to do some rescalings,

$$z_1 = v, \quad z_2 = -2^{2/3} \zeta x, \quad z_3 = y, \quad (3.36)$$

and identify  $\wp(u) = x/v^2$  and  $\wp'(u) = y/v^3$ . This immediately shows that the orbifold action indeed translates to  $\theta : u \mapsto -\zeta^2 u$ .

### Two-torus $T_2^2$ with $\mathbb{Z}_2$ symmetry

In principle every elliptic curve has a  $\mathbb{Z}_2$  symmetry, realized as  $y \mapsto -y$  in the Weierstrass equation. But we want to stick to the building principle we had used before, i.e. that each fixed point should have its own homogeneous coordinate and the degree of the polynomial should be equal to the order of the orbifold action. In that sense the  $T^2/\mathbb{Z}_2$  orbifold is special since it has four fixed points, thus with four homogeneous coordinates we will require two hypersurface equations. This ultimately leads to the elliptic curve  $\mathbb{P}_{1111}^3[2, 2]$  which we discuss in the following. The most general equation with only pure monomials are

$$\begin{aligned} a_1 z_1^2 + a_2 z_2^2 + a_3 z_3^2 + a_4 z_4^2 &= 0, \\ b_1 z_1^2 + b_2 z_2^2 + b_3 z_3^2 + b_4 z_4^2 &= 0. \end{aligned} \quad (3.37)$$

Note that if we had two generic second order equations, i.e. also including mixed monomials, we can always find a  $GL(4, \mathbb{C})$  transformation on the  $z_i$  such that all mixed monomials disappear. Therefore this choice is very convenient but not restrictive. In order to further eliminate the number of coefficients, we first do a Gauss elimination to set  $a_4$  and  $b_3$  to zero. Then we can rescale the four

### 3 GLSM description of Resolved Toroidal Orbifolds

coordinates and the two equations which sets just five of the coefficients to one, since simultaneous scaling of all coordinates and all equations with inverse scaling parameter leaves the equations invariant. Thus we are left with one parameter  $\kappa$  and the general equations become,

$$\begin{aligned} \kappa z_1^2 + z_2^2 + z_3^2 &= 0, \\ z_1^2 + z_2^2 + z_4^2 &= 0. \end{aligned} \quad (3.38)$$

This parameter represents the complex structure modulus  $\tau$  which is unfixed for  $\mathbb{Z}_2$  orbifolds. Let's first discuss the symmetries. As always we have symmetries of the form

$$\theta_i : z_i \longmapsto -z_i, \quad z_{j \neq i} \longmapsto z_j, \quad i = 1, 2, 3, 4, \quad (3.39)$$

where the combination  $\theta_1\theta_2\theta_3\theta_4$  acts trivially up to a  $U(1)$  rotation. Thus as generators for the remaining  $\mathbb{Z}_{2,\text{orbi}} \times \mathbb{Z}_{2-\text{vol}} \times \mathbb{Z}'_{2-\text{vol}}$  we choose  $\theta = \theta_1$ ,  $\alpha = \theta_2\theta_3$  and  $\alpha' = \theta_2\theta_4$ . A fixed point analysis reveals that  $\theta$  has four fixed points at  $z_1 = 0$ ,  $z_2 = \pm z_3$  and  $z_2 = \pm z_4$ , while  $\alpha$  and  $\alpha'$  are freely acting. In order to properly interpret these action we must establish a map to the classical torus, which turns out not to be as easy as for the previous cases since here we are dealing with the intersection of two hypersurfaces. Therefore we look at the following non-linear coordinate identifications

$$z_1^2 = (\epsilon_3 - \epsilon_1)v, \quad z_2^2 = \epsilon_1v - x, \quad z_3^2 = x - \epsilon_2v, \quad z_4^2 = x - \epsilon_3v. \quad (3.40)$$

These identifications fulfill the equations (3.38) precisely if  $\kappa = \frac{\epsilon_1 - \epsilon_2}{\epsilon_1 - \epsilon_3}$ . However,  $x$  and  $v$  are invariant under the actions of  $\theta_i$  and thus not sufficient as coordinates for the elliptic curve. Therefore we define

$$y = \frac{2}{\sqrt{\epsilon_1 - \epsilon_3}} z_1 z_2 z_3 z_4. \quad (3.41)$$

Then, if we also choose  $\epsilon_1 + \epsilon_2 + \epsilon_3 = 0$ , which is always possible, we find that  $(y, x, v)$  fulfill the equation,

$$y^2 = 4x^3v - fxv^3 - gv^4, \quad f = 4(\epsilon_1\epsilon_2 + \epsilon_1\epsilon_3 + \epsilon_2\epsilon_3), \quad g = -4\epsilon_1\epsilon_2\epsilon_3. \quad (3.42)$$

After the identification  $\wp(u) = x/v$ ,  $\wp'(u) = y/v^2$  this becomes the Weierstrass equation for a torus with unfixed complex structure. A closer look at the map  $(z_1, z_2, z_3, z_4) \mapsto (y, x, v)$  reveals that it is still not bijective, but rather the preimages of  $(y, x, v)$  form an orbit under  $\mathbb{Z}_{2-\text{vol}} \times \mathbb{Z}'_{2-\text{vol}}$ . Hence the map can be viewed as a holomorphic bijection of elliptic curves,

$$\frac{\mathbb{P}^3_{1111}[2, 2]}{\mathbb{Z}_{2-\text{vol}} \times \mathbb{Z}'_{2-\text{vol}}} \cong \mathbb{P}^2_{112}[4]. \quad (3.43)$$

### 3.2 Gauged Linear Sigma Models

Via the Weierstrass map of the  $\mathbb{P}_{112}^2[4]$  we find that the orbifold action  $\theta$  translates to the flat torus precisely to  $u \mapsto -u$ . In order to find out more about the discrete symmetries, we consider the maps  $\beta_i : u \mapsto u + e_i/2$ ,  $i = 1, 2$ . Via the identifications above we find them to be translated into

$$\begin{aligned}\beta_1 : (z_1, z_2, z_3, z_4) &\mapsto \left( \kappa^{-\frac{1}{4}} z_2, \kappa^{\frac{1}{4}} z_1, \kappa^{\frac{1}{4}} z_4, -\kappa^{-\frac{1}{4}} z_3 \right), \\ \beta_2 : (z_1, z_2, z_3, z_4) &\mapsto \left( i(\kappa^2 - \kappa)^{-\frac{1}{4}} z_3, (1 - \kappa^{-1})^{-\frac{1}{4}} z_4, i(\kappa^2 - \kappa)^{\frac{1}{4}} z_1, (1 - \kappa^{-1})^{\frac{1}{4}} z_2 \right).\end{aligned}\tag{3.44}$$

Details can be found in appendix A. One observes that  $\beta_1^2 = \alpha$  and  $\beta_2^2 = \alpha'$ , thus the involutions  $\alpha, \alpha'$  can be interpreted as discrete shifts  $u \mapsto u + e_{1/2}$  on a coarse torus with lattice vectors  $2e_1, 2e_2$ . Since this torus has the same complex structure, we can use the maps to identify its Klein invariant. In terms of the coefficients in the general equation (3.37) it is given by,

$$j(\tau) = 256 \frac{(c_2^2 + c_3^2 + c_4^2 - c_2 c_3 - c_2 c_4 - c_3 c_4)^3}{(c_2 - c_3)^2 (c_2 - c_4)^2 (c_3 - c_4)^2},\tag{3.45}$$

with

$$\begin{aligned}c_2 &= a_1 a_2 b_3 b_4 + b_1 b_2 a_3 a_4, & c_3 &= a_1 b_2 a_3 b_4 + b_1 a_2 b_3 a_4, \\ c_4 &= a_1 b_2 b_3 a_4 + b_1 a_2 a_3 b_4.\end{aligned}\tag{3.46}$$

This expression is nicely symmetric under the permutation of the four coordinates in the two equations, as well as under rescalings.

To sum up, there are four ways to realize a  $\mathbb{Z}_2$  orbifold out of this elliptic curve. One either divides out just  $\theta$ , then all four fixed points are at  $z_1 = 0$ , or one divides out the full  $\mathbb{Z}_{2,\text{orbi}} \times \mathbb{Z}_{2-\text{vol}} \times \mathbb{Z}'_{2-\text{vol}}$ , then there is one fixed point at each  $z_i = 0$ ,  $i = 1, 2, 3, 4$ , or one divides out just one of the involution, then one finds two fixed points at each of the vanishing loci of two coordinates.

## 3.2 Gauged Linear Sigma Models

Gauged Linear Sigma Models (GLSM) were first studied by Witten in [19]. They are two-dimensional SUSY theories that typically contain a  $U(1)^N$  gauge symmetry and some chiral fields which are charged. Such theories are not conformal since the gauge kinetic terms and the superpotential couplings are necessarily dimensionful. This is also why in CFTs one only has kinetic terms for chiral fields which thus in general have field dependent coefficients containing the information on the theory like background values of certain target space fields. Now GLSMs have the advantage that they are also able to describe this information but in a more tractable way. The kinetic terms remain field independent and the theory stays linear. We will see that the information about the target space topology is basically stored in the gaugings and in the charges of the chiral

### 3 GLSM description of Resolved Toroidal Orbifolds

fields. The values of (most of) the moduli fields are reflected by the values of the FI terms and the superpotential parameters.

Since GLSMs are not conformal, one could ask the question, what they have to do with string theory. The answer is that in the infrared limit, i.e. when one sends all dimensionful parameters to infinity simultaneously, the theory flows to a conformal theory. In this limit only the massless degrees of freedom survive. When integrating out the massive fields and after fixing the gauge, one generates non-linear kinetic terms for the massless ones, thus resulting in a typical conformal non-linear sigma model (NLSM), i.e. a suitable world sheet theory. However, one has to make sure that the parameters of the theory remain constant in this limit.

Whereas in heterotic theories the gauged SUSY stays  $N = (1, 0)$ , one increases the amount of global SUSY to  $N = (2, 0)$  in order to describe a complex geometry. For further simplification one can go to global  $N = (2, 2)$ , then one automatically describes the standard embedding. In the following we will introduce these two formalisms and discuss their properties.

#### 3.2.1 (2,2) SUSY in two dimensions

Probably the easiest way to think of  $N = (2, 2)$  in two dimensions is to take the well known  $N = 1$  SUSY formalism in four dimensions and dimensionally reduce it. For this we take the superspace coordinates  $x^\mu$ ,  $\vartheta^\pm$  and  $\bar{\vartheta}^\pm$ , and drop the dependence of the superfields of two spatial coordinates. One can think of it as compactifying on a torus and shrinking it to zero size. Then many representations of the  $N = (2, 2)$  superalgebra in two dimensions can be deduced from the respective  $N = 1$  in  $d = 4$  representations. Note that the internal parts of the Poincaré algebra become central charge and R-symmetry generators. The most common massless representations are

- The chiral multiplet  $\Psi = \phi + \vartheta^+ \psi^- + \vartheta^- \psi^+ + \vartheta \vartheta F$  with a complex scalar  $\phi$ , a non-chiral pair of complex fermions  $\psi^\pm$  and a complex auxiliary scalar  $F$ .
- The vector multiplet, here in WZ gauge,  $V = \vartheta^+ \bar{\vartheta}^+ a_+ + \vartheta^- \bar{\vartheta}^- a_- + \vartheta^- \bar{\vartheta}^+ \sigma + \vartheta^+ \bar{\vartheta}^- \bar{\sigma} + \text{gauginos} + \vartheta \vartheta \bar{\vartheta} \bar{\vartheta} D$ . The  $4d$  vector boson is decomposed into left- and right-moving  $d = 2$  components  $a_\pm$ , while the two internal components build up a complex scalar  $\sigma$ . The auxiliary scalar  $D$  plays the same role as in  $d = 4$ .
- The twisted chiral multiplet is a new feature in  $d = 2$ , i.e. it has no counterpart in  $d = 4$   $N = 1$ . It fulfills a twisted chirality constraint  $\bar{D}_+ \mathcal{F} = D_- \mathcal{F} = 0$ . In this context they are not discussed as independent fields but appear as superfield strength of the vector multiplet, which for Abelian gauge symmetries reads  $\mathcal{F} = \bar{D}_+ D_- V$ .

We will be interested in theories with a gauge group  $U(1)^N$  so we label the vector multiplets by  $V^I$  with  $I = 1, \dots, N$ . Furthermore,  $N = (2, 2)$  SUSY contains a global  $U(1)_L \times U(1)_R$   $R$ -symmetry under which the superspace coordinates  $\vartheta^\pm$  are charged. They are chosen such that  $\theta^+$  is only charged under  $U(1)_R$  and  $\theta^-$  under  $U(1)_L$ . These symmetries can be used to enforce a superpotential with finitely many terms which will turn out to be very useful.

### Action

Since our aim is to take the IR limit at the end, it is sufficient to consider only relevant and marginal terms for the action. Irrelevant terms, i.e. terms of negative mass dimension, will go to zero in this limit. However, since chiral superfields are of mass dimension zero in two dimensions, one can in principle have polynomials of arbitrary high order as coefficients of all the terms, as long as they are allowed by the symmetries. So in order not to have an infinite number of parameters, we have to make some restrictions. First of all, we set the coefficients of all kinetic terms to one. This way we might lose some information concerning e.g. the target space metric, but we will see that most of the moduli can be recovered in another fashion so we are still able to explore vast regions of the moduli space.

One important piece of the action comes from the superpotential,

$$\mathcal{L}_{\text{super}} = m \int d\vartheta^+ d\vartheta^- \mathcal{W}(\Psi_i) + \text{h.c.}, \quad (3.47)$$

where  $\mathcal{W}$  is a holomorphic polynomial in the superfields  $\Psi_i$ , and  $m$  is a parameter of mass dimension one. The superpotential must be charged under  $U(1)_L \times U(1)_R$  with charge  $(1, 1)$ . It gives rise to the  $F$ -terms in the scalar potential and fermionic bilinears,

$$\mathcal{L}_{\text{super}} = m \left( \sum_i F_i \frac{\partial \mathcal{W}}{\partial \Psi_i} + \frac{\partial^2 \mathcal{W}}{\partial \Psi_i \partial \Psi_j} \psi_i^+ \psi_j^- \right) + \text{h.c.} \quad (3.48)$$

Another important piece of the action is the the twisted superpotential containing the super field strength,

$$\mathcal{L}_{\text{twisted}} = \int d\vartheta^+ d\bar{\vartheta}^- \rho^I \mathcal{F}^I + \text{h.c.} \quad (3.49)$$

Here a priori  $\rho^I$  are neutral holomorphic functions of the chiral superfields. In compact Calabi–Yau compactification it turns out that these can only be constant,  $\rho = a + i\theta$ . In section 3.2.2 we show what happens when these terms become field dependent in  $(2, 0)$  models. When one integrates over the Grassmann coordinates, one finds that this term contains the  $D$ -term and the field

### 3 GLSM description of Resolved Toroidal Orbifolds

strength  $f$ , more precisely its  $(0, 1)$  component which makes it a topological term.

$$\mathcal{L}_{\text{twist}} = a^I D^I + \theta^I f^I. \quad (3.50)$$

After integrating out the auxiliary fields  $F_i$  and  $D^I$ , the relevant parts of the scalar potential are

$$V_{\text{scalar}} = \sum_I e_I^2 (D^I)^2 + m^2 \sum_i |F_i|^2, \quad (3.51)$$

where  $e_I$  is the dimensionful gauge coupling,  $D^I = \sum_i q_i^I |\phi_i|^2 - a^I$  and  $F_i^* = \partial\mathcal{W}/\partial\Phi_i$ .

The infrared limit can also be interpreted as sending  $e_I$  and  $m$  to infinity. In this limit we have to make sure that the parameters of the theory, i.e. the FI parameter  $\rho^I$  and the coefficients in  $\mathcal{W}$  do not renormalize. For the superpotential this follows from the non renormalization theorem. In case of the FI term, one can easily see that this imposes the tadpole cancellation condition

$$\sum_i q_i^I = 0, \quad \forall I. \quad (3.52)$$

#### Ground State Geometry

We want to discuss models which allow for a ground state with preserved SUSY and a non trivial compact (possibly singular) vacuum manifold. This will, in the conformal limit, lead to the interpretation of a string theory compactification. To ensure this, some constraints on the model have to be imposed.

In typical CY GLSM constructions one chooses a certain set of chiral superfields to have charge  $(1, 1)$  under  $U(1)_R \times U(1)_L$  and the rest to be neutral. In the following the former will be denoted by  $\mathcal{C}_a$  and the latter by  $\mathcal{Z}_i$ , with scalar components  $c_a$  and  $z_i$ , respectively. Furthermore, the charges are chosen such that there exists a basis of  $U(1)$ 's in which the charges of the  $\mathcal{Z}_i$  are positive and those of the  $\mathcal{C}_a$  are negative. This will ensure that the target space geometry stays compact. Furthermore, we choose the number of  $\mathcal{Z}_i$  to be greater than the number of  $\mathcal{C}_a$  plus the number of  $U(1)$  gaugings. Then the most general superpotential is of the form

$$\mathcal{W} = \sum_a \mathcal{C}_a \cdot P_a(\mathcal{Z}_i), \quad (3.53)$$

where  $P_a$  are polynomials with finitely many terms. The  $D$ -term equations can then be written as

$$\sum_i q_i^I |z_i|^2 + \sum_a q_a^I |c_a|^2 = a^I. \quad (3.54)$$

When all  $a^I$  are greater than zero, this will describe the geometric regime. Then, the  $D$ -term (3.54) together with the gauge fixing of the  $U(1)^N$  describes a symplectic quotient. Thus, without the  $F_{\mathcal{C}_a}$ -terms, the target space geometry is a toric variety. Now we also have to take the  $F_{\mathcal{C}_a}$  into account. Since these are holomorphic polynomials in the coordinate fields  $z_i$ ,  $F_{\mathcal{C}_a}^* = P_a(z_i)$ , their zero locus is a complete intersection in this ambient toric variety.

### 3.2.2 (2,0) SUSY in two dimensions

In true heterotic constructions, the left- and right-movers have different field content. Whereas the right-moving fermions transform in the tangent bundle of the compactification space, the left-movers live in the vector bundle that describes a non-trivial gauge background. In (2,2) SUSY theories, in which these two are equal, we can thus only have heterotic models with standard gauge embedding. To describe more general gauge backgrounds, we need to lower the amount of SUSY to (2,0).

The (2,0) multiplets in two dimensions can best be understood by reduction of the (2,2) superspace by dropping the  $\theta^+, \bar{\theta}^+$  coordinates. This way we can observe how the (2,2) multiplets decompose.

The chiral (2,2) multiplet decomposes into a (2,0) chiral multiplet and a chiral-fermi multiplet,  $\Psi_{(2,2)} = \Psi_{(2,0)} + \theta^+ \Lambda$ . Concerning the degrees of freedom, in (2,0) theories one has to count left- and right-moving dof's separately. This is because the chirality of the fermions is in one to one correspondence to their on-shell direction. Bosonic dofs, on the other hand, can always move in both directions. Furthermore, since the SUSY only transforms the right-movers, it follows that only for them the on-shell fermionic and bosonic dofs have to match. The (2,0) chiral multiplet has one scalar and one right-moving Weyl fermion,  $\Psi = z + \theta^- \psi_-$ . The chiral fermi multiplet contains a left-moving fermion and the auxiliary scalar,  $\Lambda = \psi_+ + \theta^- F$ . Note that off-shell, one cannot distinguish between left- and right-moving dof's anymore, however, still the amount of bosonic and fermionic dofs agree.

Similarly, the (2,2) vector multiplet decomposes into a (2,0) vector (or gauge) multiplet  $(V, A)$  and a fermi-gauge multiplet  $\Sigma$ ,

$$V_{(2,2)} = A + \theta^+ \Sigma + \bar{\theta}^+ \bar{\Sigma} + \theta^+ \bar{\theta}^+ V_{(2,0)}. \quad (3.55)$$

Note that the bosonic gauge multiplets always come in pairs  $(V, A)$ , where  $V$  and  $A$  do not mix under SUSY transformations, however they transform under the same (super) gauge transformations and thus need to appear together. In detail, the gauge superfields transform with a chiral superfield, whereas the fermi gauge multiplet transforms with a fermionic gauge transformation whose gauge parameter is a chiral fermi field. In Wess-Zumino gauge, the superfield

### 3 GLSM description of Resolved Toroidal Orbifolds

type	dimension	notation	R-charge	gauge charge	$\delta_{\Xi_i}$	scalar comp.
chiral	0	$\Psi_a$	0	$q_a^I$	-	$z_a$
		$\Phi_m$	1	$q_m^I$	-	$c_m$
chiral fermi	$\frac{1}{2}$	$\Lambda_\alpha$	0	$Q_\alpha^I$	$M_\alpha^i(\Psi_a)$	-
		$\Gamma_\mu$	1	$q_\mu^I$	$M_{\mu,m}^i(\Psi_a)\Phi_m$	-

Table 3.2: The  $(2, 0)$  chiral and chiral fermi superfield notation and their transformation properties.  $\delta_{\Xi_i}$  denotes the variation under fermionic gauge transformations.

expansions are

$$A = \theta^- \bar{\theta}^- a_- , \quad (3.56a)$$

$$V = a_+ + \theta^- \bar{\lambda}_+ + \bar{\theta}^- \lambda_+ + \theta^- \bar{\theta}^- D , \quad (3.56b)$$

$$\Sigma = \bar{\theta}^- \sigma + \theta^- \bar{\theta}^- \lambda_- . \quad (3.56c)$$

The degrees of freedom that are carried by these multiplets are all massive at generic points in moduli space and thus become irrelevant in the infrared limit. Instead they rather serve to introduce gauge symmetries, where here one must distinguish between bosonic and fermionic gaugings. The bosonic gaugings act in the usual way on both chiral superfields, whereas fermionic gaugings only act on chiral fermi fields,

$$\Psi_a \longmapsto e^{iq_a^I \Theta^I} \Psi_a , \quad \Lambda_\alpha \longmapsto e^{iQ_\alpha^I \Theta^I} (\Lambda_\alpha + M_\alpha^i(\Psi_a) \Xi^i) , \quad (3.57)$$

Here  $\Theta^I$  and  $\Xi^a$  are the bosonic and fermionic gauge parameter, respectively, and  $M_\alpha^i(\Psi_i)$  is a holomorphic function of the chiral superfields with charge  $Q_\alpha^I$ .

Furthermore, we assign right-moving R-charges to the various fields. For a geometric interpretation it is useful to assign R-charges zero and one to the fields, and in the following we will distinguish them in the notation, see table 3.2. Furthermore, for a compact target space, we will require the existence of a  $U(1)^N$  basis such that all  $q_a^I > 0$  and all  $Q_\mu^I < 0$ , similarly to the  $(2, 2)$  case.

#### Action

We analyze the action and the resulting target space geometry and gauge bundle. Most of the time we will work in the geometric regime where the FI parameters are positive and the  $c_m$  have zero vev. This is a rather non-trivial requirement and has to be checked for each model to be possible. The most generic superpotential is

$$\mathcal{W}_{(2,0)} = m [\Gamma_\mu P^\mu(\Psi_a) + \Lambda_\alpha \Phi_m N^{\alpha,m}(\Psi_a)] , \quad (3.58)$$



where  $P_\mu$  and  $N^{\alpha,m}$  are holomorphic polynomials of charge  $-Q_\mu$  and  $-q_m - Q_\alpha$ , respectively, and  $m$  is the mass dimension one prefactor. This superpotential must be invariant under fermionic gauge transformations, leading to the requirements

$$M_{\mu,m}^i(\Psi_a)P^\mu(\Psi_a) + M_\alpha^i(\Psi_a)N^{\alpha,m}(\Psi_a) = 0, \quad \forall m, i. \quad (3.59)$$

In  $(2,0)$  theories the chiral fermi multiplets carry the auxiliary fields  $F$ , thus for each of them we get a holomorphic equation that must be fulfilled for a SUSY vacuum. In the geometric regime, the terms  $F_\alpha^* = c_m N^{\alpha,m}(z_a)$  are automatically zero, thus we are left with the geometric  $F$ -terms  $F_\mu^* = P^\mu(z_a)$ . Thus, the ground state geometry is a complete intersection of the hypersurfaces  $P^\mu = 0$  in an ambient toric variety defined by the coordinates  $z_i$  and the  $U(1)$  gaugings. The Calabi–Yau condition now reads

$$\sum_a q_a^I + \sum_\mu Q_\mu^I = 0. \quad (3.60)$$

To identify the gauge bundle, we have to analyze the massless left-moving fermions in the chiral fermi multiplets. The fermion components of the  $\Gamma^\mu$  get a mass term from the superpotential and thus are removed in the conformal limit. Thus we have to check which of the fermions in  $\Lambda^\alpha$  remain massless. For a mass term they have to pair up with right-moving fermions which are contained in the chiral and fermi-gauge multiplets. From the superpotential (3.58) we see that in the geometrical phase we only get non-vanishing fermionic bilinears with the fields  $\Phi_m$  but not with  $\Psi_a$ . Furthermore, from the fermi gauge covariant kinetic terms we get fermionic bilinears with coefficients <sup>2</sup>  $M_\alpha^i(\Psi_a)$ . In other words, the massless left-moving fermions can be thought of as the cohomology of the monad complex,

$$0 \longrightarrow \mathcal{O}^{\oplus \#\text{ferm.gaug.}} \xrightarrow{M_\alpha^i} \bigoplus_\alpha \mathcal{O}(Q_\alpha) \xrightarrow{N_m^\alpha} \bigoplus_m \mathcal{O}(-q_m) \longrightarrow 0. \quad (3.61)$$

Then, the coefficients in the polynomials  $M_\alpha^i$  and  $N_m^\alpha$  represent the gauge bundle moduli. Accordingly, properties of the gauge bundle such as characteristic classes and cohomology groups can be deduced from this definition. We also find that there is a separation in the roles of the fields. The fields  $\Psi$  and  $\Gamma$ , combined with the bosonic gaugings, are responsible for the target space geometry and its tangent bundle, whereas the fields  $\Lambda$  and  $\Phi$ , together with the fermionic gaugings, build up the vector bundle over the geometry.

### Anomaly Cancellation

Since  $(2,0)$  theories are chiral, one has to deal with gauge anomalies that can render the theory inconsistent. More precisely, when we define the effective

---

<sup>2</sup>Alternatively one can think of these fermionic dofs being gauged away.

### 3 GLSM description of Resolved Toroidal Orbifolds

action of the gauge fields as

$$e^{iS_{\text{eff}}} = \int \mathcal{D}\mathcal{X} e^{iS_{\text{cl}}}, \quad (3.62)$$

where  $\mathcal{X}$  represents all chiral fields in the theory, the gauge anomalies can be written as

$$\delta_{\Theta^I} S_{\text{eff}} = 2\pi i \int \omega_2(\Theta). \quad (3.63)$$

The two-form  $\omega_2$  is most elegantly represented by the anomaly polynomial  $\omega_4$  via the descent equations

$$\delta_{\Theta^I} \omega_3 = d\omega_2, \quad \omega_4 = d\omega_3. \quad (3.64)$$

In  $(2, 0)$  GLSMs, only the fermions are chiral, and the left- and right-moving fermions contribute to the anomaly with different sign. Thus we find

$$\omega_4 = \frac{1}{2} \mathcal{A}_{IJ} \frac{f^I}{2\pi} \wedge \frac{f^J}{2\pi}, \quad \mathcal{A}_{IJ} = q_I \cdot q_J - Q_I \cdot Q_J. \quad (3.65)$$

Here  $f^I$  are the worldsheet gauge field strengths and the dots denote summations over all chiral or chiral fermi fields, respectively.

The worldsheet gauge anomalies are directly related to the anomalies in the low energy effective target space theory. To establish this link, one finds that the worldsheet  $U(1)$  gaugings correspond to divisors or cohomology classes of  $(1, 1)$  forms  $D_I$ . More precisely, one finds that the world sheet gauge field strength  $f^I$  is the pullback of a representative of such a  $(1, 1)$  form, i.e.  $f^I = \Psi^*(D_I)$ . We rewrite the anomaly as

$$\omega_4 \propto \Psi^* \left( \begin{array}{cc} (q_a^I q_a^J - Q_\mu^I Q_\mu^J) D^I D^J & - (Q_\alpha^I Q_\alpha^J - q_m^I q_m^J) D^I D^J \\ \text{tr } \mathcal{R}^2 & - \text{tr } \mathcal{F}^2 \end{array} \right), \quad (3.66)$$

with the target space curvature  $\mathcal{R}$  and the gauge flux  $\mathcal{F}$ . Thus, when the worldsheet theory is free of gauge anomalies, then on the target space the Bianchi identity of the Kalb–Ramond field strength is fulfilled. However, for  $N$  gaugings, the WS anomaly freedom imposes  $N(N+1)/2$  conditions on the charges, while on the target space we integrate the Bianchi identity as a  $(2, 2)$  form giving  $N$  conditions when integrated over the  $N$  divisors. In that sense the GLSM conditions are more stringent. But the  $N$  integrated Bianchi identities change when e.g. going through a flop transition, thus a bundle that seems to be consistent in one phase might become inconsistent in another one. Anomaly freedom, as a WS consistency condition, ensures a consistent bundle in all phases even in singular and non-geometrical ones.

### 3.2 Gauged Linear Sigma Models

If one has a theory with  $\mathcal{A}_{IJ} \neq 0$ , there can still be the chance to cancel the WS anomalies by a Green–Schwarz like mechanism. For a more detailed discussion, see [42, 43]. For this consider a field dependent FI term in a  $(2, 0)$  model which is,

$$\mathcal{L}_{\text{FI}} = \int d\theta^- \rho_I(\Psi_a) \mathcal{F}^I + \text{h.c.} = \text{Re}(\rho_I) D^I + \text{Im}(\rho_I) f^I, \quad (3.67)$$

with super gauge field strength  $\mathcal{F}^I$ . Thus, if  $\rho_I$  transforms with a shift under gauge transformations,

$$\rho_I(\Psi_a) \longmapsto \rho_I(\Psi_a) + iT_{IJ} \alpha^J, \quad (3.68)$$

$\alpha^J = \text{Im}\Theta^J|_{\theta=0}$  being the non-super gauge parameter, we get a contribution to the variation of the effective action. Although the anomaly coefficients  $\mathcal{A}_{IJ}$  are symmetric, for the  $T_{IJ}$  this need not be the case. Instead, their lack of symmetry can be repaired by the so-called  $V$ - $A$  couplings,

$$\mathcal{L}_{VA} = \int d^2\theta^- c_{IJ} V^I A^J, \quad (3.69)$$

with antisymmetric coefficients  $c_{IJ} = -c_{JI}$ . Their variation is  $\delta_\alpha S_{VA} = c_{IJ} \int f_2^I \alpha^J$ , thus when we choose  $c_{IJ} = (T_{IJ} - T_{JI})/2$ , the variation of  $S_{FI} + S_{VA}$  becomes symmetric. Then the total anomaly cancellation condition reads ,

$$\mathcal{A}_{IJ} + c_{JI} + T_{IJ} = 0. \quad (3.70)$$

In order to realize a shift transformation of the FI terms one can either introduce new axionic superfields as was done in [48]. One can also take (linear combinations of) logarithms of a homogeneous polynomial of the linearly transforming chiral fields that one already has,

$$\rho_I(\Psi_a) = t_{IX} \log(R^X(\Psi_a)), \quad T_{IJ} = t_{IX} q_J(R^X). \quad (3.71)$$

The coefficients  $t_{IX}$  are subject to quantization conditions which come from gauge instantons on the worldsheet. More precisely, an instanton leads to a flux quantization condition of the form  $q_a^I \int f_2^I \in 2\pi\mathbb{Z}$ , thus for the partition function to be invariant under the shift of the logarithm  $\log \mapsto \log + 2\pi i$ , we roughly find that the charges  $t_{IX} q_J(R^X)$  (here without sum over  $X$ ) must be quantized like multiples of the gauge charges. In order to find the precise quantization conditions one must study the allowed instanton configurations which is very model dependent.

We interpret these results on the target space. The coefficients in the complexified Kähler form now become position-dependent,

$$\mathcal{J} + iB_2 = \sum_I \rho_I(z_a) D_I = \sum_I (b_I(z_a) + i\beta_I(z_a)) D_I, \quad (3.72)$$

### 3 GLSM description of Resolved Toroidal Orbifolds

which implies that the Kähler form is no longer closed. At the same time we get a topologically non trivial  $H_3$  background, i.e. the manifold is equipped with a torsional connection. To illustrate what happens, we assume for simplicity  $\rho = \rho_0 + \log(\Psi_1)$ . Then the Kalb–Ramond field becomes  $B_2 = \log(z_1/\bar{z}_1)D$  and we find

$$dB_2 = \left( \frac{1}{z_1} dz_1 - \frac{1}{\bar{z}_1} d\bar{z}_1 \right) D, \quad ddB_2 \propto \delta(z_1) dz_1 \wedge d\bar{z}_1 \cdot D. \quad (3.73)$$

The physical interpretation of this is that the Kalb–Ramond field is magnetically sourced by an object that is localized on the intersection of  $D$  with  $z_1 = 0$ . In non-perturbative heterotic M-theory such objects in fact exist and are called NS5 branes<sup>3</sup>. Furthermore, the presence of NS5 branes modifies the Bianchi identity of the  $H_3$  field. Starting from its definition

$$H_3 = dB_2 + \omega_3^{\text{CS,L}} - \omega_3^{\text{CS,YM}}, \quad (3.74)$$

we look at the class of  $dH_3$ ,

$$0 = [dH_3] = [ \text{NS5 branes} ] + [\text{tr } \mathcal{R}^2] - [\text{tr } \mathcal{F}^2], \quad (3.75)$$

This is reproduced by the anomaly cancellation condition (3.70) when multiplying it by the comology classes  $D^I D^J$ . The term  $\mathcal{A}_{IJ}$  encodes as usual the Chern characters of the tangent- and vector bundle, see (3.66), the  $c_{IJ}$  term vanishes due to symmetry, and the  $T_{IJ}$  term encodes the homology class of the NS5 branes.

To see the implications on the geometry, we take a look at the  $D$  terms. Due to SUSY they get a contribution from the log term of the form,

$$\sum_a q_a^I |z_a|^2 = b_I + \sum_X t_{IX} \log(|R^X(z_a)|). \quad (3.76)$$

This shows that the geometry gets deformed as one approaches the NS5 brane locus  $R^X = 0$  which can be interpreted as geometric backreaction. Furthermore, this locus is removed from the target space, as the log approaches infinity, which hints on the non-perturbative nature of the NS5, brane, i.e. it cannot properly be described by a perturbative WS theory.

## 3.3 (2,2) Models of Resolved Toroidal Orbifolds

Now we have all ingredients to construct the resolutions of toroidal orbifolds. For this, we first have to take a look at what orbifolds are possible to realize. Since most six-tori are not realizable as a complete intersection in a toric variety,

---

<sup>3</sup>Sometimes they are also called M5 branes or H5 branes.

### 3.3 (2,2) Models of Resolved Toroidal Orbifolds

Point group	twist vector(s)	$T^6$ torus lattice	exc. coord.	Invisible moduli		Indistinguishable fixed points/tori
				$h_{\text{off-diag}}^{1,1}$	$h_{\text{twisted}}^{1,2}$	
$\mathbb{Z}_3$	$\frac{1}{3}(1, 1, -2)$	$A_2^3$	27	6	0	0
$\mathbb{Z}_4$	$\frac{1}{4}(1, 1, -2)$	$D_2^2 \times A_1^2$	23	2	6	$1 \times 2 \text{ T}$
		$D_2 \times A_1 \times A_3$	12	2	2	$8 \times 2 \text{ P}$
		$A_3^2$	8	2	0	$4 \times 4 \text{ P}$
$\mathbb{Z}_{6\text{-I}}$	$\frac{1}{6}(1, 1, -2)$	$G_2^2 \times A_2$	17	2	5	$1 \times 3 \text{ T}, 1 \times 2 \text{ P}$
$\mathbb{Z}_{6\text{-II}}$	$\frac{1}{6}(1, 2, -3)$	$G_2 \times A_2 \times A_1^2$	32	0	10	0
$\mathbb{Z}_2 \times \mathbb{Z}_2$	$\frac{1}{2}(1, -1, 0),$ $\frac{1}{2}(0, 1, -1)$	$A_1^6$	48	0	0	0
$\mathbb{Z}_2 \times \mathbb{Z}_4$	$\frac{1}{2}(0, 1, -1),$ $\frac{1}{4}(1, -1, 0)$	$D_2^2 \times A_1^2$	57	0	0	$1 \times 2 \text{ T}$
$\mathbb{Z}_2 \times \mathbb{Z}_{6\text{-I}}$	$\frac{1}{2}(0, 1, -1),$ $\frac{1}{6}(1, 1, -2)$	$G_2^3$	26	0	0	$3 \times 3 \text{ T}, 1 \times 2 \text{ P}$
$\mathbb{Z}_2 \times \mathbb{Z}_{6\text{-II}}$	$\frac{1}{6}(1, -1, 0),$ $\frac{1}{2}(0, 1, -1)$	$G_2^2 \times A_2$	46	0	2	$1 \times 3 \text{ T}$
$\mathbb{Z}_3 \times \mathbb{Z}_3$	$\frac{1}{3}(1, -1, 0),$ $\frac{1}{3}(0, 1, -1)$	$A_2^3$	81	0	0	0
$\mathbb{Z}_3 \times \mathbb{Z}_6$	$\frac{1}{3}(0, 1, -1),$ $\frac{1}{6}(1, -1, 0)$	$G_2^2 \times A_2$	65	0	1	$2 \times 2 \text{ T}, 3 \times 2 \text{ P}$
$\mathbb{Z}_4 \times \mathbb{Z}_4$	$\frac{1}{4}(1, -1, 0),$ $\frac{1}{4}(0, 1, -1)$	$D_2^3$	87	0	0	0
$\mathbb{Z}_6 \times \mathbb{Z}_6$	$\frac{1}{6}(1, -1, 0),$ $\frac{1}{6}(0, 1, -1)$	$G_2^3$	80	0	0	$1 \times 2 \text{ P}$

Table 3.3: This Table shows toroidal orbifolds for which we can construct fully resolvable GLSMs. It shows all maximal, factorized models plus two non-factorizable  $\mathbb{Z}_4$  models. The column labeled “exc. coord.” indicates the number of exceptional coordinates (which come with the same number of gaugings and FI-parameters). The two columns labeled “invisible moduli” indicate the amount of geometric moduli which are not explicitly visible in the GLSM formulation: off-diagonal untwisted Kähler moduli and twisted complex structure moduli. The final column gives the number of indistinguishable fixed points (P) and fixed tori (T) in these construction.

we have to focus on those which we can realize, namely products of two-tori. Therefore we can a priori only obtain factorizable orbifolds, i.e. those for which the lattice factorizes into three orthogonal two-dimensional lattices, each of which lives in one of the complex planes on which the point group acts diagonally. For

### 3 GLSM description of Resolved Toroidal Orbifolds

such orbifolds the order of the point group as it acts in each two-torus is restricted to be 2, 3, 4 or 6, corresponding to the four elliptic curves we constructed in 3.1.2. More concretely, if all point group elements are of the form

$$P \ni \theta : (z_1, z_2, z_3) \longmapsto \left( e^{2\pi i m_\theta^1 / N_1} z_1, e^{2\pi i m_\theta^2 / N_2} z_2, e^{2\pi i m_\theta^3 / N_3} z_3 \right), \quad (3.77)$$

with minimal choices for the orders  $N_i$ , then as a starting point we choose the six torus  $T_{N_1}^2 \times T_{N_2}^2 \times T_{N_3}^2$  with coordinates  $z_{ai}$  where  $a = 1, 2, 3$  and  $i = 1, 2, 3$  if  $N_a \neq 2$  and  $i = 1, 2, 3, 4$  if  $N_a = 2$ . Then we say that the point group acts on the  $a^{\text{th}}$  torus in  $N_a^{\text{th}}$  order. In  $(2, 2)$  models these coordinates are promoted to chiral superfields which we denote by  $\mathcal{Z}_{a\rho}$ . In general we will use calligraphic capital letters for superfields and normal minuscules for their scalar component. In this convention we denote a certain fixed point by  $(i, j, k)$  corresponding to  $z_{1i} = z_{2j} = z_{3k} = 0$ . For fixed planes there will be one index less. For each torus we require one gauging, denoted by  $U(1)_{R_a}$  and with FI parameter  $a_a$ , and one (or two) superfields for the hypersurface constraints, called  $\mathcal{C}_a$  ( and  $\mathcal{C}'_a$  ). In  $(2, 0)$  models these fields will be chiral fermi fields since they induce the holomorphic hypersurface constraints.

By construction these six tori have many symmetries which appear as phase rotations of the fields. Besides the  $n$ -volution group, which comprises the  $n$ -volutions of each two-torus, there is a potential point group  $\mathbb{Z}_{N_1} \times \mathbb{Z}_{N_2} \times \mathbb{Z}_{N_3}$ . However, it is always a subgroup of this group which preserves the Calabi–Yau condition and thus is suitable for supersymmetric string model building. A summary of all realizable point groups and their factorizable geometries is shown in table 3.3.

Now, in order to generate these discrete symmetries we have to add exceptional fields  $\mathcal{X}_r$  together with exceptional gaugings  $U(1)_{E_r}$  and associated FI parameters  $b_r$ , such that for  $x_r \neq 0$  the  $U(1)$  gets broken and the discrete symmetries are recovered and modded out. This is quite analogous to the local resolution. The index  $r$  will encode the information on the point group element which is generated and the localization of the respective fixed point/plane in the torus. It will typically look like  $k, \alpha\beta\gamma$  where  $k$  labels the twisted sector corresponding to the point group element, and  $\alpha\beta\gamma$  are the information which of the  $z_{1\alpha}$ ,  $z_{2\beta}$  and  $z_{3\gamma}$  fields are charged under the  $U(1)$ .

For example, for a  $T^6/\mathbb{Z}_4$  orbifold we need exceptional coordinates for the  $\theta$  and  $\theta^2$  sector. Thus for the  $\theta$  sector we can introduce exceptional coordinates  $x_{1,\alpha\beta\gamma}$  with  $\alpha, \beta = 1, 2$  and  $\gamma = 1, 2, 3, 4$ . The  $\theta^2$  sector leaves the third torus invariant, thus we can have exceptional coordinates  $x_{2,\alpha\beta}$  with  $\alpha, \beta = 1, 2, 3$ . A detailed discussion of the  $T^6/\mathbb{Z}_4$  models is found in section 3.3.3.

One already sees that we have a huge playground to create models which will differ in the amount of exceptional gaugings. In the classification of such models the crucial point are the  $n$ -volutions. They either remain symmetries of the theory, i.e. they describe how different fixed points behave in the same way,

### 3.3 (2,2) Models of Resolved Toroidal Orbifolds

or they are modded out, then the fixed points might have different properties. However, it might happen that via the  $n$ -volutions some fixed points are created which do not stem from one exceptional gauging and thus have no exceptional coordinate. These fixed points can therefore not be resolved within these models, however, one can always add the required coordinates to make the model fully resolvable. So for a complete classification, one would distinguish the models in the choice of fixed points which can be resolved and which not. If in a model all fixed points can be resolved, we will call it “fully resolvable”.

In general we will always have the minimal models, in which none of the  $n$ -volutions is modded out. They have a minimal field content in order to describe a smooth geometry but also treat all fixed points in the same way. Thus they are the best choice to construct models without Wilson lines. Then, there are the maximal, fully resolvable models, which have maximal field content and where almost<sup>4</sup> all fixed points and tori have their own exceptional gauging. But the generality comes at the cost of complexity which makes computations e.g. of cohomologies more involved. Then, there are models in between, which can be useful for models in which a Wilson line is not switched on. Then the remaining  $n$ -volution symmetry appears as part of a potential family symmetry.

#### 3.3.1 Example: Resolution of $T^6/\mathbb{Z}_3$

The easiest and best studied orbifold is the  $\mathbb{Z}_3$  orbifold [14–16] so we will use it to demonstrate the construction of toroidal orbifold resolutions. This example will already be useful to demonstrate many properties of the toroidal orbifold resolution GLSM constructions. We will show how the geometries emerge from the choices of coordinates for the minimal and maximal model. We also will discuss models in between and find that some non-factorizable lattices can be generated. We will study the intersection ring of the model in the smooth phase, and finally we will explore the moduli space of certain simple models.

As a warm up we present the GLSM for a local  $\mathbb{C}^3/\mathbb{Z}_3$  singularity resolution. The point group acts on the coordinates as

$$\theta : (u_1, u_2, u_3) \longmapsto (\zeta u_1, \zeta u_2, \zeta u_3), \quad \zeta = e^{2\pi i/3}. \quad (3.78)$$

In order to resolve the singularity we add one exceptional gauging and coordinate corresponding to the  $\theta^1$  sector, and get the charge assignment,

$$\begin{array}{c|c|c|c|c} \text{superfield} & \mathcal{U}_1 & \mathcal{U}_2 & \mathcal{U}_3 & \mathcal{X} \\ \hline U(1)_E & 1 & 1 & 1 & -3 \end{array},$$

---

<sup>4</sup>For  $\mathbb{Z}_4$  and  $\mathbb{Z}_6$  orbifolds it occurs that some fixed points or fixed tori are always indistinguishable, i.e. they are always described by the zero set of the same coordinates. This will be elaborated further in section 3.3.3.

### 3 GLSM description of Resolved Toroidal Orbifolds

which leads to the  $D$ -term

$$|u_1|^2 + |u_2|^2 + |u_3|^2 - 3|x|^2 = b. \quad (3.79)$$

The phase structure is simple since there is just one FI parameter. For  $b < 0$ , we find that  $x \neq 0$  which induces the  $\theta$  action on the coordinates  $u_a$  with fixed point  $(0, 0, 0)$ . For  $b > 0$ , this fixed point is removed and replaced by the exceptional divisor  $E = \{x = 0\}$  which is a  $\mathbb{P}^2$ .

In order to get an orbifold of the full torus we start with the six torus  $T_3^2 \times T_3^2 \times T_3^2$ . It has superfields  $\mathcal{Z}_{a\rho}$  with  $a, i\rho = 1, 2, 3$  and  $\mathcal{C}_a$ ,  $a = 1, 2, 3$  with charge assignment shown in table 3.4. The superpotential, constrained to linear order in  $\mathcal{C}$  by  $R$ -symmetry, is

$$\mathcal{W}_{\text{torus}} = \sum_{a,i} \mathcal{C}_a \mathcal{Z}_{ai}^3, \quad (3.80)$$

and we get the  $D$ -terms

$$|z_{a1}|^2 + |z_{a2}|^2 + |z_{a3}|^2 - 3|c_a|^2 = a_a, \quad a = 1, 2, 3. \quad (3.81)$$

In the geometric phase  $a_a > 0$  from the  $F$ -terms we get  $c_a = 0$  and the  $z_{ai}$  become homogeneous coordinates for the elliptic curves  $\mathbb{P}^2[3]$ . Since we are interested in a  $\mathbb{Z}_3$  orbifold we focus on discrete symmetries which are generated by elements of the form

$$\theta_{\alpha\beta\gamma} : (z_{1\alpha}, z_{2\beta}, z_{3\gamma}) \longmapsto (\zeta z_{1\alpha}, \zeta z_{2\beta}, \zeta z_{3\gamma}), \quad \alpha, \beta, \gamma = 1, 2, 3. \quad (3.82)$$

Although this might look like a  $\mathbb{Z}_3^{27}$ , it is in fact only a  $\mathbb{Z}_3^4$  symmetry generated by the elements

$$\theta = \theta_{111}, \quad \alpha_1 = \theta_{111}^{-1} \theta_{211}, \quad \alpha_2 = \theta_{111}^{-1} \theta_{121}, \quad \alpha_3 = \theta_{111}^{-1} \theta_{112}, \quad (3.83)$$

since up to  $U(1)_{R_a}$  rotations we find  $\theta_{\alpha\beta\gamma} = \theta \alpha_1^{\alpha-1} \alpha_2^{\beta-1} \alpha_3^{\gamma-1}$ . Accordingly we will denote this symmetry by  $\mathbb{Z}_{3,\text{orbi}} \times \mathbb{Z}_{3-\text{vol}}^3$ . Then, adding an exceptional gauging  $U(1)_{E_{\alpha\beta\gamma}}$  with coordinate  $x_{\alpha\beta\gamma}$  will induce the  $\theta_{\alpha\beta\gamma}$  action.

#### Maximal Model

We start with the discussion of the most general, the maximal, fully resolvable model. The superfield content and charge assignment is shown in table 3.5. We have  $3 + 27$  gaugings, three of them corresponding to the construction of the torus and 27 for the local singularities. Accordingly their  $D$ -terms divide up into the elliptic curve  $D$ -terms and the resolved singularity  $D$ -terms :

$$|z_{a1}|^2 + |z_{a2}|^2 + |z_{a3}|^2 - 3|c_a|^2 = a_a \quad a = 1, 2, 3, \quad (3.84a)$$

$$|z_{1\alpha}|^2 + |z_{2\beta}|^2 + |z_{3\gamma}|^2 - 3|x_{\alpha\beta\gamma}|^2 = b_{\alpha\beta\gamma} \quad \alpha, \beta, \gamma = 1, 2, 3. \quad (3.84b)$$



### 3.3 (2,2) Models of Resolved Toroidal Orbifolds

Superfield	$\mathcal{Z}_{1\alpha}$	$\mathcal{Z}_{2\beta}$	$\mathcal{Z}_{3\gamma}$	$\mathcal{C}_1$	$\mathcal{C}_2$	$\mathcal{C}_3$
$R_1$	1	0	0	-3	0	0
$R_2$	0	1	0	0	-3	0
$R_3$	0	0	1	0	0	-3

Table 3.4: Charges of the superfields in the GLSM description of the  $T^6$  torus possessing a  $\mathbb{Z}_3$  orbifold symmetry.

The superpotential for the elliptic curves have to be modified by the  $\mathcal{X}$  fields in order to be gauge invariant,

$$\mathcal{W}_{\max} = \mathcal{C}_1 \sum_{\alpha} \mathcal{Z}_{1\alpha}^3 \prod_{\beta\gamma} \mathcal{X}_{\alpha\beta\gamma} + \mathcal{C}_2 \sum_{\beta} \mathcal{Z}_{2\beta}^3 \prod_{\alpha\gamma} \mathcal{X}_{\alpha\beta\gamma} + \mathcal{C}_3 \sum_{\gamma} \mathcal{Z}_{3\gamma}^3 \prod_{\alpha\beta} \mathcal{X}_{\alpha\beta\gamma}. \quad (3.85)$$

Here we see that mixed monomials in the  $\mathcal{Z}_{ai}$  could not be made gauge invariant by the  $\mathcal{X}$ 's which is why they are left out from the beginning. This restriction reflects the fact that the complex structure of the two tori is fixed to be  $\tau = \zeta$ . From this we get the geometric  $F$ -terms

$$F_{\mathcal{C}_1}^* = z_{11}^3 \prod_{\beta,\gamma} x_{1\beta\gamma} + z_{12}^3 \prod_{\beta,\gamma} x_{2\beta\gamma} + z_{13}^3 \prod_{\beta,\gamma} x_{3\beta\gamma}, \quad (3.86a)$$

$$F_{\mathcal{C}_2}^* = z_{21}^3 \prod_{\alpha,\gamma} x_{\alpha 1\gamma} + z_{22}^3 \prod_{\alpha,\gamma} x_{\alpha 2\gamma} + z_{23}^3 \prod_{\alpha,\gamma} x_{\alpha 3\gamma}, \quad (3.86b)$$

$$F_{\mathcal{C}_3}^* = z_{31}^3 \prod_{\alpha,\beta} x_{\alpha\beta 1} + z_{32}^3 \prod_{\alpha,\beta} x_{\alpha\beta 2} + z_{33}^3 \prod_{\alpha,\beta} x_{\alpha\beta 3}, \quad (3.86c)$$

plus additional  $F$ -terms  $F_{\mathcal{Z}_{ai}}$  and  $F_{\mathcal{X}_{\alpha\beta\gamma}}$ . The latter ones are linear in  $c_a$  and will therefore vanish in the geometric regime which is roughly given by  $a_a > 0$  and  $a_a \gg b_{\alpha\beta\gamma}$ . This regime includes both the orbifold and the full resolution phase, as well as all possible partial resolutions for which some  $b$  are positive while others remain negative.

The emergence of the geometry is best understood using the holomorphic quotient. For this we start in the orbifold regime where all  $b_{\alpha\beta\gamma} < 0$ . The  $D$ -terms then force  $x_{\alpha\beta\gamma} \neq 0$  and we can perform  $\mathbb{C}_{\alpha\beta\gamma}^*$  scalings to set them equal to one, leaving a discrete symmetry generated by the  $\theta_{\alpha\beta\gamma}$ . Thus we can understand the geometry in terms of the  $z_{ai}$  coordinates with the discrete symmetry being modded out. Then we immediately see that (3.86) reduce to the hypersurface equations of the elliptic curves  $T_3^2$  on which the discrete symmetries act like  $\mathbb{Z}_{3,\text{orbi}} \times \mathbb{Z}_{3-\text{vol}}^3$ . In particular, each  $\theta_{\alpha\beta\gamma}$  has fixed points at  $z_{1\alpha} = z_{2\beta} = z_{3\gamma} = 0$  which all get identified by the 3-rotations  $\alpha_a$ .

Now we can start to blow-up the fixed points individually by setting the appropriate  $b_{\alpha\beta\gamma} > 0$ . Then the corresponding fixed points are no longer able to

### 3 GLSM description of Resolved Toroidal Orbifolds

fulfill the  $D$ -term equations and are replaced by the exceptional divisor  $E_{\alpha\beta\gamma} = \{x_{\alpha\beta\gamma} = 0\}$ . As long as the  $b_{\alpha\beta\gamma}$  are small compared to the  $a_a$ , the neighborhood of the exceptional divisors looks like the neighborhood of the fixed points. In particular, the exceptional divisors do not intersect each other.

Next, we want to qualitatively find the boundaries of the blow-up and partial blow-up phases, in which the picture of locally happening resolutions breaks down. For this, in the orbifold and blow-up regime we require that coordinates which carry different labels of the same type (e.g. pairs with  $\alpha = 1, 2$  like  $z_{1,1}, z_{1,2}$  or  $z_{1,1}, x_{211}$  or  $x_{111}, x_{211}$ ) must not vanish simultaneously. This can be achieved by conditions of the form  $a_a \gg b_{\alpha\beta\gamma}$  on the FI parameters. We explain this shortly. First of all, sitting on a fixed point or the exceptional divisor, respectively, implies

$$|z_{1,\alpha}|^2 \leq \max\{b_{\alpha\beta\gamma}, 0\} . \quad (3.87)$$

In blow-up, the  $D$ -term together with the exceptional divisor condition  $x_{\alpha\beta\gamma} = 0$  imply (3.87) with  $b_{\alpha\beta\gamma}$  being the maximum. If the fixed point is not resolved, the fixed locus equation  $z_{1,\alpha} = 0$  also trivially implies (3.87). Let's look what happens if we want to sit at the same time at two fixed points / exceptional divisors in one plane. This means that two coordinates with different labels, like e.g. one coordinate with  $\alpha = 1$  and one with  $\alpha = 2$  are zero. Then the  $F$ -term implies that one of the coordinates with  $\alpha = 3$  must also be zero. Thus we get three equations of the form (3.87) which inserted into the  $U(1)_{R_1}$   $D$ -term imply

$$a_1 = |z_{1,1}|^2 + |z_{1,2}|^2 + |z_{1,3}|^2 \leq \max\{b_{1\beta_1\gamma_1}, 0\} + \max\{b_{2\beta_2\gamma_2}, 0\} + \max\{b_{3\beta_3\gamma_3}, 0\}$$

for some  $\beta_i, \gamma_i$ . In particular, in full blow-up, these conditions are

$$a_1 \leq b_{1\beta_1\gamma_1} + b_{2\beta_2\gamma_2} + b_{3\beta_3\gamma_3} \quad (3.88)$$

The precise boundaries of the blow-up phases are rather complicated to depict due to the high dimensionality of the moduli space. However, such boundaries always appear whenever the  $b_{\alpha\beta\gamma}$  become of the order of the  $a_a$ . A more precise discussion is performed in section 3.3.2.

**Inherited divisors** In [47] three types of divisors were introduced, namely ordinary, exceptional and inherited divisors. The ordinary and exceptional divisors can in the GLSM models be described nicely as zero loci of homogeneous coordinates, i.e. ordinary divisors are  $D_{ai} := \{z_{ai} = 0\}$  and exceptional divisors are  $E_{r,ijk} := \{x_{r,ijk} = 0\}$ . For the inherited divisors  $R_a$  the situation is more complicated.

To deduce the proper form of the inherited divisors  $R_a$  in the GLSM and show that it has the desired properties, we start from their definitions on the torus

$$R_a := \bigcup_{k,l=0}^2 \left\{ u_a = \zeta^k \tilde{u}_a + l \frac{\zeta - 1}{3} \right\} , \quad (3.89)$$

### 3.3 (2,2) Models of Resolved Toroidal Orbifolds

Superfield	$\mathcal{Z}_{1i}$	$\mathcal{Z}_{2j}$	$\mathcal{Z}_{3k}$	$\mathcal{C}_1$	$\mathcal{C}_2$	$\mathcal{C}_3$	$\mathcal{X}_{ijk}$
$R_1$	1	0	0	-3	0	0	0
$R_2$	0	1	0	0	-3	0	0
$R_3$	0	0	1	0	0	-3	0
$E_{\alpha\beta\gamma}$	$\delta_{i\alpha}$	$\delta_{j\beta}$	$\delta_{k\gamma}$	0	0	0	$-3\delta_{i\alpha}\delta_{j\beta}\delta_{k\gamma}$

Table 3.5: Charges of the fields needed in the maximal description of the resolved  $T^6/\mathbb{Z}_3$  orbifold. The indices  $i, j, k, \alpha, \beta, \gamma$  run from 1 to 3.

where  $\tilde{u}_a$  are some constants. The union over the nine distinct pieces is necessary for  $\mathbb{Z}_{3,\text{orbi}} \times \mathbb{Z}_{3-\text{vol}}$  invariance. Via the Weierstrass map (3.26), we can translate them into

$$y_a = p_a v_a, \quad y_a(1 - ip_a) = v_a(p_a - 3i), \quad y_a(1 + ip_a) = v_a(p_a + 3i), \quad (3.90)$$

with  $p_a := \wp'(\tilde{u}_a)$ . Each of these terms is  $\mathbb{Z}_{3,\text{orbi}}$  invariant and thus represents three pieces inside (3.89). To make the equations invariant under  $\mathbb{Z}_{3,\text{orbi}} \times \mathbb{Z}_{3-\text{vol}}$  we multiply them to obtain ,

$$0 = -(v_a^3 + v_a y_a^2)(p_a^3 + 9p_a) + (9v_a^2 y_a + y_a^3)(1 + p_a^2). \quad (3.91)$$

Using the Weierstrass equation and the substitution (3.26) we can turn these equations into polynomials in  $z_{ai}$ ,

$$0 = (p_a^3 + 9p_a) z_{a1}^3 + 6\sqrt{3}(1 + p_a^2) \cdot (z_{a2}^3 - z_{a3}^3). \quad (3.92)$$

In the GLSM, to make it fully gauge invariant, we also have to include the  $x_{ijk}$  coordinates. Then this corresponds to a homogeneous equation of the same degree as the  $F$ -term which cuts out the torus. The result is

$$R_1 := \left\{ t_{11} z_{11}^3 \prod_{j,k} x_{1jk} + t_{12} z_{12}^3 \prod_{j,k} x_{2jk} + t_{13} z_{13}^3 \prod_{j,k} x_{3jk} = 0 \right\}, \quad (3.93)$$

and  $R_2, R_3$  similarly. The coefficients  $t_{ai}(\tilde{u}_a)$  encode the information about the position of the inherited divisors set by the constants  $\tilde{u}_a$ .

From this we can easily read off the linear equivalence relations as each monomial defines one particular sum of divisors,

$$R_1 \sim 3D_{11} + \sum_{j,k} E_{1jk} \sim 3D_{12} + \sum_{j,k} E_{2jk} \sim 3D_{13} + \sum_{j,k} E_{3jk}, \quad (3.94)$$

and similarly for the divisors  $R_2$  and  $R_3$ . In this way we recover the linear equivalences from [47].

### 3 GLSM description of Resolved Toroidal Orbifolds

**The intersection ring** With the divisors and linear equivalences at hand we can determine the intersection ring in a GLSM manner. This allows us to prove the results on the intersection ring in reference [47] which were obtained by the means of an auxiliary polyhedron. For this we first obtain the intersection numbers of three distinct divisors by counting the number of solutions of the  $D$ - and  $F$ -term equations. Then we use linear equivalences to determine the self-intersection numbers. In fact it is sufficient to give intersection numbers of a real basis of divisors. Such a basis is given by the divisors  $R_a$ ,  $a = 1, 2, 3$  and all  $E_{ijk}$ . We will systematically derive their intersection numbers here in the blow-up phase only. This phase is roughly determined by  $0 < b \ll a$ , where  $b$  and  $a$  represent any FI parameter of the respective type. In this phase the geometry is a smooth Calabi–Yau space for which intersection numbers can be compared to the results of Lüst et. al. [47].

First of all, we find that in the blow-up regime,  $R_a$  does not intersect with  $E_{ijk}$ . To show this we take e.g.  $E_{111}$  and  $R_1$ . We insert the condition  $x_{111} = 0$  into the defining equation (3.93) for  $R_a$  and the  $F$ -term (3.86) and find the conditions

$$z_{12}^3 \prod_{j,k} x_{2jk} = z_{13}^3 \prod_{j,k} x_{3jk} = 0. \quad (3.95)$$

Thus, in each monomial one field must be zero which gives us three different classes of cases, roughly described by “ $z = z = 0$ ”, “ $z = x = 0$ ” or “ $x = x = 0$ ”. The first one is  $z_{12} = z_{13} = 0$ . Then, the  $D$ -term of  $U(1)_{E_{111}} - U(1)_{R_1}$  implies that  $b_{111} > a_1$ , which is beyond the blow-up regime. In the second class we choose e.g.  $z_{12} = x_{311} = 0$  to find that the  $D$ -term of  $U(1)_{E_{111}} + U(1)_{E_{311}} - U(1)_{R_1}$  implies  $b_{111} + b_{311} > a_1$ , which again violates the blow-up phase condition. The third class is handled analogously. In the same way we see that  $R_a$  and  $D_{ai}$  do not intersect. This by linear equivalences implies that  $R_a$  does not self-intersect.

Next we focus on the intersection  $R_1 R_2 R_3$ . For this we impose three conditions of the form (3.93), one for each torus. As argued above on  $R_a$  all  $x_{ijk}$  have non-zero vevs, we fix their phases against the  $U(1)_E$  gaugings, thus leaving a  $\mathbb{Z}_{3,\text{orbi}} \times \mathbb{Z}_{3-\text{vol}}^3$  symmetry acting on the  $z_{ai}$ . Then, the inherited divisor constraints together with the three  $F$ -terms can be linearly combined to eliminate all  $z_{a1}$  and we get three equations which are cubic in  $z_{a2}$  and  $z_{a3}$ . Thus they factorize into three pieces, giving three solutions each. Now we insert these solutions into the original equations, which are cubic in  $z_{a1}$  and thus again give three solution for each  $z_{a1}$ . Altogether this gives  $3^6 = 729$  solutions. The discrete symmetries identify them in groups of  $3^4 = 81$  each, such that the intersection number is  $R_1 R_2 R_3 = 9$ .

Furthermore, an intersection of  $E_{ijk}$  and  $E_{i'j'k'}$  where  $(i, j, k) \neq (i', j', k')$  would also lead to a violation of the blow-up phase condition. The argumentation goes similarly to the one for  $R_a E_{ijk} = 0$ . Finally, in the blow-up phase, we find the intersection number  $D_{1i} D_{2j} D_{3k} = 0$ , since at a common intersection the  $D$ -term

### 3.3 (2,2) Models of Resolved Toroidal Orbifolds

of  $U(1)_{E_{ijk}}$  would contradict the blow-up condition  $b_{ijk} > 0$ . Inserting linear equivalences shows,

$$\begin{aligned} 27 D_{1i} D_{2j} D_{3k} &= \left( R_1 - \sum_{\beta, \gamma} E_{i\beta\gamma} \right) \cdot \left( R_2 - \sum_{\alpha, \gamma} E_{\alpha j \gamma} \right) \cdot \left( R_3 - \sum_{\alpha, \beta} E_{\alpha\beta k} \right) \\ &= R_1 R_2 R_3 - E_{ijk}^3, \end{aligned} \quad (3.96)$$

which implies that  $E_{ijk}^3 = 9$ . Thus we have determined the complete intersection ring.

To sum up, the non-vanishing intersection numbers of inherited and exceptional divisors in the blow-up phase ( $0 < b \ll a$ ) are

$$E_{ijk}^3 = 9, \quad R_1 R_2 R_3 = 9. \quad (3.97)$$

Intersection numbers containing ordinary divisors are obtained using linear equivalences. Hence, in the GLSM we have rigorously confirmed the intersection numbers obtained in [47].

#### Minimal Model

For the  $T^6/\mathbb{Z}_3$  orbifold one can construct a minimal fully resolvable model by just having one exceptional gauging  $U(1)_{E_{111}}$  with coordinate  $x_{111}$ . The model obtained this way was used in [51] for cohomology computations. The charge assignment is the same as in table 3.5, but with  $\alpha\beta\gamma$  only being equal to  $(1, 1, 1)$ . In this case the geometry is the same as in the maximal model, but the way it is organized is quite different. The geometric  $F$ -terms are

$$F_{C_1}^* = z_{11}^3 x_{111} + z_{12}^3 + z_{13}^3, \quad (3.98a)$$

$$F_{C_2}^* = z_{21}^3 x_{111} + z_{22}^3 + z_{23}^3, \quad (3.98b)$$

$$F_{C_3}^* = z_{31}^3 x_{111} + z_{32}^3 + z_{33}^3, \quad (3.98c)$$

whereas the  $D$ -terms are a subset of the maximal model  $D$ -terms. In general one could now allow for mixed monomials between  $z_{a2}$  and  $z_{a3}$ , but a  $GL(2, \mathbb{C})$  rotation can always bring it back to the form (3.98). In particular, such mixed terms would not change the complex structure of the torus. For  $b_{111} < 0$  the coordinate  $x_{111}$  must not vanish. Then one can use  $U(1)_{E_{111}}$  to rotate it to the positive real axis, leaving a  $\mathbb{Z}_3$  ambiguity, and the associated  $D$ -term fixes its length. Therefore the geometry is described just by the coordinates  $z_{a\rho}$  with the leftover  $\mathbb{Z}_3$  acting on them as  $z_{a1} \mapsto \zeta z_{a1}$ . The fixed points are clearly at  $z_{11} = z_{21} = z_{31} = 0$ . Inserting these in the  $F$ -terms, we find that they factorize into three pieces, stating that there are three separated solutions to each of them,  $z_{a2} = -\zeta^k z_{a3}$ ,  $k = 1, 2, 3$ . So we have found 27 fixed points which are all described by the zero locus of the same homogeneous coordinates.

### 3 GLSM description of Resolved Toroidal Orbifolds

In the blow-up regime, where  $0 < b_{111} \ll a_a$ , the singularities are removed and replaced by the exceptional divisor  $E_{111} = \{x_{111} = 0\}$ . Inserting the divisor equation into the  $F$ -terms yields the same factorization so we deduce that the divisor consists of 27 separated pieces, each replacing one of the singularities. In section 3.3.2 we will focus a bit more on the precise phase structure of this model and in particular explore what happens if one overshoots the blow-up procedure.

Although topologically the target spaces of the minimal and maximal models are the same, the nomenclature for the divisors is quite different. We already saw that the one exceptional divisor in the minimal model represents the union of all exceptional divisors in the maximal model. Due to the asymmetric roles which the coordinates  $z_{a1}$  and  $z_{a\rho}$ ,  $\rho = 2, 3$  play, their zero locus divisors will also be different. For  $D_{a1} = \{z_{a1} = 0\}$  we find that the  $a^{\text{th}}$   $F$  term factorizes in the same way as before. So this divisor consists of three pieces, each of which is located in the  $a^{\text{th}}$  torus at one of the former fixed point loci. Comparing this to the maximal model, it represents the sum over all three inherited divisors in this torus. Finally, the coordinates  $z_{a2}$  and  $z_{a3}$  are of the same charge, thus we can construct a divisor as the zero locus of a two term polynomial  $\tilde{D}_a = \{t_2 z_{a2} + t_3 z_{a3} = 0\}$ . The coefficients  $t_\rho$  can be varied continuously thus moving the divisor around on the  $a^{\text{th}}$  torus. This shows that the divisor is indeed to be interpreted as an inherited divisor, which in the maximal model required a more elaborate polynomial. We summarize the correspondence.

minimal model divisor	maximal model divisor
$E_{111}$	$\sum_{\alpha\beta\gamma} E_{\alpha\beta\gamma}$
$D_{a1}$	$\sum_{\rho} D_{a\rho}$
$\tilde{D}_a \cong D_{a2} \cong D_{a3}$	$R_a$

The linear equivalences between these divisors, as shown in equation (3.94) are also valid here. To express them in the minimal model language, one has to sum over the index  $\rho$  and one indeed finds  $3D_{a1} + E_{111} \sim \tilde{D}_a$ .

#### Models in Between

We have just presented two of the many models that can be constructed in this way. The basic ingredient is always the six-torus with homogeneous coordinates  $z_{a\rho}$  and the  $F$ -term equations. Then one could add in principle an arbitrary subset of the coordinates  $x_{\alpha\beta\gamma}$  with associated gaugings, which would all result in different  $T^6/\mathbb{Z}_3$  orbifolds. This gives a total of  $2^{27} - 1$  models<sup>5</sup> so it is by far not desirable to discuss all of them. Instead, due to the high symmetry of the  $\mathbb{Z}_3$  orbifold, we can find a classification of all these models. The result is summarized in table 3.6.

---

<sup>5</sup>The one which is subtracted represents the case without  $x$  fields at all. This is simply the six-torus.

Exceptional coordinates	Discrete Group	FP Sets		Lattice	Fully resolvable by adding
		Groups	Singular		
$x_{111}$	–	$1 \times 27$	0	$A_2 \times A_2 \times A_2$	–
$x_{111}, x_{211}$	$\mathbb{Z}_3$	$3 \times 9$	9	$A_2 \times A_2 \times A_2$	$x_{311}$
$x_{111}, x_{221}$				$F_4 \times A_2$	$x_{331}$
$x_{111}, x_{222}$				$E_6$	$x_{333}$
$x_{111}, x_{211}, x_{121}$	$\mathbb{Z}_3 \times \mathbb{Z}_3$	$9 \times 3$	18	$A_2 \times A_2 \times A_2$	$x_{131}, x_{221}, x_{231},$ $x_{311}, x_{321}, x_{331}$
$x_{111}, x_{221}, x_{112}$				$F_4 \times A_2$	$x_{113}, x_{222}, x_{223},$ $x_{331}, x_{332}, x_{333}$
$x_{111}, x_{221}, x_{212}$				no Lie lattice	$x_{123}, x_{133}, x_{232},$ $x_{313}, x_{322}, x_{331}$
$x_{111}, x_{211}, x_{121}, x_{112}$	$\mathbb{Z}_3 \times \mathbb{Z}_3 \times \mathbb{Z}_3$	$27 \times 1$	23	$A_2 \times A_2 \times A_2$	rest

Table 3.6: This table summarizes the structures that can be obtained upon inclusion of exceptional gaugings. The first column specifies which exceptional fields  $x_{\alpha\beta\gamma}$  have to be introduced for each class. The second column gives the number of discrete  $\mathbb{Z}_3$  actions which are induced in addition to the orbifold action. The third column specifies how the 27 fixed points are grouped and how many of these cannot be blown up and thus stay singular. The fourth column specifies the Lie lattice underlying the torus in the various cases. In the fifth column, we specify which additional exceptional coordinates have to be included in order to be able to completely blow-up the geometry.

### 3 GLSM description of Resolved Toroidal Orbifolds

As a central criterion in the classification we take the discrete symmetries which remain from the  $U(1)_{E_r}$  when  $x_r \neq 0$ , after fixing the  $x_r$  value, and act on the  $z_{a\rho}$ . So for the classification we take all models in the orbifold phase. In principle each such  $U(1)_{E_r}$  generates a  $\mathbb{Z}_3$  symmetry, but it can come quickly to redundancies as one increases the number. The limit of such discrete symmetries is in the maximal model, where we found a  $\mathbb{Z}_{3,\text{orbi}} \times \mathbb{Z}_{3-\text{vol}}^3$ . Thus each model in between has a subgroup of this. Since the  $\mathbb{Z}_{3-\text{vol}}$  only arise from two or more exceptional gaugings simultaneously, the group is always of the form  $\mathbb{Z}_{3,\text{orbi}} \times \mathbb{Z}_{3-\text{vol}}^k$  where  $k = 0, 1, 2, 3$ . For  $k = 0$  one finds only the minimal model, up to equivalence.

To study the  $k = 1$  models, we first add one more exceptional coordinate, so w.l.o.g. we use the coordinates  $x_{111}$  and  $x_{\alpha\beta\gamma}$  for fixed  $\alpha\beta\gamma$ . This generates one  $\mathbb{Z}_{3-\text{vol}}$  with element  $\theta_{111}\theta_{\alpha\beta\gamma}^2$  so for the classification one has to analyze how it acts.

- If only one of the indices  $\alpha\beta\gamma$  differs from one, the  $\mathbb{Z}_{3-\text{vol}}$  shifts in just one torus. We find again the factorizable orbifold, but now the fixed points can be distinguished by their locus in the first torus. Such a model could describe a theory with one Wilson line switched on.
- If two indices  $\alpha\beta\gamma$  differ from one, we get a shift in two tori simultaneously, which allows for the following interpretation. If one starts with the factorizable torus and first mods out this  $\mathbb{Z}_{3-\text{vol}}$  one obtains a non-factorizable torus. Thus, modding out the  $\mathbb{Z}_{3,\text{orbi}}$  will result in a non factorizable orbifold. In appendix B we show that this is the orbifold based on the Lie algebra lattice  $A_2 \times F_4$ . Furthermore we show that this lattice can continuously be deformed to the  $A_3^3$  lattice while preserving the  $\mathbb{Z}_{3,\text{orbi}}$  symmetry by varying the off-diagonal Kähler moduli. We will refer to such an orbifold as non-factorized, as opposed to truly non-factorizable orbifolds, for which such a deformation is not possible.
- If all indices  $\alpha\beta\gamma$  differ from one, we find a situation similar to the one above, just that the  $\mathbb{Z}_{3-\text{vol}}$  shifts in all three tori simultaneously. In appendix B we show that this results in an orbifold on the  $E_6$  lattice, which also turns out to be just non-factorized. We will get back to this example when we analyze the moduli spaces in section 3.3.2, since it possesses a nice self-duality.

With the knowledge at hand we can analyze the fixed point structures of these models. We do this in terms of the homogeneous coordinates  $z_{a\rho}$ , after fixing the  $x_r$ . There are 27 fixed points of  $\theta_{111}$  at  $z_{11} = z_{21} = z_{31} = 0$  which are identified in nine triplets by  $\mathbb{Z}_{3-\text{vol}}$ . Similarly, there are 27 fixed points of  $\theta_{\alpha\beta\gamma}$  at  $z_{1\alpha} = z_{2\beta} = z_{3\gamma} = 0$ , which also get identified to nine triplets each. In addition, we find that the element  $\theta_{111}\theta_{\alpha\beta\gamma}$  has fixed points, which arise after



### 3.3 (2,2) Models of Resolved Toroidal Orbifolds

$U(1)_{Ra}$  rotations, at  $z_{1,2-\alpha} = z_{2,2-\beta} = z_{3,2-\gamma} = 0$ , where the indices are to be taken modulo three. One can again check that these are again 9 tupels of  $\mathbb{Z}_{3-\text{vol}}$  orbits. The remaining elements of the discrete group have no fixed points or are the inverses of the ones discussed. Thus we find 27 fixed points, independent of the alignment of  $\alpha\beta\gamma$ , which confirms that all these orbifolds are off-diagonal deformations of the factorizable one. The fixed points of  $\theta_{111}$  and  $\theta_{\alpha\beta\gamma}$  can be resolved by varying the FI parameters  $b_{111}$  and  $b_{\alpha\beta\gamma}$ , respectively. The remaining fixed points, however, can never be resolved, since there is no  $D$ -term which would forbid them. Thus such models can be used to describe a situation in which some fixed points stay singular while others get resolved. To make these models fully resolvable, one would have to add the coordinate  $x_{2-\alpha,2-\beta,2-\gamma}$  with the appropriate gauging. This is then a next-to-minimal, fully resolvable model.

For  $k = 2$  we again find three ways in which the  $\mathbb{Z}_{3-\text{vol}}^2$  can be aligned, see table 3.6. One needs at least three exceptional coordinates for these cases. The fixed points will be organized in nine sets of three equivalent ones per set. Therefore, to make them fully blowable, one needs exactly nine exceptional coordinates. The three cases are a factorizable orbifold, where one can now switch on two Wilson lines, and two non factorized ones, which are  $F_4 \times A_2$  and a lattice that does not fit into the Lie algebra classification.

Finally,  $k = 3$  describes the maximal models where each fixed point has its own set of  $z_{a\rho}$  coordinates to be the zero locus thereof. Here one can start with just four coordinates and go up to all 27 ones to get the maximal fully resolvable model.

#### 3.3.2 Moduli Spaces

In Kähler geometry one can write down the formula for the volumes of curves, divisors and of the whole space. Using (3.9) and inserting the  $\mathbb{Z}_3$  intersection numbers we find for example for the maximal model,

$$\begin{aligned} \text{Vol}(X) &= 9a_1a_2a_3 - \frac{3}{2} \sum_{\alpha\beta\gamma} b_{\alpha\beta\gamma}^3, \\ \text{Vol}(D_{1\alpha}) &= 3a_2a_3 - \frac{3}{2} \sum_{\beta\gamma} b_{\alpha\beta\gamma}^2, \\ \text{Vol}(E_{\alpha\beta\gamma}) &= \frac{9}{2} b_{\alpha\beta\gamma}^3, \\ \text{Vol}(D_{1\alpha}D_{2\beta}) &= a_3 - \sum_{\gamma} b_{\alpha\beta\gamma}. \end{aligned} \tag{3.99}$$

These formulæ tell us that that the Calabi–Yau has a “swiss cheese” geometry. It means that as one continues blowing up the exceptional divisors, i.e. when the  $b_r$  increase, the volume of the whole space becomes smaller and smaller. Thus one can think of the exceptional divisors as holes in a piece of swiss cheese.

### 3 GLSM description of Resolved Toroidal Orbifolds

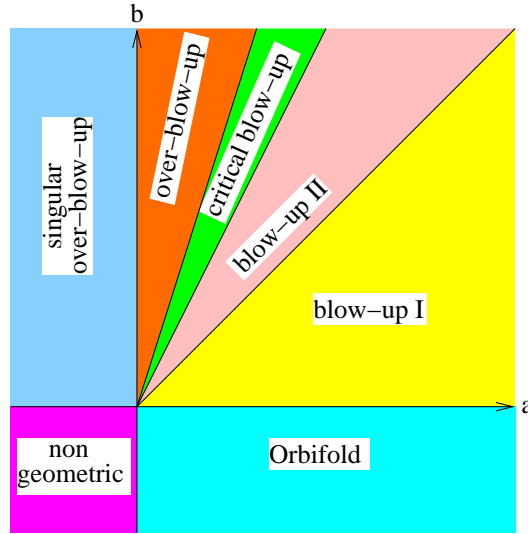


Figure 3.1: This picture displays the different phases that the minimal fully resolvable GLSM possesses.

Also the ordinary divisors  $D_{a\rho}$  and the curves in which they intersect show that structure. Thus we can qualitatively say that at some point the smooth geometry picture must break down. The volumes (3.99) suggest that this happens first when the curves  $D_{a\rho}D_{b\sigma}$  shrink to zero. Since the string theory should be well behaved when one crosses such a transition, one can ask what the theory would look like beyond this regime. The GLSM offers a tool to study these issues. Since  $(2, 2)$  models are ensured to be well behaved, we can use them to study the theories there. As was already studied in [19], the GLSM is a perfect tool to study the transition to such arbitrary phases. However, we will for simplicity not choose the maximal model, but rather the minimal one. In addition we will show that the moduli space of the fully blowable  $E_6$  model has an unexpected symmetry. Here we will focus on the classical moduli spaces only. The relation of quantum moduli spaces to the classical ones for complete intersection Calabi–Yaus is discussed in [20].

#### Phases of the Minimal Model

In the minimal model we have four FI parameters, three for the volumes of the two-tori  $a_a$  and one which blows the exceptional divisors up and down,  $b$ . For simplicity we will assume that all  $a_a$  are equal and will just call them  $a$ . This means that we study a two-real-dimensional subspace of the whole moduli space<sup>6</sup>. There are two phases of this model which were already described quite

<sup>6</sup>The dimension of the true moduli space is of course much larger, and its structure more complicated.

### 3.3 (2,2) Models of Resolved Toroidal Orbifolds

well and which also were the main purpose for constructing the models: the orbifold phase, where  $b < 0 < a$  and the resolution phase for which  $0 < b \ll a$  where the “ $\ll$ ” was so far unspecified. The discussion of these phases will not be repeated.

For a full analysis of the phases, we need to write down all the  $F$ -terms, since the field  $c_a$  which in the orbifold / blow-up phases played the role of a Lagrange multiplier for the hypersurface constraints, may become non zero and hence a homogeneous coordinate of the new target spaces,

$$F_{c_a} = z_{a1}^3 x + z_{a2}^3 + z_{a3}^3, \quad F_{\mathcal{X}} = c_1 z_{11}^3 + c_2 z_{21}^3 + c_3 z_{31}^3, \quad (3.100)$$

$$F_{z_{a1}} = 3 c_a x z_{a1}^2, \quad F_{z_{a\rho}} = 3 c_a z_{a\rho}^2. \quad (3.101)$$

It will turn out to be useful to write down the following linear combinations of  $D$  terms, as the right hand sides flop sign at the boundaries of the phases,

$$\sum_i |z_{ai}|^2 - 3 |c_a|^2 = a, \quad \sum_b |z_{b1}|^2 - 3 |x|^2 = b, \quad (3.102a)$$

$$\sum_{j \neq 1} |z_{aj}|^2 + 3 |x|^2 - \sum_{b \neq a} |z_{b1}|^2 = a - b, \quad (3.102b)$$

$$\sum_{b \neq a, j \neq 1} |z_{bj}|^2 + 3 |x|^2 - 3 \sum_{b \neq a} |c_b|^2 - |z_{a1}|^2 = 2a - b, \quad (3.102c)$$

$$\sum_{j \neq 1, a} |z_{aj}|^2 + 3 |x|^2 - 3 \sum_a |c_a|^2 = 3a - b. \quad (3.102d)$$

Similarly to the orbifold–blow-up transition, the boundaries of the phases are specified by what sets of coordinates are allowed to vanish simultaneously. Here, at the transition at  $b = 0$ , the  $D$ -term (3.102a) states that either  $\{x\}$  or  $\{z_{11}, z_{21}, z_{31}\}$  must not vanish simultaneously. The other transitions can be understood in a similar fashion. The whole phase structure is depicted in figure 3.1. Let us study the phases in the following.

**$0 < a < b < 2a$ : Blow-Up II regime** As assumed in the analysis of the Kähler geometry, the smooth blow-up phase ends when the curves  $D_{a1}D_{a2}$  shrinks to zero. Equation (3.102b) tells us that this happens at  $a = b$ . Instead, the exceptional divisor  $E$  starts to intersect with the inherited divisors, which here are  $\tilde{D}_a = \{t_2 z_{a2} + t_3 z_{a3} = 0\}$ . Thus the picture of separated singularities whose resolution happens locally is lost. The coordinates  $c_a$  are still required to vanish, so one can think of the geometry as a deformation of the smooth resolution CY.

**$a, b < 0$ : Non-geometric regime** Next we analyze a phases from the other end. This regime can be understood by taking the orbifold, whose size is just

### 3 GLSM description of Resolved Toroidal Orbifolds

given by the  $a_a$ , and shrinking it down to a point. In fact we find that in this phase, the  $D$ -terms require  $x \neq 0$  and  $c_a \neq 0$  for all  $a$ . Then the only solution to the  $F$ -terms is  $z_{a\rho} = 0$  for all  $a, \rho$ . After imposing the  $D$ -term constraints and fixing the  $U(1)$  gaugings, the resulting target space is just a point. This phase describes what is called a Landau–Ginzburg model, or rather an orbifold thereof, similarly to what was found in [19].

**$\mathbf{a} < \mathbf{0} < \mathbf{b}$ : Singular Over-blow-up regime** Here coordinates  $c_a$  are not allowed to vanish, which immediately implies  $z_{a\rho} = 0$  for  $a = 1, 2, 3$  and  $\rho = 2, 3$ . The coordinate  $x$  on the other hand is required to be zero as can be seen from (3.102d). Then only the  $F$ -term  $F_{\mathcal{X}}$  remains non-trivial. The  $D$ -terms simplify to

$$|z_{a1}| - 3|c_a|^2 = |a|, \quad |z_{11}|^2 + |z_{21}|^2 + |z_{31}|^2 = b. \quad (3.103)$$

We find that the  $c_a$  must not vanish, but are fixed by the  $D$ -terms and  $U(1)$  gaugings, leaving a  $\mathbb{Z}_3^3$  action on the  $z_{a1}$ . Analyzing the  $F$ -term, one can interpret the non-vanishing  $c_a$  as coefficients, and one would recover an elliptic curve as degree three hypersurface in  $\mathbb{P}^2$ . The  $\mathbb{Z}_3^3$  acts on it like a  $\mathbb{Z}_{3,\text{orbi}} \times \mathbb{Z}_{3-\text{vol}}$  so the target space looks like a  $T^2/\mathbb{Z}_3$  with the fixed points at  $z_{a1} = 0$ . This target space should not be thought of as a compactification space in the classical sense. Instead it gives a hybrid theory which is half geometric and half “Landau–Ginzburg-like”. Due to the apparent simplicity of the target space, one might wonder if there is a description of it in terms of a solvable CFT, which could be a hybrid of an orbifold CFT and a Landau–Ginzburg model which is fibered over the orbifold.

**$\mathbf{0} < \mathbf{3a} < \mathbf{b}$ : Over-blow-up regime** Coming from the singular over-blow-up phase, we can understand this phase as an analog of the resolution of the orbifold singularities. The target space divides up into various component.

- When all  $c_a \neq 0$ , one still finds  $z_{a2} = z_{a3} = x = 0$ , and the component can be thought of a deformation of the target space in the singular over-blow-up regime, with the fixed points removed.
- If e.g.  $c_1 = 0$ , however, we find that  $z_{12}$  and  $z_{13}$  no longer need to vanish. Instead, (3.102d) implies that  $c_a$ ,  $a = 2, 3$  must not vanish. The two new non-vanishing coordinates come with one additional non-trivial  $F$ -term, namely  $F_{\mathcal{C}_1}$ . One can fix the coordinates  $c_2, c_3, z_{21}$  and  $z_{31}$  using the  $D$ -terms of  $U(1)_E$ ,  $U(1)_{R_2}$  and  $U(1)_{R_3}$  and the  $F$ -term  $F_{\mathcal{X}}$  and obtains a target space description which can be viewed as a degenerate degree three hypersurface in  $\mathbb{P}^2$ , i.e. something of complex dimension one. This can be interpreted as a component replacing the fixed point which was removed from the first component.

### 3.3 (2,2) Models of Resolved Toroidal Orbifolds

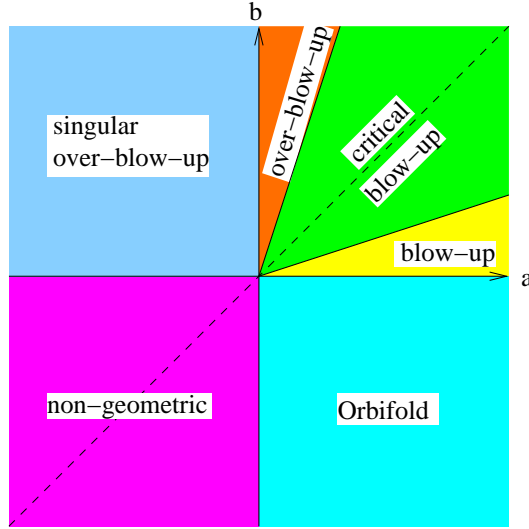


Figure 3.2: This picture displays the different phases of the fully resolvable GLSM that possesses a duality symmetry between the torus radii  $a_a$  and the blow-up cycle radii  $b_i$ .

One maybe can interpret this geometry locally as having a “squirrel-like” shape, where the body and the tail of the squirrel are both one-dimensional and intersect in a lower dimensional locus, here at  $c_1 = z_{12} = z_{13} = 0$ . As before, one should not think of it as classical compactification space but some sort of hybrid theory instead. This regime can be understood as the analogue of the blow-up regime just when coming from the singular over-blow-up phase.

**$0 < 2a < b < 3a$ : Critical regime** Finally we discuss the leftover regime, however not in that much detail. When coming from the over-blow-up regime, one can understand it as shrinking the  $c_1, c_2, c_3 \neq 0$  component to zero size. Instead a component comes up where  $c_1 = c_2 = c_3 = 0$  which is three-complex-dimensional. When shrinking  $b$  further down, this will become the target space of the blow-up and orbifold phases. The components where just one  $c_a$  is non vanishing still exist but shrink down as  $b \downarrow 2a$ .

#### Phases of the $E_6$ Model

The fully resolvable model on the  $E_6$  lattice, with three exceptional coordinates  $x_\rho = x_{\rho\rho\rho}$  has an extraordinary property. Its moduli space has a symmetry which interchanges the two-torus radii  $a_a$  and the blow-up moduli  $b_\rho$ . To make it manifest, we look at the  $D$ -terms ,

$$\sum_{\rho} |z_{a\rho}|^2 - 3|c_a|^2 = a_a , \quad \sum_a |z_{a\rho}|^2 - 3|x_\rho|^2 = b_\rho , \quad (3.104)$$

### 3 GLSM description of Resolved Toroidal Orbifolds

and the superpotential,

$$\mathcal{W} = \sum_{a,\rho} \mathcal{C}_a \mathcal{Z}_{a\rho} \mathcal{X}_\rho, \quad (3.105)$$

and find that the symmetry is given by ,

$$\mathcal{C}_a \leftrightarrow \mathcal{X}_\rho, \quad \mathcal{Z}_{a\rho} \leftrightarrow \mathcal{Z}_{\rho a}, \quad a_a \leftrightarrow b_\rho. \quad (3.106)$$

From this duality we immediately know what the singular over-blow-up and the over-blow-up phases are. They correspond to a target space which is also a  $T^6/\mathbb{Z}_3$  based on the  $E_6$  lattice and the resolution thereof. The boundary of the blow-up phase is found to be at  $a = 3b$ , so we immediately know the boundary of the over-blow-up phase at  $a = b/3$ . The situation is depicted in figure 3.2. This has an interesting consequent on the whole moduli space of the standard embedding  $\mathbb{Z}_3$  orbifold. Since each such resolution is deformable to the non-factorizable  $E_6$  orbifold, this duality should spread out over the whole moduli space. In particular we find that, if the off-diagonal Kähler moduli from the blow-up regime remain flat directions when going to the over-blow-up regime, they should correspond to moduli which take the three-dimensional “dual” resolution to a one-dimensional hybrid theory in the minimal model.

#### 3.3.3 Example: Resolution of $T^6/\mathbb{Z}_4$

In this section we present GLSMs for the  $T^6/\mathbb{Z}_4$  orbifold and its resolution. Since this orbifold has more structure than the  $\mathbb{Z}_3$  case, we encounter a few novel features: In the minimal model we need to introduce exceptional coordinates and gaugings for the different types of fixed points. Secondly, even in its fully resolvable GLSM there are two fixed tori that are not distinguished by our procedure and therefore blown up/down simultaneously. Thirdly, using our GLSM techniques we are able to describe truly non-factorizable  $T^6/\mathbb{Z}_4$  orbifolds.

To illustrate these issues and our formalism in general, we first construct the minimal fully resolvable GLSM on the factorized lattice  $D_2^2 \times A_1^2$ . Next we turn to the maximal fully resolvable model and show that one pair of fixed points remains indistinguishable. We conclude this section by explaining how we can obtain GLSMs associated with non-factorizable lattices  $A_3 \times D_2 \times A_1$  and  $A_3 \times A_3$ .

##### The minimal $T^6/\mathbb{Z}_4$ model on $D_2^2 \times A_1^2$

The  $\mathbb{Z}_4$  orbifold action on the three complex six-torus coordinates  $(u_1, u_2, u_3)$  is given by

$$\theta : (u_1, u_2, u_3) \mapsto (i u_1, i u_2, -u_3). \quad (3.107)$$

Superfield	$\mathcal{Z}_{1i}$	$\mathcal{Z}_{13}$	$\mathcal{Z}_{2j}$	$\mathcal{Z}_{23}$	$\mathcal{Z}_{3k}$	$\mathcal{C}_1$	$\mathcal{C}_2$	$\mathcal{C}_3$	$\mathcal{C}'_3$	$\mathcal{X}_{1,111}$	$\mathcal{X}_{2,ij}$
$U(1)$ charges	$z_{1i}$	$z_{13}$	$z_{2j}$	$z_{23}$	$z_{3k}$	$c_1$	$c_2$	$c_3$	$c'_3$	$x_{1,111}$	$x_{2,ij}$
$R_1$	1	2	0	0	0	-4	0	0	0	0	0
$R_2$	0	0	1	2	0	0	-4	0	0	0	0
$R_3$	0	0	0	0	1	0	0	-2	-2	0	0
$E_{1,111}$	$\delta_{i1}$	0	$\delta_{j1}$	0	$2\delta_{k1}$	0	0	0	0	-4	0
$E_{2,\alpha\beta}$	$\delta_{\alpha i}$	0	$\delta_{\beta j}$	0	0	0	0	0	0	0	$-2\delta_{\alpha i}\delta_{\beta j}$

Table 3.7: The superfield content and charge assignment for the minimal fully resolvable GLSM of  $T^6/\mathbb{Z}_4$ . The indices  $\alpha, \beta, i, j$  run from 1 to 2 and  $k$  from 1 to 4.

### 3 GLSM description of Resolved Toroidal Orbifolds

The only factorized lattice compatible with this action is of the form  $D_2^2 \times A_1^2$ , i.e. the complex structure of the first two tori is fixed to  $\tau = i$ , whereas the complex structure of the third torus stays a modulus  $\tau$ . The  $\theta$  sector has 16 fixed points whose structure factorizes as  $2 \times 2 \times 4$ . The  $\theta^2$  element acts like a  $\mathbb{Z}_2$  on the first two tori therefore naively we expect 16 fixed two-tori. But the  $\theta$  action folds four of them to  $T^2/\mathbb{Z}_2$ 's, whereas the remaining twelve get identified pairwise, i.e. they give rise to six fixed two-tori.

To understand how to obtain a global resolution model, we briefly review the local GLSM resolution of  $\mathbb{C}^3/\mathbb{Z}_4$  with the local orbifold action  $\theta(z_1, z_2, z_3) = (i z_1, i z_2, -z_3)$ . Then, to resolve the singularity we have to introduce two exceptional coordinates  $x_1$  and  $x_2$ , together with two appropriate gaugings. The charge table of the corresponding  $(2, 2)$  superfields reads:

$U(1)$ charges	$\mathcal{Z}_1$	$\mathcal{Z}_2$	$\mathcal{Z}_3$	$\mathcal{X}_1$	$\mathcal{X}_2$
$E_1$	1	1	2	-4	0
$E_2$	1	1	0	0	-2

When  $x_1 \neq 0$ , the  $U(1)_{E_1}$  reduces to the  $\mathbb{Z}_4$  orbifold action on the coordinates  $z_a$ . However, by only introducing  $x_1$  a  $\mathbb{Z}_2$  sub-singularity would remain. To make it resolvable one has to add  $x_2$ . The discrete action induced from  $U(1)_{E_2}$  when  $x_2 \neq 0$  is a  $\mathbb{Z}_2$  subgroup of  $\mathbb{Z}_4$ .

To construct the global models we first have to choose three appropriate elliptic curves. Since the orbifold  $\mathbb{Z}_4$  acts to fourth order in the first and second two-torus, and to second order in the third torus, we write the factorized six torus as  $T^6 = T_4^2 \times T_4^2 \times T_2^2$ . Hence, we need the homogeneous coordinates  $z_{1i}$ ,  $z_{2j}$  with labels  $i, j = 1, 2, 3$  and  $z_{3k}$  with  $k = 1, \dots, 4$ . To enforce the hypersurface constraints in the orbifold and blow-up regimes, we need four superfields  $\mathcal{C}_1$ ,  $\mathcal{C}_2$ ,  $\mathcal{C}_3$  and  $\mathcal{C}'_3$  which lead to the superpotential ,

$$W_{\text{torus}} = \mathcal{C}_1(\mathcal{Z}_{11}^4 + \mathcal{Z}_{12}^4 + \mathcal{Z}_{13}^2) + \mathcal{C}_2(\mathcal{Z}_{21}^4 + \mathcal{Z}_{22}^4 + \mathcal{Z}_{23}^2) \quad (3.108)$$

$$+ \mathcal{C}_3(\kappa \mathcal{Z}_{31}^2 + \mathcal{Z}_{32}^2 + \mathcal{Z}_{33}^2) + \mathcal{C}'_3(\mathcal{Z}_{31}^2 + \mathcal{Z}_{32}^2 + \mathcal{Z}_{34}^2), \quad (3.109)$$

for the corresponding superfields. Here  $\kappa$  encodes the complex structure modulus  $\tau$  in the elliptic curve description of the third torus.

In this formulation the orbifold action (3.107) acts on the homogeneous coordinates as

$$\theta : (z_{11}, z_{21}, z_{31}) \mapsto (i z_{11}, i z_{21}, -z_{31}). \quad (3.110)$$

This orbifold action can be transferred to the other coordinates by using the discrete  $U(1)_{R_a}$  rotations,

$$\theta_{R_a} : (z_{a1}, z_{a2}, z_{a3}) \mapsto (i z_{a1}, i z_{a2}, -z_{a3}), \quad a = 1, 2, \quad (3.111)$$

and the involutions  $\alpha_1, \alpha_2$  and  $\alpha_3, \alpha'_3$  of these two-tori defined in sections 3.1.2.



### 3.3 (2,2) Models of Resolved Toroidal Orbifolds

Next we investigate how many exceptional coordinates and gaugings we need to construct the minimal fully resolvable model, which by definition should be able to resolve all types of singularities. For the local resolution of a  $\mathbb{C}^3/\mathbb{Z}_4$  singularity we need two exceptional coordinates  $x_{1,111}$  and  $x_{2,11}$  with gaugings  $U(1)_{E_{1,111}}$  and  $U(1)_{E_{2,11}}$ , respectively, to resolve the  $\mathbb{Z}_4$  fixed points. Their positions are determined by the equations  $z_{11} = z_{21} = z_{31} = 0$ . The  $F_{C_a}$ -terms obtained from the superpotential (3.109),

$$\begin{aligned} z_{11}^4 + z_{12}^4 + z_{13}^2 &= 0, \\ z_{21}^4 + z_{22}^4 + z_{23}^2 &= 0, \\ \kappa z_{31}^2 + z_{32}^2 + z_{33}^2 &= 0, \\ z_{31}^2 + z_{32}^2 + z_{34}^2 &= 0, \end{aligned} \tag{3.112}$$

have  $2 \cdot 2 \cdot 2 \cdot 2 = 16$  roots, hence this corresponds to the 16  $\mathbb{Z}_4$  fixed points. The additional six fixed two-tori are located at  $z_{11} = z_{22} = 0$ ,  $z_{12} = z_{21} = 0$  and  $z_{12} = z_{22} = 0$ : For example,  $\theta^2 \theta_{R_1}^2$  has fixed tori at  $z_{12} = z_{21} = 0$ . For those the first two  $F$ -terms factorize in two times two roots. However  $\theta$  identifies the solutions pairwise, hence we find two true fixed two-tori. Similarly, there are two fixed tori of  $\theta \theta_{R_2}^2$  at  $z_{11} = z_{22} = 0$  and two  $\theta^2 \theta_{R_1}^2 \theta_{R_2}^2$  fixed tori at  $z_{12} = z_{22} = 0$ . Hence, to resolve all six fixed two-tori we need three additional exceptional coordinates  $x_{2,ij}$  and  $U(1)_{E_{2,ij}}$  with  $(i, j) = (2, 1), (1, 2), (2, 2)$ . All these together define the minimal fully resolvable model; the superfield content and the charge assignment are displayed in Table 3.7.

To show that this is indeed the minimal fully resolvable GLSM, we have to confirm that indeed all the fixed points get resolved in the blow-up regime. In this regime we have  $b_r > 0$ , yet sufficiently smaller than all the torus radii  $a_a$  to avoid running into the critical or over-blow-up regimes. From the charges in Table 3.7 we find the following  $D$ -terms

$$\begin{aligned} |z_{11}|^2 + |z_{12}|^2 + 2|z_{13}|^2 - 4|c_1|^2 &= a_1, \\ |z_{21}|^2 + |z_{22}|^2 + 2|z_{23}|^2 - 4|c_2|^2 &= a_2, \\ |z_{31}|^2 + |z_{32}|^2 + |z_{33}|^2 + |z_{34}|^2 - 2|c_3|^2 - 2|c'_3|^2 &= a_3, \\ |z_{11}|^2 + |z_{21}|^2 + 2|z_{31}|^2 - 4|x_{1,111}|^2 &= b_{1,111}, \\ |z_{1i}|^2 + |z_{2j}|^2 - 2|x_{2,ij}|^2 &= b_{2,ij}, \quad i, j = 1, 2. \end{aligned} \tag{3.113}$$

These equations clearly forbid setting  $z_{11} = z_{22} = 0$ ,  $z_{21} = z_{21} = 0$  or  $z_{12} = z_{22} = 0$ , because  $b_{1,111}, b_{2,ij}$  are all positive in the blow-up phase. Consequently, all the orbifold fixed points have been removed and replaced by the corresponding exceptional divisors  $E_{1,111} := \{x_{1,111} = 0\}$  and  $E_{2,ij} := \{x_{2,ij} = 0\}$ .

To show that these are glued in at the appropriate positions, we look at the  $F$ -terms in blow-up. In this regime the  $b_{1,111}, b_{2,ij}$  are sufficiently smaller than

Superfield	$\mathcal{Z}_{1i}$	$\mathcal{Z}_{13}$	$\mathcal{Z}_{2j}$	$\mathcal{Z}_{23}$	$\mathcal{Z}_{3k}$	$\mathcal{C}_1$	$\mathcal{C}_2$	$\mathcal{C}_3$	$\mathcal{C}'_3$	$\mathcal{X}_{1,ijk}$	$\mathcal{X}_{2,ij}$
$U(1)$ charges	$z_{1i}$	$z_{13}$	$z_{2j}$	$z_{23}$	$z_{3k}$	$c_1$	$c_2$	$c_3$	$c'_3$	$x_{1,ijk}$	$x_{2,ij}$
$R_1$	1	2	0	0	0	-4	0	0	0	0	0
$R_2$	0	0	1	2	0	0	-4	0	0	0	0
$R_3$	0	0	0	0	1	0	0	-2	-2	0	0
$E_{1,\alpha\beta\gamma}$	$\delta_{i\alpha}$	0	$\delta_{j\beta}$	0	$2\delta_{k\gamma}$	0	0	0	0	$-4\delta_{i\alpha}\delta_{j\beta}\delta_{k\gamma}$	0
$E_{2,\alpha\beta}$	$\delta_{i\alpha}$	$\delta_{3\alpha}$	$\delta_{j\beta}$	$\delta_{3\beta}$	0	0	0	0	0	0	$-2\delta_{\alpha i}\delta_{\beta j}$

Table 3.8: The superfield content and charge assignment for the maximal GLSM model of  $T^6/\mathbb{Z}_4$ . The indices  $k, \gamma$  run from 1 to 4. The indices  $i, j, \alpha, \beta$  run from 1 to 2 for  $x_{1,ijk}$  and  $U(1)_{E_{1,ijk}}$ , and from 1 to 3 for  $x_{2,ij}$  and  $U(1)_{E_{2,ij}}$ .

### 3.3 (2,2) Models of Resolved Toroidal Orbifolds

$a_a$ , such that the  $F$ -terms associated with  $z_{ai}$  force  $c_a = 0$ . Hence the only remaining  $F$ -terms are:

$$\begin{aligned} z_{11}^4 x_{1,111} x_{2,11} x_{2,12} + z_{12}^4 x_{2,21} x_{2,22} + z_{13}^2 &= 0, \\ z_{21}^4 x_{1,111} x_{2,11} x_{2,21} + z_{22}^4 x_{2,12} x_{2,22} + z_{23}^2 &= 0, \\ \kappa z_{31}^2 x_{1,111} + z_{32}^2 + z_{33}^2 = 0, \quad z_{31}^2 x_{1,111} + z_{32}^2 + z_{34}^2 &= 0. \end{aligned} \quad (3.114)$$

Thus in blow-up one recovers the resolved  $\mathbb{Z}_4$  singularities by setting  $x_{1,111} = 0$ . The factorization of the  $F$ -term (3.114) then shows that there are the same 16 components as in the orbifold case discussed above. Similarly, by setting  $x_{2,ij} = 0$  with  $(i, j) = (2, 1), (1, 2), (2, 2)$ , we find the roots associated with the  $\mathbb{Z}_2$  fixed two-tori. This confirms that this model indeed resolves all singularities of the  $T^6/\mathbb{Z}_4$  orbifold.

#### The Maximal $T^6/\mathbb{Z}_4$ model on $D_2^2 \times A_1^2$

In the maximal model we have 16 separate exceptional coordinates  $x_{1,ijk}$  with gaugings  $U(1)_{E_{1,ijk}}$ , where  $i, j = 1, 2$  and  $k = 1, \dots, 4$  in the  $\mathbb{Z}_4$  sector, see Table 3.8. In addition, we have 9 coordinates  $x_{2,ij}$  and gaugings  $U(1)_{E_{2,jk}}$  with  $i, j = 1, 2, 3$  in the  $\mathbb{Z}_2$  sector. The resulting  $D$ -terms are given by

$$\begin{aligned} |z_{11}|^2 + |z_{12}|^2 + 2|z_{13}|^2 - 4|c_1|^2 &= a_1, \\ |z_{21}|^2 + |z_{22}|^2 + 2|z_{23}|^2 - 4|c_2|^2 &= a_2, \\ |z_{31}|^2 + |z_{32}|^2 + |z_{33}|^2 + |z_{34}|^2 - 2|c_3|^2 - 2|c'_3|^2 &= a_3, \\ |z_{1i}|^2 + |z_{2j}|^2 + 2|z_{3k}|^2 - 4|x_{1,ijk}|^2 &= b_{1,ijk}, \\ i, j = 1, 2, \quad k = 1, \dots, 4. \end{aligned} \quad (3.115)$$

In the orbifold and blow-up phases the  $F$ -terms reduce to

$$\begin{aligned} z_{11}^4 \prod_j x_{2,1j}^2 \prod_{j,k} x_{1,1jk} + z_{12}^4 \prod_j x_{2,2j}^2 \prod_{j,k} x_{1,2jk} + z_{13}^2 \prod_j x_{2,3j} &= 0, \\ z_{21}^4 \prod_i x_{2,i1}^2 \prod_{i,k} x_{1,i1k} + z_{22}^4 \prod_i x_{2,i2}^2 \prod_{i,k} x_{1,i2k} + z_{23}^2 \prod_i x_{2,i3} &= 0, \\ \kappa z_{31}^2 \prod_{i,j} x_{1,ij1} + z_{32}^2 \prod_{i,j} x_{1,ij2} + z_{33}^2 \prod_{i,j} x_{1,ij3} &= 0, \\ z_{31}^2 \prod_{i,j} x_{1,ij1} + z_{32}^2 \prod_{i,j} x_{1,ij2} + z_{34}^2 \prod_{i,j} x_{1,ij4} &= 0. \end{aligned} \quad (3.116)$$

As expected in the maximal model each  $\mathbb{Z}_4$  fixed point has its own exceptional coordinate and gauging. Indeed, in the blow-down regime we find  $\mathbb{Z}_4$  fixed points at  $z_{1i} = z_{2j} = z_{3k} = 0$ ,  $i, j \neq 3$ , and in blow-up their exceptional divisor counterparts  $x_{1,ijk} = 0$ .

### 3 GLSM description of Resolved Toroidal Orbifolds

However, some of the  $\mathbb{Z}_2$  fixed tori at  $z_{1i} = z_{2j} = 0$  cannot be uniquely identified. As long as  $(i, j) \neq (3, 3)$ , for each  $i, j$  we obtain a single fixed torus in a similar manner as above for the  $\mathbb{Z}_4$  fixed points. Contrary, in the case  $z_{13} = z_{23} = 0$  we find two distinct solutions to the relevant  $F$ -terms. To see this, we first fix all the values of all the non-zero  $x$  in the orbifold regime. It is then easy to see that each  $F$ -term has four solutions,  $z_{a1} = i^{n+1/2} z_{a2}$ ,  $n = 1, 2, 3, 4$ , i.e. 16 solutions altogether. The discrete actions in each of the two tori  $(z_{a1}, z_{a2}) \mapsto (i z_{a1}, -i z_{a2})$  identify the solutions in four quadruplets. The orbifold  $\mathbb{Z}_4$  further identifies pairs of them, so that in the end we still have two independent solutions. This shows that two  $\mathbb{Z}_2$  fixed two-tori remain indistinguishable. This can be understood by inspecting the space group of the orbifold. The fixed points/lines are in one to one correspondance to conjugacy classes with non-trivial twist. The GLSM just sees the Abelianization of the space group which is the point group times the involution group. Such indistinguishable fixed points/tori occur precisely if multiple conjugacy classes are mapped to one element of the Abelianization.

#### Non-Factorizable $T^6/\mathbb{Z}_4$ models

In the previous subsections we have discussed the minimal and maximal fully resolvable GLSMs of the  $T^6/\mathbb{Z}_4$  orbifold on the factorized lattice  $D_2^2 \times A_1^2$ . As for the  $T^6/\mathbb{Z}_3$  it is possible to construct a variety of models which have more gaugings than the minimal, yet less than the maximal models. Since the classification of all  $\mathbb{Z}_4$  models is straightforward but a little more complicated than for the  $\mathbb{Z}_3$  case, we refrain from presenting it here. Instead we demonstrate that in two special cases a novel possibility arises which was not present for the  $\mathbb{Z}_3$  models: We can construct  $\mathbb{Z}_4$  models on truly non-factorizable lattices.

For both orbifolds the construction of non-factorized lattices is the same: We choose exceptional gaugings that generate  $n$ -volutions which act on more than one two-torus simultaneously. As we discussed in subsection 3.3.1 in the  $\mathbb{Z}_3$  case it is always possible to find an off-diagonal Kähler deformation to bring the non-factorized lattice back to a the factorized form. In the  $\mathbb{Z}_4$  case there are some non-factorized lattices that cannot be deformed to a factorized version, because the required off-diagonal Kähler deformations simply do not exist. Hence, these are genuinely non-factorizable. As a consequence, these models have a different amount of fixed tori than the factorizable case, and thus correspond to truly different topologies.

Below we present two GLSMs which yield  $\mathbb{Z}_4$  orbifolds based on the lattices  $A_3 \times D_2 \times A_1$  and  $A_3 \times A_3$ . In particular we show that as the lattice becomes less factorizable the number of fixed tori decreases, whereas the amount of fixed  $T^2/\mathbb{Z}_2$ 's and  $\mathbb{Z}_4$  fixed points stays the same. Together with the factorizable case on  $D_2^2 \times A_1^2$  we thus can realize all  $\mathbb{Z}_4$  orbifolds classified in theorem 1 of [21] (see also Table 2.1 of [47]).

### 3.3 (2,2) Models of Resolved Toroidal Orbifolds

#### Non-factorizable GLSM on $A_3 \times D_2 \times A_1$

In the first model we just add one extra coordinate to the minimal model: We choose the coordinates  $x_{1,111}$  and  $x_{1,122}$  with their  $U(1)$  gaugings. Moreover, in order to resolve the  $\mathbb{Z}_2$  singularities we also need all  $x_{2,ij}$  with  $i, j = 1, 2$  plus gaugings, even though they do not introduce further discrete symmetries. In this setup we focus on the action of  $\theta_{1,111}\theta_{1,122}^3$ :

$$\alpha_1 = \theta_{1,111}\theta_{1,122}^3 : (z_{21}, z_{22}, z_{31}, z_{32}) \longmapsto (i z_{21}, -i z_{22}, -z_{31}, -z_{32}). \quad (3.117)$$

This is a freely acting  $\mathbb{Z}_2$  element on the homogeneous torus coordinates, thus a simultaneous shift in the second and third torus. In appendix B we show that modding it out of the torus results in the root lattice of the Lie algebra  $A_3 \times D_2 \times A_1$ . Contrary to the  $\mathbb{Z}_3$  orbifold, the off-diagonal Kähler modulus which would mix the second and third torus is not orbifold invariant and thus does not exist. Therefore, in this case our construction gives a truly non-factorizable lattice.

The topology of the resulting non-factorizable orbifold is indeed different from its factorized counterpart. To show this, we inspect the fixed point and fixed torus structure. There are eight  $\theta_{1,111}$  fixed points at  $z_{11} = z_{21} = z_{31} = 0$  and eight  $\theta_{1,122}$  fixed points at  $z_{11} = z_{22} = z_{32} = 0$ . The fixed tori in the  $\mathbb{Z}_2$  sector are described by the same zero loci as in the minimal model. The factorization of the  $F$ -terms shows that there are two fixed tori at  $z_{11} = z_{21} = 0$  and two at  $z_{11} = z_{22} = 0$ , but just one at  $z_{12} = z_{21} = 0$  and  $z_{12} = z_{22} = 0$  each. One can easily convince oneself that there are no more fixed points when  $\theta^2$  actions are combined with  $U(1)_R$  rotations. This is exactly the right amount of fixed tori expected on this lattice, see e.g. [47]. Note that due to the presence of the coordinates  $x_{2,ij}$ , all fixed tori can be blown up, thus this model is fully resolvable.

#### Non-factorizable GLSM on $A_3 \times A_3$

In the case discussed above we went from the minimal model on the factorized lattice  $D_2^2 \times A_1^2$  to the non-factorizable case  $A_3 \times D_2 \times A_1$  by modding out one discrete  $\mathbb{Z}_2$  element. We can repeat this operation again to obtain a  $\mathbb{Z}_4$  orbifold on the  $A_3 \times A_3$  lattice. The GLSM realization of this, as a fully resolvable model, requires the fields  $x_{1,111}$ ,  $x_{1,122}$ ,  $x_{1,213}$  and  $x_{1,224}$ . Again, resolving the  $\mathbb{Z}_2$  singularities requires the coordinates  $x_{2,ij}$  with  $i, j = 1, 2$ , which are the same ones as for the minimal model.

Let us look at the discrete symmetries that get induced on the  $z_{ak}$  in this setup. They form a  $\mathbb{Z}_4 \times \mathbb{Z}_2 \times \mathbb{Z}_2$  group, generated by  $\theta_{1,111}$ ,  $\alpha_1$  as defined in (3.117) and

$$\alpha_2 := \theta_{1,111}\theta_{1,213}^3 : (z_{11}, z_{12}, z_{31}, z_{33}) \longmapsto (i z_{11}, -i z_{12}, -z_{31}, -z_{33}). \quad (3.118)$$

### 3 GLSM description of Resolved Toroidal Orbifolds

The  $\theta_{1,224}$  induced by a vev of  $x_{1,224}$  is generated as  $\theta_{1,111}\alpha_1\alpha_2$  together with some  $U(1)_R$  rotations. Therefore, including  $x_{1,224}$  does not enhance the discrete symmetry group. Rather the  $U(1)_{E_{1,224}}$  gauging is necessary to be able to resolve the fixed points which would be present at  $z_{12} = z_{22} = z_{34} = 0$  otherwise.

The topology of this non-factorizable orbifold is again different from the previous case. Inspecting the  $F$ -terms we find a multiplicity of four for each of these fixed points, i.e. again there are 16 fixed points altogether. Furthermore, we find fixed tori of the various  $\theta_{1,ijk}^2$  actions, with  $(i, j, k) = (1, 1, 1), (1, 2, 2), (2, 1, 3)$  and  $(2, 2, 4)$ , at  $z_{1i} = z_{2j} = 0$ , respectively. Each of them has multiplicity one, i.e. there are four fixed tori, each of which is orbifolded to  $T^2/\mathbb{Z}_2$  by the residual  $\mathbb{Z}_2$ . One can check that there are indeed no further fixed tori than the ones identified here. This again agrees with the results on this lattice by [47].

## 3.4 (2,0) Models

In  $(2, 2)$  models one always obtains target space theories with gauge group  $E_6 \times E_8$  and with the number of **27** and  $\overline{\mathbf{27}}$  given by the Hodge numbers  $h^{1,1}$  and  $h^{2,1}$ . Since  $E_6$  contains the SM gauge group in a nice chain of GUT subgroups, and the decomposition of the **27** representation contains all required matter and Higgs multiplets, one could take such a theory as a starting point for realistic models. The further gauge symmetry breaking could e.g. be realized by free discrete symmetries and the associated free Wilson lines. However, such a situation is difficult to find, and in heterotic orbifold resolutions the net number of **27**s, which is half the Euler number, is too high to reduce it to the required three families by dividing out free symmetries. Thus it is phenomenologically more appealing to study  $(2, 0)$  models which allow for a wider class of vector bundles and thus for four-dimensional spectra. However, many nice properties of the  $(2, 2)$  models are lost like the automatic anomaly freedom and stability of the bundle. These things have to be checked explicitly in  $(2, 0)$  constructions which makes them much harder to study. In particular, for good phenomenological models one has to switch on almost all of the Wilson lines, which implies that a GLSM construction would require many  $U(1)$  gaugings and thus be restricted by many anomaly cancellation conditions. One could try to cure this with the WS GS mechanism presented in section 3.2.2 but this would deform the geometry such that the smooth connection to the singular orbifold theory, which is well defined, would be lost. Here we will not be able to show a fully consistent  $(2, 0)$  model. Instead we present how a possible line bundle model would look in the GLSM realization. One problem of such a line bundle would be that it does not provide additional chiral fields whose charges are opposite to the coordinate chiral fields. Thus the Landau–Ginzburg phase, where the FI parameters take negative values, of such models would not be defined. The hope is that a cure of this problem could also cure the anomaly conditions, eventually in such a way

that in the geometric regime no additional bundle dofs are generated besides the line bundle. But this is left for future investigation.

### 3.4.1 Line and Vector Bundles

The GLSM offers a framework to construct vector bundles on the target space in terms of the monad complex. The basic bundle dofs are the chiral-fermi multiplets  $\Lambda^A$  whose lowest component is a left-moving fermion. Having only these fields one would describe a sum over line bundles where the charges  $Q_I^A = Q_I(\Lambda^A)$  are the coefficients of its curvature, or equivalently its first Chern class, in terms of the divisors,

$$F^A = c_1(\mathcal{O}(Q_I^A)) = \sum_I Q_I^A \tilde{D}^I, \quad (3.119)$$

where  $\tilde{D}^I$  are divisors whose defining polynomials are only charged under the  $I^{\text{th}}$   $U(1)$ , as in section 3.1. Such a line bundle is rather easy to study since its properties only depend on  $c_1$ . In heterotic orbifold resolutions there is evidence that such line bundles arise from single oscillatorless blow-up modes, as will be discussed in section 4.1.

Now there are two possibilities to restrict the bundle dofs. The first one is to introduce chiral fields  $\Phi^i$  whose charge is such that in the geometric regime their bosonic components are not allowed to get vevs. This has to be ensured by the  $F$ -terms of the chiral fermi fields  $\Lambda^A$  by superpotential couplings of the form (3.58). As discussed, this generates mass terms in which the left-moving  $\Lambda$  fermionic components pair up with the right-moving fermions in  $\Phi$  to build a massive Dirac fermion which decouples in the IR limit. This results in a vector bundle which is the kernel of the maps  $N(\Psi)$  in (3.58). If this kernel still has a global sections, they need to be removed by introducing fermionic gaugings. In these fermionic gaugings the holomorphic functions  $M(\Psi)$  represent the global sections which are to be gauged away.

We in particular want to discuss the quantization conditions on the line bundles which arise in heterotic models on resolved orbifolds. There are three different approaches to these quantization conditions and we will show at an example that they are all equivalent. The first one is the identification of the bundle vectors with the local orbifold shifts. The second one is the SUGRA quantization requirement, stating that the integral of the flux over each curve must lie in the  $E_8 \times E_8$  lattice. This will be discussed in section 4.1. The third one comes from the GLSM where one requires that the charges of the fields  $\Lambda$  must be quantized in the same units as the coordinate fields  $\Psi$ .

Superfield	$\mathcal{Z}_{1i}$	$\mathcal{Z}_{2j}$	$\mathcal{Z}_{3k}$	$\mathcal{X}_{1,jk}$	$\mathcal{X}_{2,ik}$	$\mathcal{X}_{3,ij}$	$\mathcal{C}_1, \mathcal{C}'_1$	$\mathcal{C}_2, \mathcal{C}'_2$	$\mathcal{C}_3, \mathcal{C}'_3$	$\Gamma^A$
$U(1)_{R_1}$	1	0	0	0	0	0	-2	0	0	0
$U(1)_{R_2}$	0	1	0	0	0	0	0	-2	0	0
$U(1)_{R_3}$	0	0	1	0	0	0	0	0	-2	0
$U(1)_{E_{1,\beta\gamma}}$	0	$\delta_{\beta j}$	$\delta_{\gamma k}$	$-2\delta_{\beta j}\delta_{\gamma k}$	0	0	0	0	0	$Q_{E_{1,\beta\gamma}}^A$
$U(1)_{E_{2,\alpha\gamma}}$	$\delta_{\alpha i}$	0	$\delta_{\gamma k}$	0	$-2\delta_{\alpha i}\delta_{\gamma k}$	0	0	0	0	$Q_{E_{2,\alpha\gamma}}^A$
$U(1)_{E_{3,\alpha\beta}}$	$\delta_{\alpha i}$	$\delta_{\beta j}$	0	0	0	$-2\delta_{\alpha i}\delta_{\beta j}$	0	0	0	$Q_{E_{3,\alpha\beta}}^A$

Table 3.9: The superfield content and charge assignment for the maximal fully resolvable GLSM of  $T^6/\mathbb{Z}_2 \times \mathbb{Z}_2$ . The indices  $\alpha, \beta, \gamma$  and  $i, j, k$  run from 1 to 4. As this is a  $(2, 0)$  model, the  $\mathcal{Z}$  and  $\mathcal{X}$  fields are  $(2, 0)$  chiral fields, whereas the  $\mathcal{C}$  and  $\Gamma^A$  are chiral fermi.



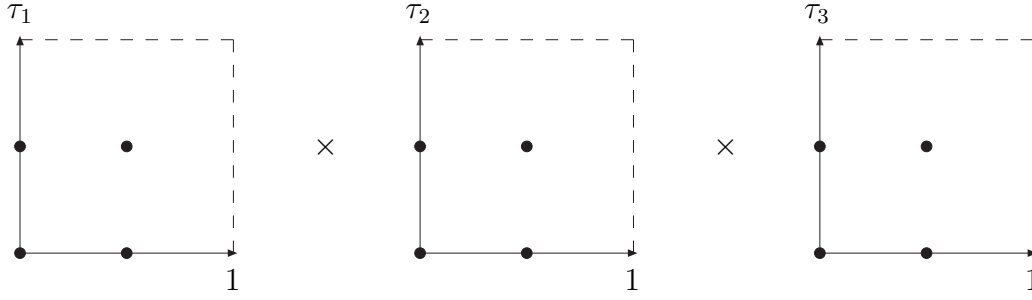


Figure 3.3: Geometry of the  $\mathbb{Z}_2 \times \mathbb{Z}_2$  orbifold. The dots show where the fixed lines are located in each torus. The product of two points corresponds to a fixed torus. The product of three dots is a point in which fixed tori intersect.

### The Model: Line Bundles on $\mathbb{Z}_2 \times \mathbb{Z}_2$ on $A_1^6$

As a model to study these issues we choose the  $T^6/\mathbb{Z}_2 \times \mathbb{Z}_2$  orbifold on a factorizable lattice  $A_1^6$ . First we review the classical construction. The torus is based on a factorizable lattice where the complex structure  $\tau_a$  in each torus is unconstrained, i.e. each two-lattice is spanned by 1 and  $\tau_a$ . The point group acts on the coordinates  $u_a$  as

$$\theta_a : u_b \mapsto -(-1)^{\delta_{ab}} u_b, \quad a, b = 1, 2, 3, \quad (3.120)$$

i.e.  $\theta_a$  rotates all coordinates by  $\pi$  except  $u_a$ . In other terms, the twist vectors are

$$v_1 = (0, 1/2, -1/2), \quad v_2 = (-1/2, 0, 1/2), \quad v_3 = (1/2, -1/2, 0). \quad (3.121)$$

Each  $\theta_a$  has 16 fixed lines called  $F_{a,\rho\sigma}$  where

$$F_{a,\rho\sigma} = \{u_b = u_b^\rho, u_c = u_c^\sigma\}, \quad \text{with } a \neq b < c \neq a, \quad (3.122)$$

$$\vec{u}_d = (0, 1/2, \tau_d/2, (1 + \tau_d)/2).$$

Thus altogether there are 16 fixed lines  $F_{1,\beta\gamma}$ ,  $F_{2,\alpha\gamma}$  and  $F_{3,\alpha\beta}$ . These lines intersect at 64 fixed points given by  $(u_1^\alpha, u_2^\beta, u_3^\gamma)$ . The Abelianization of the space group is a group isomorphic to  $\mathbb{Z}_2^8$ , where, as usual, a  $\mathbb{Z}_2 \times \mathbb{Z}_2$  factor represents the point group, whereas the other  $\mathbb{Z}_2$ 's represent the six lattice basis vectors. Therefore, the orbifold CFT has two independent shift vectors  $V_1$  and  $V_2$  and six Wilson line  $W_1, \dots, W_6$ , each of them being of order two.

On the GLSM side we use the maximal GLSM construction for this in order to obtain maximal independent data. It has precisely 51  $U(1)$  gaugings which divide into three corresponding to the untwisted (1, 1) forms  $du^a \wedge d\bar{u}^a$ , and 48, one for each twisted sector, so it does not miss any (1, 1) form on the resolution.

### 3 GLSM description of Resolved Toroidal Orbifolds

The charge assignment is shown in table 3.9. The  $D$ -terms for this case are

$$\sum_{\rho=1}^4 |z_{a\rho}|^2 - 2|c_a|^2 - 2|c'_a|^2 = a_a, \quad a = 1, 2, 3, \quad (3.123a)$$

$$|z_{2,\beta}|^2 + |z_{3,\gamma}|^2 - 2|x_{1,\beta\gamma}|^2 = b_{1,\beta\gamma}, \quad \beta, \gamma = 1, 2, 3, 4, \quad (3.123b)$$

$$|z_{1,\alpha}|^2 + |z_{3,\gamma}|^2 - 2|x_{2,\alpha\gamma}|^2 = b_{2,\alpha\gamma}, \quad \alpha, \gamma = 1, 2, 3, 4, \quad (3.123c)$$

$$|z_{1,\alpha}|^2 + |z_{2,\beta}|^2 - 2|x_{3,\alpha\beta}|^2 = b_{3,\alpha\beta}, \quad \alpha, \beta = 1, 2, 3, 4. \quad (3.123d)$$

We will work in the blow-up regime where  $0 < b_{1,\beta\gamma}, b_{2,\alpha\gamma}, b_{3,\alpha\beta} \ll a_a$  to ensure a smooth geometry. We define the divisors

$$\begin{aligned} D_{a,\rho} &:= \{z_{a,\rho} = 0\}, & E_{k,\rho\sigma} &:= \{x_{k,\rho\sigma} = 0\}, \\ R_a &:= \left\{ \sum c_{a\rho} z_{a\rho}^2 \prod x^2 = 0 \right\}, \end{aligned} \quad (3.124)$$

where the “ $\prod x^2$ ” stands for an appropriate monomial in the  $x_{k,\rho\sigma}$  in order to make the polynomial neutral under the  $U(1)_{E_{k,\rho\sigma}}$ . The  $R_a$  are not rigid, but rather the  $c_{a\rho}$  encode the information on their locus. For the  $\mathbb{Z}_2 \times \mathbb{Z}_2$  case the topology of the resolution is not unique. Instead, for each local resolution there are four possible triangulations which are related by flop transitions. To see this, for fixed and dropped indices  $\alpha\beta\gamma$ , we look at the following linear combinations of the  $D$ -terms:

$$(3.123b) + (3.123c) - (3.123d) :$$

$$2(|x_3|^2 + |z_3|^2 - |x_1|^2 - |x_2|^2) = b_1 + b_2 - b_3, \quad (3.125)$$

$$(3.123b) - (3.123c) + (3.123d) :$$

$$2(|x_2|^2 + |z_2|^2 - |x_1|^2 - |x_3|^2) = b_1 - b_2 + b_3, \quad (3.126)$$

$$- (3.123b) + (3.123c) + (3.123d) :$$

$$2(|x_1|^2 + |z_a|^2 - |x_2|^2 - |x_3|^2) = -b_1 + b_2 + b_3. \quad (3.127)$$

These  $D$ -terms look like conifold  $D$ -terms and thus we can identify flop transitions. E.g. at  $b_1 + b_2 > b_3$  we find that the curve  $E_1 E_2$  exists and the curve  $D_3 E_3$  does not, whereas for  $b_1 + b_2 < b_3$  it is the other way around. In [41] it was shown that when identifying the  $b_r$  and  $a_a$  with the Kähler parameters of the Kähler form, then the flops occur at exactly the same positions which one can view as a hint for a linear relation between them. For more details on the local phase structure we refer to [41] and [44]. Here we will just need the intersection numbers to perform further calculations in the classical geometric regime.

In [41] they were obtained by the means of an auxiliary polyhedron which was introduced in [47]. Here, however, we can deduce the intersection numbers in a rigorous way from the GLSM setup. Although the method of [47] reproduced the correct intersection numbers for the factorizable orbifold, it was not able to construct the correct intersection numbers for non-factorizable orbifolds. For example, the intersection numbers on the resolved  $\mathbb{Z}_2 \times \mathbb{Z}_2$  orbifold on the  $A_3 \times A_1^3$  lattice, which is equivalent to the quotient of the factorizable case divided by a freely acting involution, as will be presented in 3.4.2, cannot be obtained. Instead they were calculated in [41], and these calculations are confirmed using the GLSM constructions introduced here.

After we identified the boundaries of the phases, we can label them by

Name	Condition
“ $E_1$ ”	$b_1 > b_2 + b_3$
“ $E_2$ ”	$b_2 > b_1 + b_3$
“ $E_3$ ”	$b_3 > b_1 + b_2$
“symm”	else

Going back to the global picture, this would give an enormous bunch of different triangulations. Naively, for each of the 64 choices of  $\alpha\beta\gamma$  there are four possible triangulations so one would expect a total number of  $4^{64}$ , when one does not consider symmetries. However, in the GLSM approach one can show that not all of these phases exist. The reason is that the GLSM reveals that the phases are controlled by the FI parameters  $b_r$ , thus only phases are realized for which one can find a choice of FI parameters which reproduces it. For example, consider the following triangulation.

Fixed Point ( $\alpha\beta\gamma$ )	Triangulation	Condition
(1, 1, 1)	“ $E_1$ ”	$b_{1,11} > b_{2,11} + b_{3,11}$
(1, 2, 1)	“ $E_2$ ”	$b_{2,11} > b_{1,21} + b_{3,12}$
(2, 2, 1)	“ $E_1$ ”	$b_{1,21} > b_{2,21} + b_{3,22}$
(2, 1, 1)	“ $E_2$ ”	$b_{2,21} > b_{1,11} + b_{3,21}$

When we add up these conditions, we obtain  $b_{3,11} + b_{3,12} + b_{3,22} + b_{3,21} < 0$ , which contradicts the full resolution condition for which all  $b_r$  have to be positive. It is very hard to tell how many of the  $4^{64}$  phases are realized, since performing the counting would be an exorbitant effort. But this at least tells that if one works in a particular global triangulation, one should first check if it is indeed allowed for some choice of FI parameters.

For simplicity we will work in phases where the triangulation is the same for all local resolutions ( $\alpha\beta\gamma$ ). This is easily achieved by equalizing all FI parameters of the same type, i.e.  $b_{1,\beta\gamma} \equiv b_1$ ,  $b_{2,\alpha\gamma} \equiv b_2$  and  $b_{3,\alpha\beta} \equiv b_3$ . Then we are left with four smooth phases. The intersection numbers of the  $E_r$  and  $R_a$  divisors are given in table 3.10. The intersection numbers involving the divisors  $D_{a,\sigma}$  can be

### 3 GLSM description of Resolved Toroidal Orbifolds

Int( $S_1 S_2 S_3$ ) \ Triangulation	“ $E_1$ ”	“ $E_2$ ”	“ $E_3$ ”	“ <i>symm</i> ”
$E_{1,\beta\gamma} E_{2,\alpha\gamma} E_{3,\alpha\beta}$	0	0	0	1
$E_{1,\beta\gamma} E_{2,\alpha\gamma}^2, E_{1,\beta\gamma} E_{3,\alpha\beta}^2$	-2	0	0	-1
$E_{2,\alpha\gamma} E_{1,\beta\gamma}^2, E_{2,\alpha\gamma} E_{3,\alpha\beta}^2$	0	-2	0	-1
$E_{3,\alpha\beta} E_{1,\beta\gamma}^2, E_{3,\alpha\beta} E_{2,\alpha\gamma}^2$	0	0	-2	-1
$E_{1,\beta\gamma}^3$	0	8	8	4
$E_{2,\alpha\gamma}^3$	8	0	8	4
$E_{3,\alpha\beta}^3$	8	8	0	4
$R_1 R_2 R_3$	2			
$R_1 E_{1,\beta\gamma}^2, R_2 E_{2,\alpha\gamma}^2, R_3 E_{3,\alpha\beta}^2$	-2			

Table 3.10: The upper part gives the intersection numbers when using the same triangulation at all 64 fixed points. The lower part gives the triangulation-independent intersection numbers.

obtained from them using the linear equivalence relations among them. These linear equivalence relations are found by taking the definition of the inherited divisors in (3.124) and taking the limit  $c_{\alpha\rho} \rightarrow \delta_{\rho\sigma}$ . Then the defining equation for  $R_a$  factorizes and we find

$$\begin{aligned}
 R_1 &\sim 2D_{1\alpha} + \sum_{\gamma} E_{2,\alpha\gamma} + \sum_{\beta} E_{3,\alpha\beta}, \\
 R_2 &\sim 2D_{2\beta} + \sum_{\gamma} E_{1,\beta\gamma} + \sum_{\alpha} E_{3,\alpha\beta}, \\
 R_3 &\sim 2D_{3\gamma} + \sum_{\beta} E_{1,\beta\gamma} + \sum_{\alpha} E_{2,\alpha\gamma}.
 \end{aligned} \tag{3.128}$$

Next, we put a sum of line bundles on the resolved space. In the GLSM this is done by adding chiral fermi fields  $\Lambda^I = \lambda^I + \dots$  with  $I = 1, \dots, 16$  with charges  $Q_r^I$ . These charges need to be specified a bit more. Since our intention is to get contact to an orbifold CFT in blow-down, we have to reproduce the correct transformation behavior under the space group. The fermionic formulation of the heterotic string, we have 16 left-moving fermions  $\lambda^I$  which under a space group element transform as  $\lambda^I \mapsto e^{2\pi i V_g^I} \lambda^I$ , where  $V_g$  is the local shift. In the blow-down limit of the orbifold in the GLSM description we do not recover the whole space group, but rather its Abelianization. In particular, the class of the space group element  $g$  which creates the fixed point  $F_{k,\rho\sigma} = \{z_{i\rho} = z_{j\sigma} = 0\}$ , where  $i \neq j \neq k \neq i$ , precisely corresponds to the  $\mathbb{Z}_2$  group which is generated by breaking the  $U(1)_{E_{k,\rho\sigma}}$  by the vev of  $x_{k,\rho\sigma}$ . Applying this on the left-moving

fermion on both sides we find the identification

$$Q_{E_{k,\rho\sigma}}^I = 2V_g^I \pmod{2}. \quad (3.129)$$

The charges w.r.t. to  $U(1)_{R_a}$  are chosen to be zero since they would be visible on the orbifold in terms of non-trivial flux on the two-tori. Altogether, this provides some link between the orbifold CFT data in terms of shift vectors and Wilson lines, and the GLSM charges of the chiral fermi fields.

### Modular Invariance versus Anomaly

On both, the CFT and the GLSM side we have consistency conditions in form of quadratic equations. On the orbifold side, they come from one-loop diagrams where the worldsheet is described as a genus one Riemann surface, i.e. a two-torus. The invariance of the one-loop partition function under the modular group  $SL(2, \mathbb{Z})$  implies conditions on the shift vectors and Wilson lines, which can be summarized as

$$2 \cdot (V_g^2 - v_g^2) = 0 \pmod{2} \quad \text{for all local twists } V_g \text{ and } v_g^2 = v_a^2 = 1/2. \quad (3.130)$$

The fact that these conditions are mod conditions reflects that the shifts and Wilson lines need only be specified up to  $\Lambda_{E_8 \times E_8}$  lattice vectors<sup>7</sup>. The (2,0) gauge anomaly conditions on the other hand are

$$\sum_m q_r^m q_s^m - \sum_\mu Q_r^\mu Q_s^\mu = 0. \quad (3.131)$$

Here  $m$  runs over all chiral fields,  $\mu$  runs over all chiral fermi fields and  $r$  and  $s$  run over all  $U(1)$  factors. These conditions are much more stringent since on the one hand they are no longer mod conditions, and on the other hand they also involve mixed products. In particular, using such line bundles only it is not possible to solve all anomaly conditions simultaneously, since e.g. the anomalies involving the  $U(1)_{R_a}$  are not addressed at all. Writing down a fully anomaly free (2,0) GLSM with just line bundles and a connectivity to an orbifold CFT is a yet unsolved problem which is subject to future investigation. However, the conditions for the pure  $U(1)_{E_{k,\rho\sigma}}^2$  anomalies are

$$6 - \sum_A Q_{E_{k,\rho\sigma}}^A Q_{E_{k,\rho\sigma}}^A = 0, \quad (3.132)$$

where now the sum runs only over the fields  $\Lambda^A$ , so using the identification (3.129) they indeed reproduce the modular invariance conditions.

---

<sup>7</sup>In fact, shifting  $V_a$  and  $W_\alpha$  by a lattice vector can lead to a modification of the projection conditions in the twisted sectors. This corresponds to switching on discrete torsion phases [24] which in turn can be used to undo this shift. Thus one can say that  $V_a$  and  $W_\alpha$  defined up to lattice vectors if one considers discrete torsion.

### Flux Quantization in the GLSM

One could ask the question if one can allow for line bundles on resolved orbifolds which do not allow for an identification like (3.129). This is equivalent to the question, what the quantization conditions are on the charges of the chiral fermi fields. For a well defined transformation property on the target space, the fermion charges must be quantized in the same units as the coordinate fields. In other words, they may only take values in the lattice spanned by the charges of the chiral fields. For the maximal  $\mathbb{Z}_2 \times \mathbb{Z}_2$  it might look like all integer charges are allowed since each  $U(1)$  has a field with charge one, however this is not the case. The  $U(1)$  basis shown in table 3.9 is chosen such because it is nicely symmetric in the fixed points  $(\alpha\beta\gamma)$  and, from its structure, it reveals the interpretation of the target space as (resolved) orbifold. But we can identify certain "mixed"  $U(1)$ s which are fractional linear combinations of the given  $U(1)$ 's but still all chiral fields have integral charges, and thus also the  $\Lambda^A$  must so. In principle one must also include the chiral fermi fields  $\mathcal{C}_a, \mathcal{C}'_a$  in the quantization conditions, but this is trivially fulfilled since their charges are chosen such that they neutralize a homogeneous polynomial of the chiral fields. Let us inspect such fractional mixed  $U(1)$ s. First, we find 64 of the form,

$$\frac{1}{2} (U(1)_{E_{1,\beta\gamma}} + U(1)_{E_{2,\alpha\gamma}} + U(1)_{E_{3,\alpha\beta}}) . \quad (3.133)$$

They imply quantization conditions,

$$Q_{E_{1,\beta\gamma}}^A + Q_{E_{2,\alpha\gamma}}^A + Q_{E_{3,\alpha\beta}}^A = 0 \text{ mod } 2 . \quad (3.134)$$

Furthermore, involving also the  $U(1)_{R_a}$ , one finds 24 more such mixed  $U(1)$ s, namely

$$\begin{aligned} & \frac{1}{2} \left( U(1)_{R_1} + \sum_{\beta} U(1)_{E_{3,\alpha\beta}} \right) , & \frac{1}{2} \left( U(1)_{R_1} + \sum_{\gamma} U(1)_{E_{2,\alpha\gamma}} \right) , \\ & \frac{1}{2} \left( U(1)_{R_2} + \sum_{\alpha} U(1)_{E_{3,\alpha\beta}} \right) , & \frac{1}{2} \left( U(1)_{R_2} + \sum_{\gamma} U(1)_{E_{1,\beta\gamma}} \right) , \\ & \frac{1}{2} \left( U(1)_{R_3} + \sum_{\alpha} U(1)_{E_{2,\alpha\gamma}} \right) , & \frac{1}{2} \left( U(1)_{R_3} + \sum_{\beta} U(1)_{E_{1,\beta\gamma}} \right) , \end{aligned} \quad (3.135)$$

where the unsummed index runs from  $1, \dots, 4$ . They imply that

$$\begin{aligned} \sum_{\beta} Q_{E_{3,\alpha\beta}}^A &= 0 \text{ mod } 2 , & \sum_{\gamma} Q_{E_{2,\alpha\gamma}}^A &= 0 \text{ mod } 2 , \\ \sum_{\alpha} Q_{E_{3,\alpha\beta}}^A &= 0 \text{ mod } 2 , & \sum_{\gamma} Q_{E_{1,\beta\gamma}}^A &= 0 \text{ mod } 2 , \\ \sum_{\alpha} Q_{E_{2,\alpha\gamma}}^A &= 0 \text{ mod } 2 , & \sum_{\beta} Q_{E_{1,\beta\gamma}}^A &= 0 \text{ mod } 2 . \end{aligned} \quad (3.136)$$

There is a further condition on the charges. In order to result in an  $E_8 \times E_8$  string theory, the first Chern class of the bundle must be an even class. This implies that  $\sum_I Q_r^I = 0 \pmod{2}$  for all  $r$ , i.e. the  $Q^r$  must be root vectors of  $SO(16)$ . Vectors in the spinor lattice of  $SO(16)$  are not realizable this way, but for many models one can perform a Weyl reflection in the  $E_8 \times E_8$  lattice such that they all lie in the  $SO(16)$  root lattice. In appendix C we show that the conditions (3.134) and (3.136) imply that the charges must indeed fulfill the conditions (3.129). Thus, in this context one finds no obstruction that all consistent GLSM models can be traced back to orbifold models formulated as free CFTs. Later, in section 4.1 we will observe that the same conditions arise from the flux quantization in the SUGRA theory.

### 3.4.2 Freely Acting Discrete Symmetries

In typical Calabi–Yau models one needs a freely acting discrete symmetry for a hypercharge preserving  $SU(5)$  GUT breaking [52]. The model we constructed in [40, 41] is such an example which builds up on a  $\mathbb{Z}_2 \times \mathbb{Z}_2$  orbifold on which an involutive  $\mathbb{Z}2free$  acts, and a blow-up is performed in a way which preserves the  $\mathbb{Z}2free$ . By modding out a discrete freely acting symmetry  $G$  obtains a non-simply connected manifold where the fundamental group is equal to  $G$ . By extending the  $G$  action into the gauge degrees of freedom one obtains the possibility to switch on discrete Wilson lines, to which we will refer as free Wilson lines. Now a theorem in algebraic geometry states that a complete intersection in a toric variety is always simply connected, if it is not an elliptic curve or a product thereof. This means that by standard GLSMs with it is not possible to generate such freely acting discrete symmetries as remnants of  $U(1)$  gaugings. We will demonstrate this for the  $\mathbb{Z}_2 \times \mathbb{Z}_2$  orbifold where we can identify a huge group of torus involutions, however, only those can be generated by broken  $U(1)$ s which preserve the simply-connectedness. However, such symmetries can still be identified but then must be modded out by hand, which might lead to linear identifications between the coordinates and gaugings.

**Example:**  $\mathbb{Z}_2 \times \mathbb{Z}_2 \times \mathbb{Z}_{2,free}$

As a first example we demonstrate the freely acting  $\mathbb{Z}2free$  symmetries in a factorizable  $\mathbb{Z}_2 \times \mathbb{Z}_2$  orbifold. The lattice identifications are

$$u_a \sim u_a + 1 \sim u_a + \tau_a, \quad a = 1, 2, 3, \quad (3.137)$$

$\tau_a$  being the complex structure modulus in each torus, and the point groups acts as

$$\theta_a : z_{b \neq a} \mapsto -z_b, \quad z_a \mapsto z_a, \quad a = 1, 2, 3. \quad (3.138)$$

### 3 GLSM description of Resolved Toroidal Orbifolds

The fixed point structure is the following. Each  $\theta_a$  leaves the  $a^{\text{th}}$  plane invariant and acts to second order in the other two planes, which results in  $4 \times 4 = 16$  fixed lines, which get twisted by the remaining  $\mathbb{Z}_2$ . Altogether this results in  $3 \times 16 = 48$  fixed lines which are labeled by  $(1, \beta\gamma)$ ,  $(2, \alpha\gamma)$  and  $(3, \alpha\beta)$ . To make this more concretely, we show the maximal GLSM model for this geometry. The field content with charges is shown in table 3.9. In the orbifold limit, when all FI parameters  $b_{1,\beta\gamma}$ ,  $b_{2,\alpha\gamma}$  and  $b_{3,\alpha\beta}$  are negative, we obtain a map to the flat coordinates  $u_a$  by the Weierstrass identifications done in section 3.1.2.

The action of the  $\mathbb{Z}_2^{\text{free}}$  on the flat coordinates is given by

$$\theta_{\text{free}} : (u_1, u_2, u_3) \mapsto \left( u_1 + \frac{\tau_1}{2}, u_2 + \frac{\tau_2}{2}, u_3 + \frac{\tau_3}{2} \right). \quad (3.139)$$

Using the Weierstrass map which was established in section 3.1.2, we can translate the  $\theta_{\text{free}}$  action to the homogeneous coordinates. It acts like  $\beta_2$  in equation (3.45) on all coordinates  $z_{ai}$  simultaneously. However, when interpreting equation (3.45) for this case, the values of the  $x$  fields have already been set to one against the  $\mathbb{C}^*$  scalings. Thus, in order to make  $\theta_{\text{free}}$  a symmetry of the whole theory, we have to extend it on the other objects in the theory. From the action on the  $z_{ai}$  we see that  $\theta_{\text{free}}$  basically permutes the indices  $\alpha\beta\gamma$  as  $1 \leftrightarrow 3$  and  $2 \leftrightarrow 4$ . Thus, we have to identify the exceptional coordinates and gaugings, and in the GLSM also the FI parameters, in the same way,

$$(x_{1\beta\gamma}, U(1)_{E_{1\beta\gamma}}, b_{1\beta\gamma}) \leftrightarrow (x_{1,\beta+2,\gamma+2}, U(1)_{E_{1,\beta+2,\gamma+2}}, b_{1,\beta+2,\gamma+2}), \quad (3.140)$$

$$(x_{2\alpha\gamma}, U(1)_{E_{2\alpha\gamma}}, b_{2\alpha\gamma}) \leftrightarrow (x_{2,\alpha+2,\gamma+2}, U(1)_{E_{2,\alpha+2,\gamma+2}}, b_{2,\alpha+2,\gamma+2}), \quad (3.141)$$

$$(x_{3\alpha\beta}, U(1)_{E_{3\alpha\beta}}, b_{3\alpha\beta}) \leftrightarrow (x_{3,\alpha+2,\beta+2}, U(1)_{E_{3,\alpha+2,\beta+2}}, b_{3,\alpha+2,\beta+2}), \quad (3.142)$$

where the addition of the indices is taken modulo four. In the symplectic quotient there might appear some factors in the identifications in order to make the  $D$ -terms invariant. However, in the holomorphic quotient construction the map always works without prefactors if the fan possesses the required symmetry. One drawback of such a construction would be that the  $\mathbb{Z}_{2,\text{free}}$  enters a semidirect product with the  $U(1)$  gaugings on the worldsheet, thus making the group non-Abelian.

Another possibility would be to start with the minimal model of the  $\mathbb{Z}_2 \times \mathbb{Z}_2$  orbifold and identify the  $\mathbb{Z}_{2,\text{free}}$  action there. Since on the  $\mathbb{Z}_2 \times \mathbb{Z}_2$  orbifold the geometry of all fixed tori and their intersection points is the same, we only need one set of exceptional coordinates to obtain a fully resolvable model. The field content and the charges can be obtained from the maximal model by reducing the exceptional coordinates and gaugings such that the indices just are  $\alpha = \beta =$



$\gamma = 1$  and thus can be dropped. Then the  $F$ -terms become

$$\begin{aligned}
 \kappa_1 z_{11}^2 x_2 x_3 + z_{12}^2 + z_{13}^2 &= 0, \\
 z_{11}^2 x_2 x_3 + z_{12}^2 + z_{14}^2 &= 0, \\
 \kappa_2 z_{21}^2 x_1 x_3 + z_{22}^2 + z_{23}^2 &= 0, \\
 z_{21}^2 x_1 x_3 + z_{22}^2 + z_{24}^2 &= 0, \\
 \kappa_3 z_{31}^2 x_1 x_2 + z_{32}^2 + z_{33}^2 &= 0, \\
 z_{31}^2 x_1 x_2 + z_{32}^2 + z_{34}^2 &= 0.
 \end{aligned} \tag{3.143}$$

On the fixed points,  $z_{11} = z_{21} = z_{31} = 0$ , the  $F$  terms become quadratic equation in two (homogeneous) variables and thus factorize into two solutions each. Thus it immediately describes all 64 fixed points which lie at  $z_{a3}/z_{a2} = \pm 1$ ,  $z_{a4}/z_{a2} = \pm 1$ . In fact we have a  $\mathbb{Z}_2^6$  involutive symmetry which interchanges all the fixed points and acts precisely by sign flips of the homogeneous coordinates. Thus the  $\mathbb{Z}_{2,\text{free}}$  can be realized as a subgroup of this and modded out by hand. One realization of this would be

$$\theta_{\text{free}}(z_{a1}, z_{a2}, z_{a3}, z_{a4}) \longmapsto (-z_{a1}, z_{a2}, -z_{a3}, z_{a4}), \tag{3.144}$$

for all  $a$  simultaneously. In fact we saw that if one adds more exceptional coordinates and gaugings, part of this involution group can indeed be modded out. The extreme case was the maximal model where the whole involution group is modded out. Thus one could hope that this freely acting symmetry is realizable in some intermediate model. However, one can argue that this is not possible. As a first argument, the involutions one creates this way always arise due to multiple exceptional gaugings  $U(1)_{E_{k,\rho\sigma}}$  in the same sector  $k$  which differ in the indices  $\rho$  and  $\sigma$  which belong to the two tori. Therefore such involutions always act in one or two tori simultaneously, but never in three as is required for  $\theta_{\text{free}}$ . Another argument is that the resulting space, if it is blown up, is a smooth complete intersection CY in an ambient toric variety. Now a theorem states that such spaces are always simply connected, whereas the  $\theta_{\text{free}}$ , as a freely acting element, creates a non-simply connected space. However, these constructions can still be used to deduce the intersection ring on the resolved spaces and use it for SUGRA models.

### 3 *GLSM description of Resolved Toroidal Orbifolds*

## 4 Phenomenology on Orbifold Resolutions

After having put so much effort in constructing the resolutions of toroidal orbifolds, it is our intention to study the physics which comes out of the compactification of heterotic string. In particular we are interested in what happens during the resolution process to see how the observable parameters depend on the geometrical moduli. Now the only framework where we can perform the resolution process continuously is the GLSM, but there it is very hard to get precise statements about properties of the target space theory. Instead we take the GLSM as a confirmation that such an interpolation is possible and will only work in the limiting regions where we can more easily do calculations. These regions are on the one hand the full string orbifold CFT which was introduced in chapter 2. The second theory is compactification of heterotic ten-dimensional supergravity on a smooth Calabi–Yau manifold with line bundles. The situation is depicted in figure 4.1. In fact, in cases where the resolution is not unique as  $\mathbb{Z}_2 \times \mathbb{Z}_2$ , there will be a whole bunch of resolution theories. Since the SUGRA theory is an approximation in the string length, stringy effects will a priori not be visible. One can think of these theories being valid approximations to string theories if the radii of the compactification space are large compared to the string length. We will find that the comparison of the various SUGRA limits with each other and the orbifold CFT will reveal concrete hints for stringy effects that would not have been visible in the theories themselves.

### 4.1 Effective SUGRA

Ten-dimensional heterotic supergravity is well known to an extent which is required here. The field content consists of the massless string modes, namely the graviton  $g_{MN}$ , the Kalb–Ramond field  $B_{MN}$ , the dilaton  $\phi$  and 496 gauge bosons  $A_M^a$  of  $E_8 \times E_8$ . The fermions are not mentioned here explicitly since their content follows from supersymmetry. The action up to second order in derivatives is roughly

$$S_{10D} \sim \int *R + H_3 \wedge *H_3 + d\phi \wedge *d\phi + \text{tr } F_2 \wedge *F_2 + B_2 \wedge X_8. \quad (4.1)$$

Here  $R$  is the curvature scalar,  $H_3 = dB_2 + \text{tr } \Omega_1 \wedge R_2 - \text{tr } A_1 \wedge F_2$ , where  $\Omega_1$  is the spin connection,  $R_2$  its curvature, and  $X_8$  is a polynomial in  $F_2$  and  $R_2$ .

#### 4 Phenomenology on Orbifold Resolutions

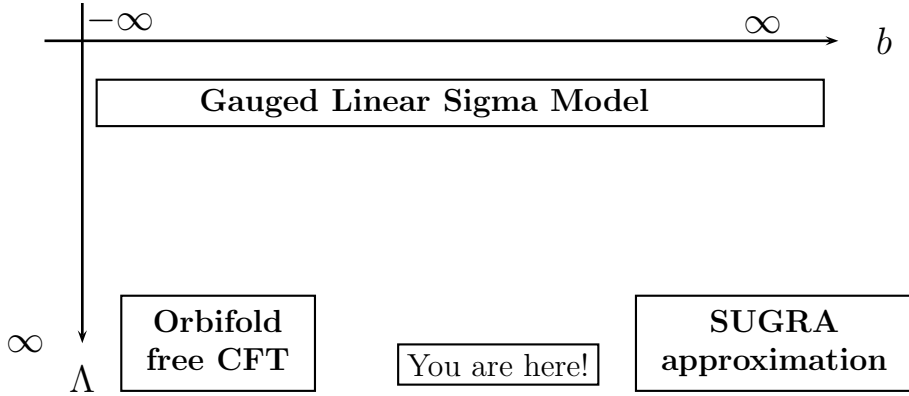


Figure 4.1: The theories we are working with, plotted in a plane spanned by the GLSM mass scale  $\Lambda$  and the blow-up parameter  $b$ . The interpolation between singular orbifold and smooth resolution is doable in the GLSM framework at finite  $\Lambda$ . The string theories / SUGRA approximations are conformal  $\Lambda = \infty$  but only work for limiting cases of  $b$ . A realistic theory, however, will lie somewhere in between.

The first four terms can be interpreted as kinetic terms for the bosons. The last term is required for Green–Schwarz anomaly cancellation in ten dimensions.

In the compactification to four dimensions we have to split the fields according to the decomposition of representation under the reduction of the Lorentz group  $SO(1, 9) \rightarrow SO(1, 3) \times SO(6)$ . We assume compactification on a Calabi–Yau manifold  $X$  with a stable vector bundle  $V$  on it. The Bianchi identity of  $H_3$ , i.e. the exactness of  $dH_3$  imply topological conditions on the bundle, which can be summarized in terms of the Chern characters as  $\text{ch}_2(TX) = \text{ch}_2(V)$ . In section 3.2.2 we showed that in a GLSM setup, these conditions follow from  $(2, 0)$  anomaly freedom.

The Calabi–Yau property implies  $h^{1,0}(X) = h^{2,0}(X) = 0$  and the existence of a holomorphic non vanishing three form, i.e.  $h^{3,0}(X) = 1$ . Furthermore, the stability of the bundle implies that  $h^0(V) = 0$ , where  $V$  is the bundle in any representation. The fields have to be expanded in eigenmodes of the internal Laplacian, in the spirit of Kaluza–Klein. In fact, we will only be interested in the zero modes corresponding to massless particles, since we are interested in an effective theory at energies smaller than the inverse compactification scale. These zero modes are precisely the harmonic forms which furthermore are in one to one correspondence with cohomology groups. Thus the amount of massless modes can be deduced purely from the topological properties of the compactification space. As a last step, one has to specify the background values for the four-dimensional scalar fields. They correspond to the moduli of the internal space and the vector bundle. Let us focus a bit more on the splitting. For this, notice

10 d field	component reduction	multiplicity	name
10d graviton	$g_{\mu\nu}$	$h^0(X) = 1$	4d graviton
	$g_{\mu m}$	$2h^{1,0}(X) = 0$	-
	$g_{mn}$	$2h^{2,1}(X)$	complex structure moduli
		$h^{1,1}(X)$	Kähler moduli
Kalb–Ramond	$B_{\mu\nu}$	$h^0(X) = 1$	universal axion
	$B_{\mu m}$	$2h^{1,0}(X) = 0$	-
	$B_{mn}$	$h^{1,1}(X)$	axions
dilaton	$\phi$	$h^0(X) = 1$	dilaton
10d vector boson ( $\mathbf{1}, \mathbf{ad}(\mathbf{H})$ )	$A_\mu$	$h^0(\mathcal{O}) = 1$	4d vector boson
	$A_m$	$h^1(\mathcal{O}) = 0$	-
10d vector boson ( $\mathbf{ad}(\mathbf{G}), \mathbf{1}$ )	$A_\mu$	$h^0(\text{End}(V)) = 0$	-
	$A_m$	$h^1(\text{End}(V))$	bundle moduli
10d vector boson ( $(\mathbf{R}, \mathbf{R}')$ )	$A_\mu$	$h^0(V_{\mathbf{R}}) = 0$	-
	$A_m$	$h^1(V_{\mathbf{R}})$	chiral matter

Table 4.1: Decomposition of 10d bosonic fields into 4d fields and multiplicities.

#### 4 Phenomenology on Orbifold Resolutions

that the  $E_8 \times E_8$  gets split into  $G \times H$  where  $G$  is the structure group of the gauge bundle and  $H$  is its commutant. Accordingly, the vector bosons in the adjoint will split as

$$\mathbf{248} \longmapsto (\mathbf{ad}(\mathbf{G}), \mathbf{1}) \oplus (\mathbf{1}, \mathbf{ad}(\mathbf{H})) \oplus \bigoplus (\mathbf{R}, \mathbf{R}'). \quad (4.2)$$

Thus we will distinguish if the bosons are in the adjoint of  $G$ , in the adjoint of  $H$  or in any other representation. The decomposition of the fields and their multiplicities are shown in table 4.1. To sum up, from the 10d gravity multiplet we get a 4d gravity multiplet together with some chiral fields which fall into three categories

- $h^{2,1}(X)$  complex structure moduli, which by themselves are complex ,
- $h^{1,1}(X)$  complexified Kähler moduli,  $\alpha_r + ia_r$ ,  $r = 1, \dots, h^{1,1}(X)$  where  $a_r$  are the Kähler moduli and  $\alpha_r$  are axions originating from the Kalb–Ramond field ,
- One axion-dilaton,  $a_{\text{uni}} + i\phi$ , where the universal axion is dual to the Kalb–Ramond field in four dimensions,  $da_{\text{uni}} = *_4 dB_2$ . .

From the 10d gauge multiplets we get the 4d gauge multiplets of the commutant  $H$  of the bundle, a bunch of  $H$  neutral bundle moduli and chiral fields transforming in non-trivial representations of  $H$  and chiral fields transforming in both the bundle structure group and the four dimensional gauge group. The only thing one has to do to get their amount is to compute the dimensions of cohomology groups. The easiest of them are  $h^{p,q}(X)$  which can in the resolved orbifold case be done by counting the untwisted and twisted contributions separately. For the bundle cohomologies, these calculations are doable [54], but it turns out that their difficulty increases exponentially with the number of gaugings, which in the maximal models is roughly  $h^{1,1}(X)$ . Thus for generic orbifold resolutions in terms of maximal models they are not feasible. Instead, the computation of the net multiplicity can in the be done in a much easier way. Using the bundle stability and Serre duality we find

$$\chi(V) = h^0(V) - h^1(V) + h^2(V) - h^3(V) \quad (4.3)$$

$$= 0 - h^1(V) + h^1(V^\vee) - 0 \quad (4.4)$$

$$= \#\text{antichirals} - \#\text{chirals}. \quad (4.5)$$

The Euler number  $\chi(V)$  can be computed by an index theorem as a topological integral over  $X$ . In the cases we study here, the vector bundle will simply be a sum over line bundles. In these cases, the field strength is equal to the bundle first Chern class and can thus be expanded in a basis of divisors,

$$F = \sum_r E_r V_r^I H^I, \quad (4.6)$$

where the  $H^I$  can be seen as generators of the Cartan subalgebra of  $E_8 \times E_8$ , and the coefficients  $V_r^I$  are called bundle vectors. For line bundles, the statement that the commutant of the bundle structure group in  $E_8 \times E_8$  stays unbroken is not quite correct. Since line bundles are Abelian bundles, one would expect from SUGRA that their structure- $U(1)$ 's remain unbroken, since they commutes with themselves. However, the coupling of the Kalb–Ramond field to the gauge fields via the Chern–Simons term generates a Stückelberg mechanism in four dimensions which gives mass to the gauge boson. To see this, we expand  $B_2$  in the internal  $(1, 1)$  forms with the parameters being the four-dimensional axions,

$$B_2|_X = \sum_r E_r \beta_r. \quad (4.7)$$

We do the same for the three-form flux  $H_3$  including the gauge Chern–Simons term and insert the line bundle,

$$H_3 \supset dB_2 - \text{tr} A \wedge F \supset \sum_r E_r \wedge (d_4 \beta_r - V_r^I A^I). \quad (4.8)$$

Under an Abelian gauge transformation  $\delta A^I = d_4 \varphi^I$  with gauge parameter  $\varphi^I$ , in order for  $H_3$  to be inert, the axion must transform with a shift  $\delta \beta_r = V_r^I \varphi^I$ . Then one can gauge  $\beta_r$  away and its kinetic term becomes a mass term for the vector boson  $A$ , with the mass being proportional to the axion scale. So one can raise the question, how to obtain a massless  $U(1)$  gauge theory in such a smooth CY compactification. One can either try to find a bundle with structure group  $G \subset E_8 \times E_8$  such that its commutant contains a  $U(1)$  factor which is orthogonal to  $G$ , but, in the context of MSSM-like models, no such working case is known yet. Another possibility is to construct a CY with a non-trivial fundamental group. Then one can wrap Wilson lines around the non-contractible cycles. Since the fundamental group of such a CY is typically finite, the Wilson lines are discrete. They can then be used to break some non-Abelian group down to something with  $U(1)$  factors for which there are no axions making them massive. This is a famous scenario for  $SU(5)$  GUT breaking to assure an unbroken hypercharge. In the context of orbifold and resolutions we encountered this in [40, 41].

For the case of an orbifold resolution where one insists on the interpretation as the blow-up of a singular orbifold theory, we choose the sum to run over the exceptional divisors only, since there the two-tori are free of flux. Then one can argue that the bundle vectors must be equal to the local shift vectors, up to  $E_8 \times E_8$  lattice vectors, as was done in [37, 39],

$$V_r = V_g \text{ mod } \Lambda_{E_8 \times E_8}. \quad (4.9)$$

In a line bundle scenario, the index theorem takes a rather simple form,

$$\chi(V) = \int_X \left( \frac{1}{6} F^3 - \frac{1}{24} \text{tr} R^2 \cdot F \right), \quad (4.10)$$

#### 4 Phenomenology on Orbifold Resolutions

Flux quantization in triangulation “ $E_1$ ”			
$E_{1,\beta\gamma}E_{2,\alpha\gamma}$	$2V_{2,\alpha\gamma} \cong 0$	$D_{1,\alpha}E_{1,\beta\gamma}$	$V_{1,\beta\gamma} - V_{2,\alpha\gamma} - V_{3,\alpha\beta} \cong 0$
$E_{1,\beta\gamma}E_{3,\alpha\beta}$	$2V_{3,\alpha\beta} \cong 0$	$D_{1,\alpha}E_{2,\alpha\gamma}$	$4V_{2,\alpha\gamma} - \sum_{\beta} V_{1,\beta\gamma} \cong 0$
$E_{2,\alpha\gamma}E_{3,\alpha\beta}$	$0$	$D_{1,\alpha}E_{3,\alpha\beta}$	$4V_{3,\alpha\beta} - \sum_{\gamma} V_{1,\beta\gamma} \cong 0$
$D_{2,\beta}E_{1,\beta\gamma}$	$-\sum_{\alpha} V_{3,\alpha\beta} \cong 0$	$D_{3,\gamma}E_{1,\beta\gamma}$	$-\sum_{\alpha} V_{2,\alpha\gamma} \cong 0$
$D_{2,\beta}E_{2,\alpha\gamma}$	$0$	$D_{3,\gamma}E_{2,\alpha\gamma}$	$-\sum_{\beta} V_{1,\beta\gamma} \cong 0$
$D_{2,\beta}E_{3,\alpha\beta}$	$-\sum_{\gamma} V_{1,\beta\gamma} \cong 0$	$D_{3,\gamma}E_{3,\alpha\beta}$	$0$
$R_i E_{i,\rho\sigma}$	$2V_{i,\rho\sigma} \cong 0$	$R_i R_j$	$0$
$R_i D_{j,\rho}$	$-\sum_{\sigma} V_{i,\rho\sigma} \cong 0 \quad (i \neq j)$		

Table 4.2: The flux quantization  $\int_C F$  on curves  $C$  using triangulation “ $E_1$ ” at all  $\mathbb{Z}_2 \times \mathbb{Z}_2$  orbifold fixed points.

which is also called multiplicity operator. An alternative, more physics related approach to the multiplicity operator is by extracting it from the reduction of the ten-dimensional anomaly polynomial to the four-dimensional one [35]. There it appears as prefactor of the contributions of the chiral fields and thus only knows about the net multiplicity.

#### Flux Quantization on resolution Calabi–Yau

In section 3.4.1 we showed that the integrality condition on the GLSM charges of the chiral fermi multiplets is equivalent to the conditions stemming from the identification with the orbifold CFT in the blow-down limit. If one works in the target space theory on the resolution one can study the relation between the flux quantization conditions and the identifications with the orbifold local shifts. This, however, has to be done case by case. Here we do the analysis for the factorizable  $\mathbb{Z}_2 \times \mathbb{Z}_2$  orbifold and show that these conditions are indeed equivalent. For a line bundle (4.6) the flux quantization conditions take the form

$$\int_C F \cong 0, \quad (4.11)$$

where  $C$  is any integral curve on the CY manifold and here  $\cong$  means equal up to  $E_8 \times E_8$  lattice vectors. A priori, these conditions depend on the amount of



Flux quantization in triangulation “S”			
$E_{1,\beta\gamma}E_{2,\alpha\gamma}$	$-V_{1,\beta\gamma} - V_{2,\alpha\gamma} + V_{3,\alpha\beta} \cong 0$	$D_{1,\alpha}E_{1,\beta\gamma}$	0
$E_{1,\beta\gamma}E_{3,\alpha\beta}$	$-V_{1,\beta\gamma} + V_{2,\alpha\gamma} - V_{3,\alpha\beta} \cong 0$	$D_{1,\alpha}E_{2,\alpha\gamma}$	$\sum_{\beta} V_{3,\alpha\beta} \cong 0$
$E_{2,\alpha\gamma}E_{3,\alpha\beta}$	$V_{1,\beta\gamma} - V_{2,\alpha\gamma} - V_{3,\alpha\beta} \cong 0$	$D_{1,\alpha}E_{3,\alpha\beta}$	$\sum_{\gamma} V_{2,\alpha\gamma} \cong 0$
$D_{2,\beta}E_{1,\beta\gamma}$	$\sum_{\alpha} V_{3,\alpha\beta} \cong 0$	$D_{3,\gamma}E_{1,\beta\gamma}$	$\sum_{\alpha} V_{2,\alpha\gamma} \cong 0$
$D_{2,\beta}E_{2,\alpha\gamma}$	0	$D_{3,\gamma}E_{2,\alpha\gamma}$	$\sum_{\beta} V_{1,\beta\gamma} \cong 0$
$D_{2,\beta}E_{3,\alpha\beta}$	$\sum_{\gamma} V_{1,\beta\gamma} \cong 0$	$D_{3,\gamma}E_{3,\alpha\beta}$	0
$R_i E_{i,\rho\sigma}$	$2V_{i,\rho\sigma} \cong 0$	$R_i R_j$	0
$R_i D_{j,\rho}$	$-\sum_{\sigma} V_{i,\rho\sigma} \cong 0 \quad (i \neq j)$		

Table 4.3: The flux quantization  $\int_C F$  on curves  $C$  using the triangulation “symm” at all  $\mathbb{Z}_2 \times \mathbb{Z}_2$  orbifold fixed points.

curves on the space and should be studied for each non-equivalent topology case by case. For an orbifold resolution, they might change between the different triangulations. We show in the example of the  $\mathbb{Z}_2 \times \mathbb{Z}_2$  resolution that in all triangulations we recover the same set of conditions. Taking the intersection numbers from table 3.10 and the line bundle ansatz (4.6), we can compute these conditions. The results for the triangulations “symm” and “ $E_1$ ” are written down in tables 4.2 and 4.3. First we observe that for each bundle vector  $V_r$  we get the condition that is a half  $E_8 \times E_8$  lattice vector. Then, we find conditions of the form

$$V_{1,\beta\gamma} + V_{2,\alpha\gamma} + V_{3,\alpha\beta} \cong 0, \quad (4.12)$$

$$\sum_{\rho} V_{k,\rho\sigma} \cong \sum_{\sigma} V_{k,\rho\sigma} \cong 0. \quad (4.13)$$

These conditions look very similar to the GLSM quantization conditions found in equations (3.134) and (3.136), and thus also imply the orbifold identifications, as shown in appendix C.

The fact that for this the bundle the bundle vectors have to be identified with the GLSM charges,  $Q_r/2 \cong V_r$ , is not surprising. In fact, we have expanded the bundle vectors in a basis of  $E_r = \{x_r = 0\}$  divisors, which can be seen as duals of the  $U(1)_{E_r}$  gaugings, since the fields  $x_r$  are only charged under  $U(1)_{E_r}$ . The factor in the identification comes from the charge  $-2$  of  $x_r$ , so the exact identifications are  $V_r = -Q_r/2$ .

### First Identification of States

In an ideal picture of a blow-up procedure, one starts at the orbifold point and moves along a flat directions in moduli space. In general a non-vanishing FI term of the orbifold anomalous U(1) will drive this process. What happens from this point of view is comparable to the standard model Higgs mechanism. The gauge symmetries, under which the moduli fields are charged, get broken. At the same time the vevs might generate mass terms in the superpotential for pairs of chiral fields which thus disappear from the low energy spectrum. Having brought such a theory to a point where the volumes are large and one can take the SUGRA approximation to describe the theory. We assume to have one blow-up mode at each fixed point which should lead to a line bundle model on the resolution. There the things look a bit different. Here the breaking of the gauge symmetry comes from a Stückelberg mechanism involving the axions  $\beta_r$ . One can understand this by identifying the blow-up mode  $\Psi_r$ , i.e. the field that gets a vev, with the complexified Kähler modulus  $T_r = b_r + i\beta_r$  as

$$\Psi_r = e^{T_r} . \tag{4.14}$$

This is motivated by the fact that the blow-up mode is a field transforming linearly under gauge transformations, so here we identify the bundle vector to be its charge. Then the expansion around the vev of the kinetic term gives precisely the axion coupling, with the axion scale being determined by  $b$ . In [39,41] we showed that the Bianchi identities often force the blow-up modes to be oscillatorless states by fixing the length on  $V_r^2$ . In the GLSM one can show that this is always the case. For this assume a very simple setup of just a local  $\mathbb{C}^3/\mathbb{Z}_N$  singularity where we just focus on one particular sector corresponding to the twist  $\theta = \text{diag}(e^{2\pi i m_1/N}, e^{2\pi i m_2/N}, e^{2\pi i m_3/N})$ , with  $0 \leq m_i < N$  and  $m_1 + m_2 + m_3 = N$ . The GLSM for just this sector with a line bundle reads:

field	$\mathcal{Z}_1$	$z\mathcal{Z}_2$	$\mathcal{Z}_3$	$\mathcal{X}$	$\Lambda^A$
U(1) charge	$m_1$	$m_2$	$m_3$	$-N$	$Q^I$

Then the bundle vector of charge of the blow-up mode is  $V^I = Q^I/N$ . The U(1)<sup>2</sup> gauge anomaly cancellation reads

$$m_1^2 + m_2^2 + m_3^2 + N^2 = \sum_I (Q^I)^2 . \tag{4.15}$$

Dividing this by  $N^2$ , we obtain a formula for the length of the blow-up mode charge vector. Inserting it into the orbifold mass equation (2.11) we indeed find that the blow-up mode can only be massless if all oscillators are switched off.

A next difficulty in the matching are the charges of the twisted chiral fields. On the resolution all chiral fields come from the adjoint of  $E_8 \times E_8$  and thus their charges are the  $E_8 \times E_8$  roots. The charges of orbifold twisted states, on

the other hand, are shifted by the local shift  $V_g$  and are in particular no longer in the root lattice. For this to be repaired, one finds that the states have to be redefined by the blow-up modes,

$$\Psi_{\text{orbifold}} = e^{f(T_r)} \Psi_{\text{blow-up}}. \quad (4.16)$$

where  $f(T_r)$  is a linear polynomial. The naive assumption would be to use  $f(T_r) = T_r$  when  $\Psi$  comes from the twisted sector corresponding to  $r$ . In the examples we studied in [41, 45] we show that this is not always the case, but rather more general linear polynomials must appear. This will be elaborated in to some more detail in the next section.

## 4.2 Stringy Effects

We want to shed a light in stringy effects which are not seen from the pure SUGRA theories, but rather are revealed by comparing the theories at different points in moduli space. For example, as the multiplicity operator is a topological integral, it might happen that the multiplicity of certain states jumps during a flop transition. From a pure SUGRA point of view this would just correspond to two different theories, since going through a flop, the geometry would become singular and the pure field theory on it would be ill defined. However, if one views the SUGRA theory as an approximation to an underlying string theory, then both sides of the flop should be connected since the string can deal with singularities. Such a stringy smooth interpolation of different SUGRA theories was first studied in [19] in the context of type II theories. There it was observed that an infinite number of worldsheet instantons could smoothly extrapolate between Yukawa couplings calculated in the SUGRA regimes on the two sides of the flop.

Furthermore, a matching with the orbifold states can be performed. The states at this point and their interactions are known. In the example we present, we will observe that there are massless states in the SUGRA theory, which have no orbifold counterpart and thus cannot be perturbative orbifold states. From the SUGRA point of view these states have to disappear in the blow-down limit, which can only be explained by including non-perturbative stringy corrections.

### Example: A $\mathbb{Z}_2 \times \mathbb{Z}_2$ Model with Flop Transitions

A concrete and simple setup to study this phenomenon is the standard embedding on the  $\mathbb{Z}_2 \times \mathbb{Z}_2$  orbifold. The orbifold model is specified by the shifts

$$V_1 = \left(0, \frac{1}{2}, -\frac{1}{2}, 0^5\right) \left(0^8\right) \quad \text{and} \quad V_2 = \left(-\frac{1}{2}, 0, \frac{1}{2}, 0^5\right) \left(0^8\right) \quad (4.17)$$

and vanishing Wilson lines  $W_i = 0$ ,  $i = 1, \dots, 6$ . The resulting 4d model has  $E_6 \times U(1)^2 \times E_8$  gauge group and the charged matter spectrum consists of  $3(\mathbf{27}, \mathbf{1}) +$

#### 4 Phenomenology on Orbifold Resolutions

U sector		$\theta_1$ -sector	$\theta_2$ -sector	$\theta_3$ -sector
$(\mathbf{27}, \mathbf{1})_{(-2,-2)}$	$(\overline{\mathbf{27}}, \mathbf{1})_{(2,2)}$	$16(\overline{\mathbf{27}}, \mathbf{1})_{(2,0)}$	$16(\overline{\mathbf{27}}, \mathbf{1})_{(-1,1)}$	$16(\overline{\mathbf{27}}, \mathbf{1})_{(-1,-1)}$
$(\mathbf{27}, \mathbf{1})_{(-2,2)}$	$(\overline{\mathbf{27}}, \mathbf{1})_{(2,-2)}$	$16(\mathbf{1}, \mathbf{1})_{(-6,0)}$	$16(\mathbf{1}, \mathbf{1})_{(3,-3)}$	$16(\mathbf{1}, \mathbf{1})_{(3,3)}$
$(\mathbf{27}, \mathbf{1})_{(4,0)}$	$(\overline{\mathbf{27}}, \mathbf{1})_{(-4,0)}$	$32(\mathbf{1}, \mathbf{1})_{0,2}$	$32(\mathbf{1}, \mathbf{1})_{(3,1)}$	$32(\mathbf{1}, \mathbf{1})_{(3,-1)}$
$(\mathbf{1}, \mathbf{1})_{(6,-2)}$	$(\mathbf{1}, \mathbf{1})_{(-6,2)}$	$32(\mathbf{1}, \mathbf{1})_{(0,-2)}$	$32(\mathbf{1}, \mathbf{1})_{(-3,-1)}$	$32(\mathbf{1}, \mathbf{1})_{(-3,1)}$
$(\mathbf{1}, \mathbf{1})_{(6,2)}$	$(\mathbf{1}, \mathbf{1})_{(-6,-2)}$			
$(\mathbf{1}, \mathbf{1})_{(0,4)}$	$(\mathbf{1}, \mathbf{1})_{(0,-4)}$			

Table 4.4: The massless spectrum of the  $\mathbb{Z}_2 \times \mathbb{Z}_2$  standard embedding orbifold model with gauge group  $E_6 \times U(1)^2 \times E_8$ .

51 $(\overline{\mathbf{27}}, \mathbf{1})$  and 246 singlets (charged under  $U(1)^2$ ). It is listed in detail in table 4.4.

The blow-up model is obtained with the bundle vectors

$$V_{1,\beta\gamma} = \left(0, -\frac{1}{2}, -\frac{1}{2}, 1, 0, 0, 0, 0\right) \left(0, 0, 0, 0, 0, 0, 0, 0\right), \quad (4.18)$$

$$V_{2,\alpha\gamma} = \left(-\frac{1}{2}, 0 - \frac{1}{2}, 0, 1, 0, 0, 0, 0\right) \left(0, 0, 0, 0, 0, 0, 0, 0\right), \quad (4.19)$$

$$V_{3,\alpha\beta} = \left(-\frac{1}{2}, -\frac{1}{2}, 0, 0, 0, 1, 0, 0\right) \left(0, 0, 0, 0, 0, 0, 0, 0\right), \quad (4.20)$$

which fulfill the Bianchi identities for any triangulation. This corresponds to choosing the blow-up modes in three different directions inside  $\overline{\mathbf{27}}$  of  $E_6$  which induces a gauge symmetry breaking  $E_6 \times U(1)^2 \rightarrow SU(3) \times SU(2) \times U(1)^5$ . (In detail: The blow-up modes associated to  $V_{1,\beta\gamma}$  lead to a breaking to  $SO(10) \times U(1)$  and all  $\overline{\mathbf{27}}$  are branched to  $\overline{\mathbf{16}} + \mathbf{10} + \mathbf{1}$ . The blow-up modes associated to  $V_{2,\alpha\gamma}$  acquire a VEV in the  $\overline{\mathbf{16}}$ . This induces further breaking  $SO(10) \rightarrow SU(5) \times U(1)$ , and the  $\overline{\mathbf{16}}$  branches to  $\overline{\mathbf{10}} + \mathbf{5} + \mathbf{1}$ . And finally the blow-up modes associated to  $V_{3,\alpha\beta}$  branches the  $\overline{\mathbf{10}}$  of  $SU(5)$ .) Since we chose the same blow-up mode in each fixed plane of a given twisted sector, the discussion is the same for all 64 local resolutions. Thus, here we may drop the fixed point labels  $\alpha$ ,  $\beta$  and  $\gamma$ . The  $U(1)$ 's are chosen such that the charge vectors of the blow-up modes are  $Q(\phi_1) = (10, 0, 0, 0, 0)$ ,  $Q(\phi_2) = (0, 10, 0, 0, 0)$  and  $Q(\phi_3) = (0, 0, 10, 0, 0)$ . In this way the axions corresponding to the blow-up modes have no effect in anomaly cancellation for the last two  $U(1)$  factors. In fact, these  $U(1)$ 's have no anomaly at all, as can be checked by directly inspecting the anomaly polynomial. This matches with the fact that the two  $U(1)$ 's present in the orbifold model are non-anomalous, but notice that the non-anomalous  $U(1)$ 's in the orbifold and those in the resolution cannot be identified with each other directly, since the blow-up modes are generically charged under the orbifold  $U(1)$ 's.

In table 4.5 we list the twisted spectrum of the standard embedding model, after branching it in representations of  $SU(3) \times SU(2)$ , and we match it with the spectra obtained in the resolutions “ $E_1$ ” and “ $S$ ”. The untwisted spectrum has no chiral counterpart in the resolution, so we do not consider it. Note that some orbifold states are not listed here since they received a mass term from Yukawa couplings with the blow-up mode, which becomes large in the SUGRA regime. We provide the  $U(1)$  charges in the basis discussed above, that differs from the basis used in table 4.4 for the reasons explained above. In what follows we also face the details of the matching in the specific case of states in  $(\mathbf{1}, \mathbf{2})$  representations, but the mechanisms at work for the other representation are essentially the same.

### Flopping states: the $(\mathbf{1}, \mathbf{2})$ case

To face the phenomenon of extra states appearing on the resolutions, we discuss here as an example the matching and appearance of novel states for the  $SU(2)$  doublets  $d_i$  listed in table 4.5. We focus in particular on the states named  $d_1$  and  $d_2$ . The multiplicities of the orbifold states and of the states appearing in each of the four triangulations of the  $64 \mathbb{Z}_2 \times \mathbb{Z}_2$  fixed points are shown in table 4.5. As the charges of the orbifold states and the states on the resolution do not completely match we need to perform field redefinitions of the orbifold states using the blow-up modes of the respective sectors given by:

$$d_{i,\text{BU}} = e^{2\pi T_r} d_{i,\text{orbi}} \text{ for } i = 1 \dots 6 \text{ and } d_{7,\text{BU}} = e^{-2\pi T_r} d_{7,\text{orbi}} . \quad (4.21)$$

Table 4.5 indicates that orbifold and resolution multiplicities of the states  $d_1$  and  $d_2$  are identical, except for resolution “ $E_2$ ”, where the multiplicity is  $-48$  rather than  $16$ . The negative multiplicity is interpreted such that on that resolution one does not see the  $d_1$  and  $d_2$  states, but rather their charge conjugates which we call  $\underline{d}_1$  and  $\underline{d}_2$ . In order to explain this we first consider the (lowest order) superpotential terms for  $d_1$  and  $d_2$  that can be written from the orbifold perspective, namely  $W = d_{1,\text{orbi}} d_{2,\text{orbi}} \phi_2$ . This term indicates that all states get a mass term in blow-up. From the blow-up perspective the corresponding superpotential can be obtained after field redefinition, and reads  $W = d_1 d_2 e^{-2\pi(U_1+U_3-U_2)}$ . We observe that in all triangulations but “ $E_2$ ” the conditions on the blow-up moduli are such that we can interpret this superpotential term as instantonic mass terms. Thus,  $d_1$  and  $d_2$  have the same multiplicity both in the orbifold point and in resolution, since they are massless modes in a perturbative expansion of the theory, receiving instantonic mass corrections. When we pass to triangulation “ $E_2$ ” from any other triangulation, the twisted moduli fulfill the condition  $b_2 > b_1 + b_3$  and the  $d_1 d_2$  mass term cannot be thought of as an instantonic correction to a well defined perturbative theory any more.

In other words, the supergravity construction fails as soon as  $b_2$  is not smaller than  $b_1 + b_3$ , and we lose control on the “perturbative” computation of the

#### 4 Phenomenology on Orbifold Resolutions

spectrum: the non-perturbative corrections take over, and a new “perturbative” computation comes at hand, i.e. the supergravity construction made in resolution “ $E_2$ ”, where the states  $d_1$  and  $d_2$  indeed disappear from the spectrum. This argument holds in the very same way for the pairs  $d_3, d_4$  and  $d_5, d_6$ , disappearing in resolution “ $E_1$ ” and “ $E_3$ ”, respectively. For the  $d_7$  states the orbifold mass term is such that in no triangulation it can be seen as an instantonic correction to a perturbatively massless set of states: in supergravity, independently of the resolution type, these states have a large  $O(M_s)$  mass and are removed from the massless spectrum.

We explained the fate of the orbifold states when passing in blow-up and when passing from one triangulation to the other. This is not all, since we have underlined states to explain as well. Their fate is somewhat dual to that of non-underlined states. Let us consider the  $\underline{d}_1$  and  $\underline{d}_2$  states in triangulation “ $E_2$ ”: it is reasonable to assume that their superpotential is

$$W = \underline{d}_1 \underline{d}_2 e^{2\pi(T_1+T_3-T_2)} \quad (4.22)$$

and these states are present as massless states with instantonic mass terms only if the moduli are chosen such that we are in triangulation “ $E_2$ ”, in all the other cases the instantonic correction grows, a perturbative perspective is non-tenable, and the underlined states drop from the massless spectrum.

State	Orb. Mult.			Resolution Mult.				U(1) charges
	$\theta_1$	$\theta_2$	$\theta_3$	" $E_1$ "	" $E_2$ "	" $E_3$ "	" $S$ "	
$d_1$	16			16	-48	16	16	( 7,-5, 3, 1, 2)
$d_2$		16		16	-48	16	16	( 3,-5, 7,-1,-2)
$d_3$		16		16	16	-48	16	( 3, 7,-5,-2,-1)
$d_4$	16			16	16	-48	16	( 7, 3,-5, 2, 1)
$d_5$		16		-48	16	16	16	(-5, 3, 7, 1,-1)
$d_6$		16		-48	16	16	16	(-5, 7, 3,-1, 1)
$d_7$	16	16	16	-80	-80	-80	-80	(-5,-5,-5, 0, 0)
$\bar{t}_1$	16			16	-48	-48	-48	( 8,-4,-4, 1, 1)
$t_2$		16	16	32	-32	-32	-32	( 2,-6,-6,-1,-1)
$\bar{t}_3$		16		-48	-48	16	-48	(-4,-4, 8, 0,-1)
$t_4$	16	16		-32	-32	32	-32	(-6,-6, 2, 0, 1)
$\bar{t}_5$		16		-48	16	-48	-48	(-4, 8,-4,-1, 0)
$t_6$	16		16	-32	32	-32	-32	(-6, 2,-6, 1, 0)
$t_7$	16			16	16	16	16	( 6, 2, 2, 2, 2)
$t_8$		16		16	16	16	16	( 2, 6, 2,-2, 0)
$t_9$		16		16	16	16	16	( 2, 2, 6, 0,-2)
$\bar{q}_1$	16			16	16	16	16	(-7, 1, 1, 1, 1)
$\bar{q}_2$		16		16	16	16	16	( 1,-7, 1,-1, 0)
$\bar{q}_3$		16		16	16	16	16	( 1, 1,-7, 0,-1)
$\phi_1$	16			1 <sup>st</sup> Blow-up mode				(10, 0, 0, 0, 0)
$\phi_2$		16		2 <sup>nd</sup> Blow-up mode				( 0,10, 0, 0, 0)
$\phi_3$		16		3 <sup>rd</sup> Blow-up mode				( 0, 0,10, 0, 0)
$s_1$	16			16	16	16	16	( 6, 2, 2,-3,-3)
$s_2$		16		16	16	16	16	( 2, 6, 2, 3, 0)
$s_3$		16		16	16	16	16	( 2, 2, 6, 0, 3)
$s_4$	16		-16	-64	0	64	0	(-8, 0, 8, 1, 2)
$s_5$				-64	0	0	0	(-2,10, 2,-1,-2)
$s_6$				0	0	-64	0	( 2,10,-2, 1, 2)
$s_7$	16	-16		-64	64	0	0	(-8, 8, 0, 2, 1)
$s_8$				-64	0	0	0	(-2, 2,10,-2,-1)
$s_9$				0	64	0	0	( 2,-2,10, 2, 1)
$s_{10}$		16	-16	0	-64	64	0	( 0,-8, 8,-1, 1)
$s_{11}$				0	-64	0	0	(10,-2, 2, 1,-1)
$s_{12}$				0	0	64	0	(10, 2,-2,-1, 1)

Table 4.5: Orbifold and resolution multiplicities of the states in the standard embedding (but in non-standard blow-up). The first column lists the labels of  $SU(3) \times SU(2)$  representations: " $d_x$ " for  $(\mathbf{1}, \mathbf{2})$ , " $t_x$ " for  $(\mathbf{3}, \mathbf{1})$ , " $q_x$ " for  $(\mathbf{3}, \mathbf{2})$ ,  $\phi_x$  for the blow-up modes, and " $s_x$ " denote the singlets. An overlined label indicates the corresponding conjugate representation. In giving the multiplicities in the orbifold we indicate the twisted sector to which they belong ( $\theta_1$ ,  $\theta_2$ , and  $\theta_3$ ).

## 4 *Phenomenology on Orbifold Resolutions*



## 5 Conclusions and Outlook

Motivated by the success in the approaching the standard model of particle physics from heterotic orbifold compactifications, we studied how such models behave when going away from the orbifold point in moduli space in order to get a more realistic vacuum. One important step was to find a framework in which the moduli spaces are accessible without losing control of the theory. This was realized in terms of GLSMs by describing toroidal orbifolds as complete intersections. This way we could rigorously obtain the topological data of the resolved geometry in order to be able to study the SUGRA approximation.

We studied the behavior of  $(2, 2)$  models in different corners of moduli space and discovered new phases with interesting interpretations as hybrid theories. To our knowledge this is the first example of complete intersection Calabi–Yaus that possess a limit with a fully geometric solvable CFT description. It would be interesting to study the phases which seem to allow for CFT descriptions, like the non-geometric phases and singular over-blow-up phases, in order to get more perspectives on the physics which happen at low energies.

The GLSM resolution models might also be applied in the context of type II theories. For this one has to elaborate how to formulate the open string boundary conditions to study D-brane models in this setup.

In the context of  $(2, 0)$  models which are required for a realistic compactification, we found that it is very hard to write down a fully consistent model with an orbifold limit. Here there is still a lot of potential to be discovered. For example one try to describe line bundles in a less naive way than how it was done here, such that the gauge anomalies cancel. Then one could not only see the bundle moduli in a GLSM fashion as superpotential parameters, but one might also get an impression of how the associated  $(2, 0)$  moduli spaces look. Furthermore, the realization of more general vector bundles and their relation to the orbifold point is of particular interest.

The observation of states with jumping multiplicities showed that the spectrum computation in SUGRA theories is subject to string corrections. Since in realistic models the compactification scale cannot be too far away from the string scale, such corrections have high impact on the low energy theory and cannot be ignored. Here a  $(2, 0)$  version of quantum cohomology [55], which includes such non-perturbative corrections, might be helpful. A more distant goal is to deduce more physical statements directly from the GLSM, so that one can make statements at any point in moduli space.

## 5 *Conclusions and Outlook*

# A Discrete Actions on elliptic Curves and Tori

In this appendix we show the equivalence of some discrete group actions on elliptic curves and translations on tori they correspond to. We focus here on the  $\mathbb{Z}_3$ ,  $\mathbb{Z}_4$  and  $\mathbb{Z}_2$  tori discussed in section 3.1.2. To establish this equivalence the following addition formulae for the Weierstrass function and its derivative are of crucial importance:

$$\begin{aligned}\wp(u_1 + u_2) &= \frac{1}{4} \left( \frac{\wp'(u_1) - \wp'(u_2)}{\wp(u_1) - \wp(u_2)} \right)^2 - \wp(u_1) - \wp(u_2), \\ \wp'(u_1 + u_2) &= -\frac{1}{4} \left( \frac{\wp'(u_1) - \wp'(u_2)}{\wp(u_1) - \wp(u_2)} \right)^3 + 3 \frac{\wp'(u_1) - \wp'(u_2)}{\wp(u_1) - \wp(u_2)} \wp(u_2) \\ &\quad + \wp'(u_1) - 2 \wp'(u_2).\end{aligned}\tag{A.1}$$

## $\mathbb{Z}_3$ Torus

On the flat torus the orbifold map is  $\theta : u \rightarrow \zeta u$ . We find

$$\wp(\zeta u) = \zeta \wp(u), \quad \wp'(\zeta u) = \wp'(u),\tag{A.2}$$

thus, using (3.24) and (3.26) we find that  $\theta_1 : z_1 \rightarrow \zeta z_1$  is indeed the orbifold action. Next we want to identify the Wilson line action. For this, we first look at the fixed points of  $\theta$ . They are precisely at

$$u_1 = 0, \quad u_2 = \omega_1 \cdot \frac{e^{2\pi i/3} - 1}{3}, \quad u_3 = \omega_1 \cdot 2 \frac{e^{2\pi i/3} - 1}{3}.\tag{A.3}$$

The Wilson line action identifies these three fixed points so it is a shift by  $a := \omega_1 \cdot \frac{e^{2\pi i/3} - 1}{3}$ . Using the formula (A.1) together with the identities  $\wp(a) = 0$ ,  $\wp'(a) = -i$ , we find

$$\begin{aligned}\wp(u + a) &= \frac{\wp'(u)^2 + 2i\wp'(u) - 1 - 4\wp^3(u)}{4\wp(u)^2} \\ &= \frac{2\wp(u)}{-i\wp'(u) - 1}.\end{aligned}\tag{A.4}$$

## A Discrete Actions on elliptic Curves and Tori

Now lets take a look at what we assume are our Wilson line actions on the algebraic torus. There the free WL action was

$$\theta_{\text{WL}} : (z_1, z_2, z_3) \mapsto (z_1, \zeta^2 z_2, \zeta z_3). \quad (\text{A.5})$$

mapping this to the coordinates  $(x, y, v)$  yields

$$\theta_{\text{WL}} : \begin{pmatrix} y \\ v \end{pmatrix} \mapsto -\frac{1}{2} \begin{pmatrix} 1 & 3i \\ i & 1 \end{pmatrix} \begin{pmatrix} y \\ v \end{pmatrix}, \quad x \mapsto x \quad (\text{A.6})$$

Together with our Weierstrass identification (3.26) this gives

$$\wp(u) = \frac{x}{v} \mapsto \frac{x}{-\frac{i}{2}y - \frac{1}{2}v} = \frac{-2\frac{x}{v}}{i\frac{y}{v} + 1} = \frac{-2\wp(u)}{i\wp'(u) + 1}, \quad (\text{A.7})$$

which is exactly the same as we found on the flat torus. This proves that the Wilson line action on the algebraic torus (A.5) is the Wilson line action on the flat torus.

## $\mathbb{Z}_4$ Torus

On the flat torus the simplest choice for  $\mathbb{Z}_{4, \text{Orbi}}$  would be  $u \mapsto iu$ . However, we find that via the map given above the Orbifold action rotates around the fixed point  $u_{\text{fix}} = \frac{e_1}{2+2i}$ , i.e. it acts as  $\theta : u \mapsto iu + \frac{e_1}{2}$ . This we show using the identities

$$\wp(e_1/2) = \frac{1}{2}, \quad \wp'(e_1/2) = 0, \quad \wp(iu) = -\wp(u), \quad \wp'(iu) = i\wp(u), \quad (\text{A.8})$$

here:

$$\begin{aligned} \wp(u) &\mapsto \wp(iu + e_1/2) \\ &= \frac{1}{4} \left( \frac{\wp'(iu) - \wp'(e_1/2)}{\wp(iu) - \wp(e_1/2)} \right)^2 - \wp(iu) - \wp(e_1/2) \\ &= \frac{1}{2} \frac{\wp(u) - 1/2}{\wp(u) + 1/2} \end{aligned} \quad (\text{A.9})$$

Now lets look at the  $\mathbb{Z}_{4, \text{Orbi}}$  action on the algebraic torus which is given by  $(z_1, z_2, z_3) \mapsto (iz_1, z_2, z_3)$ . Translating it via (3.30) yields

$$\theta : \begin{pmatrix} x \\ v \end{pmatrix} \mapsto \frac{1+i}{2} \begin{pmatrix} 1 & -1/2 \\ 2 & 1 \end{pmatrix} \begin{pmatrix} x \\ v \end{pmatrix}, \quad y \mapsto y \quad (\text{A.10})$$

which using the identifications above gives,

$$\wp(u) = \frac{x}{v} \mapsto \frac{x - v/2}{2x + v} = \frac{1}{2} \frac{x/v - 1/2}{x/v + 1/2} = \frac{1}{2} \frac{\wp(u) - 1/2}{\wp(u) + 1/2}, \quad (\text{A.11})$$

as expected.

Next we investigate in the Wilson line action. On the flat torus it is given by  $u \mapsto u + \frac{e_1 + e_2}{2}$ . Here we need the identities

$$\wp((e_1 + e_2)/2) = 0, \quad \wp'((e_1 + e_2)/2) = 0, \quad (\text{A.12})$$

which quickly show

$$\begin{aligned} \wp(u) &\mapsto \wp(u + (e_1 + e_2)/2) \\ &= \frac{1}{4} \left( \frac{\wp'(u) - \wp'((e_1 + e_2)/2)}{\wp(u) - \wp((e_1 + e_2)/2)} \right)^2 - \wp(u) - \wp((e_1 + e_2)/2) \\ &= \frac{-\wp(u)}{4\wp(u)^2} = \frac{-1}{4\wp(u)}. \end{aligned} \quad (\text{A.13})$$

On the algebraic torus our free  $\mathbb{Z}_{2,\text{WL}}$  acts as  $(z_1, z_2, z_3) \mapsto (iz_1, -iz_2, z_3)$  which via (3.30) translates into

$$\theta : \begin{pmatrix} x \\ v \end{pmatrix} \mapsto \begin{pmatrix} 0 & -1/2 \\ 2 & 0 \end{pmatrix} \begin{pmatrix} x \\ v \end{pmatrix}, \quad y \mapsto y \quad (\text{A.14})$$

so we find,

$$\wp(u) = \frac{x}{v} \mapsto \frac{-v/2}{2x} = \frac{-v}{4x} = \frac{-1}{4\wp(u)}, \quad (\text{A.15})$$

so this agrees with the Wilson line action on the flat torus.

## Generic two-Torus

The generic Weierstrass equation is

$$y^2 = 4v(x - \epsilon_1 v)(x - \epsilon_2 v)(x - \epsilon_3 v). \quad (\text{A.16})$$

To establish that the discrete actions on the elliptic curve and the flat torus are identical we first consider the effect of the translations on the Weierstrass function and its derivative using (A.1) and the fact that the  $\epsilon_i$  define the zeros of  $\wp'$ :

$$\wp\left(u + \frac{1}{2}e_i\right) = \frac{\epsilon_i \wp(u) + \epsilon_{i+1} \epsilon_{i+2} + \epsilon_i^2}{\wp(u) - \epsilon_i}, \quad (\text{A.17a})$$

$$\wp'\left(u + \frac{1}{2}e_i\right) = -(\epsilon_{i+1} \epsilon_{i+2} + 2\epsilon_i^2) \frac{\wp'(u)}{(\wp(u) - \epsilon_i)^2} \quad (\text{A.17b})$$

## A Discrete Actions on elliptic Curves and Tori

where  $e_1 = 1, e_2 = \tau$  and  $e_3 = 1 + \tau$ . Using the mapping

$$\wp(u) = \frac{x}{v}, \quad \wp'(u) = 2 \frac{y}{v^2}, \quad (\text{A.18})$$

one can show that these actions on  $(x, y, v)$  are given by

$$\alpha_i : \begin{pmatrix} x \\ v \end{pmatrix} \mapsto \frac{1}{\sqrt{-\epsilon_{i+1}\epsilon_{i+2} - 2\epsilon_i^2}} \begin{pmatrix} \epsilon_i & \epsilon_{i+1}\epsilon_{i+2} + \epsilon_i^2 \\ 1 & -\epsilon_i \end{pmatrix} \begin{pmatrix} x \\ v \end{pmatrix}, \quad \alpha_i : y \mapsto -y, \quad (\text{A.19})$$

The fixed point mappings follows from applying (A.19) to the factors in (A.16). In detail we have

$$\alpha_i : \quad v \mapsto \frac{x - \epsilon_i v}{\sqrt{\epsilon_{i+1}\epsilon_{i+2} + 2\epsilon_i^2}}, \quad x - \epsilon_i \mapsto \sqrt{\epsilon_{i+1}\epsilon_{i+2} + 2\epsilon_i^2} \cdot v, \quad (\text{A.20a})$$

$$\alpha_i : \quad x - \epsilon_{i+1}v \mapsto \frac{gve_i - \epsilon_{i+1}}{\sqrt{\epsilon_{i+1}\epsilon_{i+2} + 2\epsilon_i^2}}(x - \epsilon_{i+2}v), \quad x - \epsilon_{i+2}v \mapsto \frac{\epsilon_i - \epsilon_{i+2}}{\sqrt{\epsilon_{i+1}\epsilon_{i+2} + 2\epsilon_i^2}}(x - \epsilon_{i+1}v). \quad (\text{A.20b})$$

This show how the factors and therefore the zeros are pairwise permuted.

## $\mathbb{Z}_2$ Torus

We want to translate the maps (A.20b) to the  $\mathbb{P}^3[2, 2]/\mathbb{Z}_2 \times \mathbb{Z}_2$  torus, i.e. the  $T^2(\mathbb{Z}_2)$ . For this we define the map

$$\mathbb{P}_{1,2,1}^2[4] \rightarrow \mathbb{P}^3[2, 2]/\mathbb{Z}_2 \times \mathbb{Z}_2 : \quad (x, y, v) \mapsto (z_1, z_2, z_3, z_4), \quad (\text{A.21})$$

as follows: On  $\mathbb{P}^3[2, 2]/\mathbb{Z}_2 \times \mathbb{Z}_2$  we have three sign ambiguities, one from  $U(1)_R$  and two from  $\mathbb{Z}_2 \times \mathbb{Z}_2$ . Thus we can define

$$z_1 = \sqrt{(\epsilon_3 - \epsilon_1)v}, \quad z_2 = \sqrt{-x + \epsilon_1v}, \quad z_3 = \sqrt{x - \epsilon_2}, \quad z_4 = \frac{-iy}{2z_1z_2z_3}. \quad (\text{A.22})$$

One could also define  $z_4 = \pm\sqrt{x - \epsilon_3v}$  where the sign has to be chosen such that  $y = 2iz_1z_2z_3z_4$ , as there are no more sign ambiguities. This way we find that the discrete  $\mathbb{Z}_2 \times \mathbb{Z}_2$  shifts, given in (A.20b) translate to the actions given in (3.45).

# B Compactification Lattice Analyses

## The $T^6/\mathbb{Z}_3$ Orbifold

The aim of this Appendix is two-fold: i) We briefly describe the factorized Lie-algebra lattice  $A_2^3$ , and non-factorized lattices, underlying the  $T^6/\mathbb{Z}_3$  orbifolds encountered in Section 3.3.1. To this end we work out in detail how dividing out the free discrete actions on the torus induce refined and often non-factorized lattices. ii) When possible we classify the result lattice as some Lie algebra lattice. iii) And finally, we show that each of the non-factorized ones can be obtained from the factorized  $A_2^3$  lattice by a change of Kähler structure.

In our conventions for  $\mathbb{Z}_3$  compatible tori defined in Section 3.1.2, the lattice underlying two-tori to be spanned by 1 and the complex structure  $\tau = \zeta$ . Therefore, our reference basis vectors  $e_1, \dots, e_6$  for the lattice  $A_2^3$  in  $\mathbb{R}^6$  are given by

$$e_1 = \begin{pmatrix} 1 \\ 0 \\ 0 \\ 0 \\ 0 \\ 0 \end{pmatrix}, \quad e_2 = \begin{pmatrix} -\frac{1}{2} \\ \frac{\sqrt{3}}{2} \\ 0 \\ 0 \\ 0 \\ 0 \end{pmatrix}, \quad e_3 = \begin{pmatrix} 0 \\ 0 \\ 1 \\ 0 \\ 0 \\ 0 \end{pmatrix}, \quad e_4 = \begin{pmatrix} 0 \\ 0 \\ -\frac{1}{2} \\ \frac{\sqrt{3}}{2} \\ 0 \\ 0 \end{pmatrix}, \quad e_5 = \begin{pmatrix} 0 \\ 0 \\ 0 \\ 0 \\ 1 \\ 0 \end{pmatrix}, \quad e_6 = \begin{pmatrix} 0 \\ 0 \\ 0 \\ 0 \\ -\frac{1}{2} \\ \frac{\sqrt{3}}{2} \end{pmatrix}.$$

These basis vectors have norm squared 1 rather than 2, which is the conventional choice for simple roots.

The basis vectors, which is obtained by dividing out the free discrete actions, are referred to as  $\hat{e}_1, \dots, \hat{e}_6$ . Where necessary we include normalization factors, to ensure that we can identify the Lie algebra the lattice corresponds by computing the Cartan matrix

$$A_{mn} = \frac{2 \hat{e}_m \cdot \hat{e}_n}{\hat{e}_m \cdot \hat{e}_m}, \quad (\text{B.1})$$

where  $x \cdot y$  denotes the standard inner product on  $\mathbb{R}^6$ .

To establish that the refined (non-factorized) lattice can be turned  $A_2^3$  lattice by a Kähler deformation, we have to find a basis of this lattice such that the  $\mathbb{Z}_3$

## B Compactification lattice analyses

action on it, looks like the standard  $\mathbb{Z}_3$  action

$$e_{2a-1} \mapsto e_{2a}, \quad e_{2a} \mapsto -e_{2a} - e_{2a-1}, \quad (\text{B.2})$$

with  $a = 1, 2, 3$  on  $A_2^3$  basis vectors  $e_1, \dots, e_6$ . We refer to  $\tilde{e}_1, \dots, \tilde{e}_6$ . To discuss Kähler deformations we define the inner product

$$\langle x, y \rangle_G = x^T G y, \quad x, y \in \mathbb{R}^6, \quad (\text{B.3})$$

w.r.t. a metric  $G$ ; the standard inner product  $x \cdot y$  is obtained when the metric  $G$  is taken to be the identity. To establish that the basis vectors  $\tilde{e}_1, \dots, \tilde{e}_6$  of the non-factorized lattice is equivalent to our standard  $A_2^3$  basis up to a Kähler deformation, we need to show that there is a Kähler metric  $G$  such that

$$\langle e_m, e_n \rangle_G = \tilde{e}_m \cdot \tilde{e}_n, \quad (\text{B.4})$$

for all  $m, n = 1, \dots, 6$ .

To make (B.4) explicit, we write out our reference basis and give a general parameterization of a Kähler metric  $G$ . To construct the general metric  $G$  that includes all Kähler moduli, we start from a generic Kähler form

$$J = \frac{i}{2} J_{ab} d\bar{u}_a \wedge du_b. \quad (\text{B.5})$$

Its reality condition reads  $J_{ab} = \bar{J}_{ba}$ , so we rewrite it in terms of real parameters defined as

$$J_{aa} = b_a, \quad J_{ab} = c_{ab} + id_{ab} \quad \text{for } a < b. \quad (\text{B.6})$$

Then, decomposing into real coordinates,  $u_a = x_{2a-1} + ix_{2a}$  the metric becomes

$$G = \begin{pmatrix} b_1 & 0 & c_{12} & d_{12} & c_{13} & d_{13} \\ 0 & b_1 & -d_{12} & c_{12} & -d_{13} & c_{13} \\ c_{12} & -d_{12} & b_2 & 0 & c_{23} & d_{23} \\ d_{12} & c_{12} & 0 & b_2 & -d_{23} & c_{23} \\ c_{13} & -d_{13} & c_{23} & -d_{23} & b_3 & 0 \\ d_{13} & c_{13} & d_{23} & c_{23} & 0 & b_3 \end{pmatrix}. \quad (\text{B.7})$$

The inner product of the  $A_2^3$  lattice vectors  $e_i$  using this metric reads

$$\langle e_m, e_n \rangle_G = \begin{pmatrix} b_1 & -\frac{b_1}{2} & c_{12} & -\frac{c_{12}-\sqrt{3}d_{12}}{2} & c_{13} & -\frac{c_{13}-\sqrt{3}d_{13}}{2} \\ -\frac{b_1}{2} & b_1 & -\frac{c_{12}+\sqrt{3}d_{12}}{2} & c_{12} & -\frac{c_{13}+\sqrt{3}d_{13}}{2} & c_{13} \\ c_{12} & -\frac{c_{12}+\sqrt{3}d_{12}}{2} & b_2 & -\frac{b_2}{2} & c_{23} & -\frac{c_{23}-\sqrt{3}d_{23}}{2} \\ -\frac{c_{12}-\sqrt{3}d_{12}}{2} & c_{12} & -\frac{b_2}{2} & b_2 & -\frac{c_{23}+\sqrt{3}d_{23}}{2} & c_{23} \\ c_{13} & -\frac{c_{13}+\sqrt{3}d_{13}}{2} & c_{23} & -\frac{c_{23}+\sqrt{3}d_{23}}{2} & b_3 & -\frac{b_3}{2} \\ -\frac{c_{13}-\sqrt{3}d_{13}}{2} & c_{13} & -\frac{c_{23}-\sqrt{3}d_{23}}{2} & c_{23} & -\frac{b_3}{2} & b_3 \end{pmatrix}. \quad (\text{B.8})$$



We obtain the standard  $A_2^3$  metric  $\cdot$  is of course obtained for  $b_i = 1$ ,  $c_{ij} = d_{ij} = 0$ .

The free discrete  $\mathbb{Z}_3$  action  $\alpha_a$  (given in (3.27)) acts on the torus coordinates as

$$u_b \mapsto u_b + \frac{\zeta - 1}{3} \delta_{ab} . \quad (\text{B.9})$$

Therefore, modding out such free actions, lead to a refinement of the  $A_2^3$  lattice: This lattice gets replaced by a lattice spanned by the  $A_2^3$  basis vectors  $e_1, \dots, e_6$  and the corresponding combinations of the vectors

$$\hat{\alpha}_1 = \frac{1}{3}(e_2 - e_1) , \quad \hat{\alpha}_2 = \frac{1}{3}(e_4 - e_3) , \quad \hat{\alpha}_3 = \frac{1}{3}(e_6 - e_5) , \quad (\text{B.10})$$

corresponding to  $\alpha_1, \alpha_2, \alpha_3$ , respectively. Using this technique we will construct each of the non-factorized  $\mathbb{Z}_3$  lattices below and compute the standard inner products of all its basis vectors and thereby simply read off the metric  $G$  using (B.8).

### The $F_4 \times A_2$ Lattice

When the discrete action (B.9) acts in two of the three tori (e.g. the first and the second), this results in a new non-factorized lattice with basis vectors

$$\hat{e}_1 := -\frac{e_2}{\sqrt{2}} , \quad \hat{e}_2 := \frac{1}{3} \left( \frac{e_2 - e_1}{\sqrt{2}} + e_4 - e_3 \right) , \quad \hat{e}_3 := -e_4 , \quad \hat{e}_4 := e_3 + e_4 , \quad (\text{B.11})$$

and  $\hat{e}_5 = e_5$ ,  $\hat{e}_6 = e_6$ . In order to match the resulting lattice to a Lie lattice, we have changed to normalization of the basis vectors in the first two-tori, to obtain the Lie lattice of  $F_4 \times A_2$ .

Next we demonstrate that it is possible to factorize this non-factorized  $F_4 \times A_2$  lattice into factorized  $A_2^3$  lattice. To do so, we have to find a basis of  $F_4 \times A_2$  lattices such that the  $\mathbb{Z}_3$  action looks like (B.2). Taking the vectors (B.11) such a basis is given by

$$\tilde{e}_1 := \sqrt{2} \hat{e}_2 , \quad \tilde{e}_2 := \sqrt{2}(\hat{e}_1 + \hat{e}_2 + \hat{e}_3) , \quad \tilde{e}_3 := \hat{e}_3 + \hat{e}_4 , \quad \tilde{e}_4 := -\hat{e}_3 . \quad (\text{B.12})$$

In this case we find the product matrix

$$\tilde{e}_i \cdot \tilde{e}_j = \begin{pmatrix} 1 & -\frac{1}{2} & -\frac{1}{\sqrt{2}} & \frac{1}{\sqrt{2}} & 0 & 0 \\ -\frac{1}{2} & 1 & 0 & -\frac{1}{\sqrt{2}} & 0 & 0 \\ -\frac{1}{\sqrt{2}} & 0 & 1 & -\frac{1}{2} & 0 & 0 \\ \frac{1}{\sqrt{2}} & -\frac{1}{\sqrt{2}} & -\frac{1}{2} & 1 & 0 & 0 \\ 0 & 0 & 0 & 0 & 1 & -\frac{1}{2} \\ 0 & 0 & 0 & 0 & -\frac{1}{2} & 1 \end{pmatrix} . \quad (\text{B.13})$$

This we can obtain from (B.8) by setting  $b_i = 1$ ,  $c_{12} = -1/\sqrt{2}$ ,  $d_{12} = 1/\sqrt{6}$ , and the rest to zero. Thus, we obtain the  $F_4 \times A_2$  lattice from the  $A_2^3$  lattice upon switching on some of the off-diagonal Kähler moduli.

## The $E_6$ Lattice

When the discrete action (B.9) acts in all three tori simultaneously, we obtain a new lattice with basis vectors

$$\begin{aligned}\hat{e}_1 &:= e_3 + e_4, & \hat{e}_2 &:= -e_4, & \hat{e}_3 &:= \frac{1}{3}(-e_1 + e_2 - e_3 + e_4 - e_5 + e_6), \\ \hat{e}_4 &:= -e_6, & \hat{e}_5 &:= e_5 + e_6, & \hat{e}_6 &:= -e_2,\end{aligned}\tag{B.14}$$

we find their metric to be (one half times) the Cartan matrix of  $E_6$ .

Here we demonstrate that it is possible to factorize the  $E_6$  lattice into  $A_2^3$ . To do so, we have to find a basis of the  $E_6$  lattice such that the  $\mathbb{Z}_3$  action looks like (B.2). Taking the vectors (B.14) such a basis is given by

$$\begin{aligned}\tilde{e}_1 &:= \hat{e}_1 + \hat{e}_2, & \tilde{e}_2 &:= -\hat{e}_2, & \tilde{e}_3 &:= \hat{e}_3, \\ \tilde{e}_4 &:= \hat{e}_3 + \hat{e}_2 + \hat{e}_4 + \hat{e}_6, & \tilde{e}_5 &:= \hat{e}_4 + \hat{e}_5, & \tilde{e}_6 &:= -\hat{e}_4.\end{aligned}\tag{B.15}$$

In this case we find the product matrix

$$\tilde{e}_i \cdot \tilde{e}_j = \begin{pmatrix} 1 & -\frac{1}{2} & -\frac{1}{2} & 0 & 0 & 0 \\ -\frac{1}{2} & 1 & \frac{1}{2} & -\frac{1}{2} & 0 & 0 \\ -\frac{1}{2} & \frac{1}{2} & 1 & -\frac{1}{2} & -\frac{1}{2} & \frac{1}{2} \\ 0 & -\frac{1}{2} & -\frac{1}{2} & 1 & 0 & -\frac{1}{2} \\ 0 & 0 & -\frac{1}{2} & 0 & 1 & -\frac{1}{2} \\ 0 & 0 & \frac{1}{2} & -\frac{1}{2} & -\frac{1}{2} & 1 \end{pmatrix}.\tag{B.16}$$

This we can obtain from (B.8) by setting  $b_i = 1$ ,  $c_{12} = c_{23} = -1/2$ ,  $d_{12} = -d_{23} = -1/(2\sqrt{3})$ , and the rest to zero. Thus, we obtain the  $E_6$  lattice from the  $A_2^3$  lattice upon switching on some of the off-diagonal Kähler moduli.

## A non-Lie Lattice

It is also possible we have two discrete actions (B.9). The first one mixes first and second two-torus and the second one mixes the second and third two-torus. Each action by itself is similar the  $F_4$  case, but they get “intermingled” in such a way that this lattice does not correspond to any Lie algebra lattice.

From the two free discrete actions we obtain two new lattice vectors

$$\hat{e}_1 := \frac{1}{3}\left(\frac{e_2 - e_1}{\sqrt{2}} + e_4 - e_3\right), \quad \hat{e}_2 := \frac{e_2}{\sqrt{2}}, \quad \hat{e}_4 := e_4,\tag{B.17}$$

$$\hat{e}_3 := \frac{1}{3}\left(\frac{e_6 - e_5}{\sqrt{2}} + e_4 - e_3\right), \quad \hat{e}_5 := \frac{e_5}{\sqrt{2}}, \quad \hat{e}_6 := \frac{e_6}{\sqrt{2}}.\tag{B.18}$$

As in the  $F_4$  case, we have scaled the first and the third torus via  $(e_1, e_2, e_5, e_6) \mapsto 1/\sqrt{2}(e_1, e_2, e_5, e_6)$ .

Here we demonstrate that it is possible to factorize the non-Lie lattice into  $SU(3)^3$ . To do so, we have to find a basis of the non-Lie lattice such that the  $\mathbb{Z}_3$  action looks like (B.2). Taking the vectors (B.18) such a basis is given by

$$\begin{aligned} \tilde{e}_1 &:= \hat{e}_1, & \tilde{e}_2 &:= \hat{e}_1 - \hat{e}_2 - \hat{e}_4, & \tilde{e}_3 &:= \hat{e}_3, \\ \tilde{e}_4 &:= \hat{e}_3 - \hat{e}_4 - \hat{e}_6, & \tilde{e}_5 &:= \hat{e}_5, & \tilde{e}_6 &:= \hat{e}_6. \end{aligned} \quad (\text{B.19})$$

In this case we find the product matrix

$$\tilde{e}_i \cdot \tilde{e}_j = \begin{pmatrix} 1 & -\frac{1}{2} & \frac{2}{3} & -\frac{1}{3} & 0 & 0 \\ -\frac{1}{2} & 1 & -\frac{1}{3} & \frac{2}{3} & 0 & 0 \\ \frac{2}{3} & -\frac{1}{3} & 1 & -\frac{1}{2} & -\frac{1}{2} & \frac{1}{2} \\ -\frac{1}{3} & \frac{2}{3} & -\frac{1}{2} & 1 & 0 & -\frac{1}{2} \\ 0 & 0 & -\frac{1}{2} & 0 & 1 & -\frac{1}{2} \\ 0 & 0 & \frac{1}{2} & -\frac{1}{2} & -\frac{1}{2} & 1 \end{pmatrix}. \quad (\text{B.20})$$

This we obtain from (B.8) by setting  $b_i = 1$ ,  $c_{12} = 2/3$ ,  $c_{23} = -1/2$ ,  $d_{23} = 1/(2\sqrt{3})$ , and the rest to zero. Thus, we obtain the non-Lie lattice from the  $A_2^3$  lattice upon switching on some of the off-diagonal Kähler moduli.

## Non-factorizable Lattices for the $T^6/\mathbb{Z}_4$ Orbifold

In this appendix we describe the non-factorizable lattices we find for  $\mathbb{Z}_4$  orbifolds in section 3.3.3. We start with the factorizable lattice  $D_2^2 \times A_1^2$ . The torus  $T^2(\mathbb{Z}_4) \times T^2(\mathbb{Z}_4) \times T^2 I(\mathbb{Z}_2)$  obtained from it is mapped to the elliptic curves as described in Appendix A. When we add exceptional coordinates and  $U(1)$  gaugings, we induce discrete actions on this torus which we can identify on the torus as we did for the  $\mathbb{Z}_3$  orbifold. Let us describe the factorizable lattice by the lattice vectors  $e_i$ ,  $i = 1, \dots, 6$ . The inner product of this basis is<sup>1</sup>

$$G = \begin{pmatrix} b_1 & 0 & c_{12} & d_{12} & 0 & 0 \\ 0 & b_1 & -d_{12} & c_{12} & 0 & 0 \\ c_{12} & -d_{12} & b_2 & 0 & 0 & 0 \\ d_{12} & c_{12} & 0 & b_2 & 0 & 0 \\ 0 & 0 & 0 & 0 & b_3 & 0 \\ 0 & 0 & 0 & 0 & 0 & b_3 \end{pmatrix}. \quad (\text{B.21})$$

The  $\mathbb{Z}_4$  acts as

$$\begin{aligned} e_1 &\mapsto e_2, & e_2 &\mapsto -e_1, & e_3 &\mapsto e_4, \\ e_4 &\mapsto -e_3, & e_5 &\mapsto -e_5, & e_6 &\mapsto -e_6. \end{aligned} \quad (\text{B.22})$$

---

<sup>1</sup>We neglect possible complex structure deformations in the third torus since they are not relevant here.

### The $A_3 \times D_2 \times A_1$ Lattice

In the first truly non-factorizable model we find the discrete action

$$\tilde{\theta}_1 : (z_{21}, z_{22}, z_{31}, z_{32}) \mapsto (iz_{21}, -iz_{22}, -z_{31}, -z_{32}). \quad (\text{B.23})$$

Via the Weierstrass map to the torus it translates into a shift by  $\frac{e_3+e_4+e_5}{2}$ , i.e. a shift in two two-tori simultaneously. For the non-factorizable torus obtained in this way we choose a basis

$$\hat{e}_1 := \frac{e_3 + e_4 + e_5}{2}, \quad \hat{e}_2 := \frac{-e_3 + e_4 - e_5}{2}, \quad \hat{e}_3 := \frac{-e_3 - e_4 + e_5}{2}, \quad (\text{B.24a})$$

$$\hat{e}_4 := e_1, \quad \hat{e}_5 := e_2, \quad \hat{e}_6 := e_6. \quad (\text{B.24b})$$

On the first three basis vectors their inner product reads

$$\hat{e}_i \cdot \hat{e}_j = \begin{pmatrix} b_2/2 + b_3/4 & -b_3/4 & -b_2/2 + b_3/4 \\ -b_3/4 & b_2/2 + b_3/4 & -b_3/4 \\ -b_2/2 + b_3/4 & -b_3/4 & b_2/2 + b_3/4 \end{pmatrix}. \quad (\text{B.25})$$

This product cannot be given a factorized structure. Choosing  $b_3 = 4$  and  $b_2 = 2$  it becomes the Cartan matrix for the Lie algebra  $A_3$ . The  $\mathbb{Z}_4$  acts as

$$\hat{e}_1 \mapsto \hat{e}_2, \quad \hat{e}_2 \mapsto \hat{e}_3, \quad \hat{e}_3 \mapsto -\hat{e}_1 - \hat{e}_2 - \hat{e}_3, \quad (\text{B.26})$$

i.e. as a rotation of the extended Dynkin diagram.

### The $A_3 \times A_3$ Lattice

Analogously to the case above, we find here in addition the discrete action

$$\tilde{\theta}_2 : (z_{11}, z_{12}, z_{31}, z_{33}) \mapsto (iz_{11}, -iz_{12}, -z_{31}, -z_{33}). \quad (\text{B.27})$$

which translates into a shift by  $\frac{e_1+e_2+e_6}{2}$ . Now the basis consists of  $\hat{e}_i$ ,  $i = 1, 2, 3$  as defined in (B.24a) but we replace (B.24b) by

$$\hat{e}_4 := \frac{e_1 + e_2 + e_6}{2}, \quad \hat{e}_5 := \frac{-e_1 + e_2 - e_6}{2}, \quad \hat{e}_6 := \frac{-e_1 - e_2 + e_6}{2}. \quad (\text{B.28})$$

Altogether this gives the inner product,

$$\hat{e}_i \cdot \hat{e}_j = \frac{1}{2} \begin{pmatrix} b_2 + b_3/2 & -b_3/2 & -b_2 + b_3/2 & c & d & -c \\ -b_3/2 & b_2 + b_3/2 & -b_3/2 & -d & c & d \\ -b_2 + b_3/2 & -b_3/2 & b_2 + b_3/2 & -c & -d & c \\ c & -d & -c & b_1 + b_3/2 & -b_3/2 & -b_1 + b_3/2 \\ d & c & -d & -b_3/2 & b_1 + b_3/2 & -b_3/2 \\ -c & d & c & -b_1 + b_3/2 & -b_3/2 & b_1 + b_3/2 \end{pmatrix}, \quad (\text{B.29})$$

which for  $b_3 = 4$ ,  $b_1 = b_2 = 2$  and  $c = d = 0$  becomes the Cartan matrix of  $A_3 \times A_3$ .

## C Flux Quantization

We show that on the factorizable  $\mathbb{Z}_2 \times \mathbb{Z}_2$  orbifold resolution the identification of the bundle vectors with the local orbifold shifts is equivalent to the resolution flux quantization conditions for all triangulations, which in turn is equivalent to the GLSM condition by the identifications  $2V_r = Q_r$ .

The orbifold identifications read,

$$V_{1,\beta\gamma} \cong V_1 + n_{3,\beta}W_3 + n_{4,\beta}W_4 + n_{5,\gamma}W_5 + n_{6,\gamma}W_6, \quad (\text{C.1a})$$

$$V_{2,\alpha\gamma} \cong V_2 + n_{1,\alpha}W_1 + n_{2,\alpha}W_2 + n_{5,\gamma}W_5 + n_{6,\gamma}W_6, \quad (\text{C.1b})$$

$$V_{3,\alpha\beta} \cong V_3 + n_{1,\alpha}W_1 + n_{2,\alpha}W_2 + n_{3,\beta}W_3 + n_{4,\beta}W_4, \quad (\text{C.1c})$$

using

$$n_{1,\alpha} = (0, 0, 1, 1), \quad n_{2,\alpha} = (0, 1, 0, 1), \quad (\text{C.2a})$$

$$n_{3,\beta} = (0, 0, 1, 1), \quad n_{4,\beta} = (0, 1, 0, 1), \quad (\text{C.2b})$$

$$n_{5,\gamma} = (0, 0, 1, 1), \quad n_{6,\gamma} = (0, 1, 0, 1), \quad (\text{C.2c})$$

We also give the flux quantization conditions for the triangulations “ $S$ ” and “ $E_1$ ”, see tables 6. and 7. in our paper. These conditions are summarized to three types of conditions. The first one,

$$2V_{k,\rho\sigma} \cong 0, \quad k = 1, 2, 3, \quad \rho, \sigma = 1, \dots, 4, \quad (\text{C.3})$$

just states that all flux vectors are of order two. These conditions are always found on the curves  $R_k E_{k,\rho\sigma}$ . The second conditions read

$$(*, \alpha, \beta, \gamma) : \quad V_{1,\beta\gamma} + V_{2,\alpha\gamma} + V_{3,\alpha\beta} \cong 0, \quad \alpha, \beta, \gamma = 1, \dots, 4. \quad (\text{C.4})$$

We will refer to them as  $(*, \alpha, \beta, \gamma)$ . In the symmetric triangulation these conditions are found on any of the compact curves  $E_i E_j$ . Now if the fixed point  $(\alpha, \beta, \gamma)$  has another triangulation, say “ $E_1$ ”, then this condition is found of the curve  $D_{1,\alpha} E_{1,\beta\gamma}$ . The third conditions are of the form

$$(**, k, \sigma) : \quad \sum_{\rho} V_{k,\rho\sigma} \cong \sum_{\rho} V_{k,\sigma\rho} \cong 0, \quad k = 1, 2, 3, \sigma = 1, \dots, 4. \quad (\text{C.5})$$

These conditions live e.g. on the triangulation independent curves  $R_k D_{j,\sigma}$  are will be referred to as  $(**, k, \sigma)$ .

## Constructive Proof

First of all we define the orbifold data, i.e. the shift vectors and Wilson lines, in terms of the flux vectors.

$$V_1 := V_{1,11}, \quad V_2 := V_{2,11}, \quad V_3 := V_{3,11}, \quad (\text{C.6})$$

$$W_1 := V_{2,31} - V_{2,11}, \quad W_2 := V_{2,21} - V_{2,11}, \quad (\text{C.7a})$$

$$W_3 := V_{3,13} - V_{3,11}, \quad W_4 := V_{3,12} - V_{3,11}, \quad (\text{C.7b})$$

$$W_5 := V_{1,13} - V_{1,11}, \quad W_6 := V_{1,12} - V_{1,11}. \quad (\text{C.7c})$$

This way the  $V_k$  and  $W_i$  are automatically order two.  $(*, 1, 1, 1)$  then immediately implies that  $V_3 \cong V_1 + V_2$ . In the following we show that with these definitions we can express all flux vectors like (C.1c).

We start with the conditions  $(**, k, 1)$ . For e.g.  $k = 1$  we find

$$\begin{aligned} & V_{1,11} + V_{1,12} + V_{1,13} + V_{1,14} \cong 0 \\ \Rightarrow & V_1 + (V_1 + W_6) + (V_1 + W_5) + V_{1,14} \cong 0 \\ \Rightarrow & V_{1,14} \cong V_1 + W_5 + W_6, \end{aligned} \quad (\text{C.8})$$

and analogous expressions for  $V_{2,41}$  and  $V_{3,14}$ .

Up to now the Wilson lines are just related to just one twisted sector. So we use the conditions  $(*, \underline{\rho}, 1, 1)$ ,  $\rho = 2, 3, 4$ , underline denotes permutations, to relate them to the others. As an example we take  $(*, 1, 2, 1)$  and find,

$$\begin{aligned} & V_{1,21} + V_{2,11} + V_{3,12} \cong 0 \\ \Rightarrow & V_{1,21} + V_2 + V_3 + W_4 \cong 0 \\ \Rightarrow & V_{1,21} \cong V_1 + W_4. \end{aligned} \quad (\text{C.9})$$

So with these relations we are able to express all  $V_{k,\rho\sigma}$  as (C.1c) if  $\rho = 1$  or  $\sigma = 1$ .

In the last step we show the general case. For this we take the conditions  $(*, \underline{\rho}, \underline{\sigma}, 1)$  for  $\rho, \sigma = 2, 3, 4$ . Again we demonstrate this with an example, say  $(*, 1, 3, 4)$ ,

$$\begin{aligned} & V_{1,34} + V_{2,14} + V_{3,13} \cong 0 \\ \Rightarrow & V_{1,34} + (V_2 + W_5 + W_6) + (V_3 + W_3) \cong 0 \\ \Rightarrow & V_{1,34} \cong V_1 + W_3 + W_5 + W_6. \end{aligned} \quad (\text{C.10})$$

This way we have shown that all bundle vectors  $V_{k,\rho\sigma}$  are expressible in terms of the orbifold data  $V_1, V_2$  and  $W_i$ ,  $i = 1, \dots, 6$ .

# Bibliography

- [1] G. Aad *et al.* [ATLAS Collaboration], “Observation of a new particle in the search for the Standard Model Higgs boson with the ATLAS detector at the LHC,” arXiv:1207.7214 [hep-ex].
- [2] H. P. Nilles, “Supersymmetry, Supergravity and Particle Physics,” Phys. Rept. **110** (1984) 1.
- [3] H. Georgi and S. L. Glashow, “Unity of All Elementary Particle Forces,” Phys. Rev. Lett. **32** (1974) 438.
- [4] K. Becker, M. Becker and J. H. Schwarz, “String theory and M-theory: A modern introduction,” Cambridge, UK: Cambridge Univ. Pr. (2007) 739 p
- [5] M. B. Green, J. H. Schwarz and E. Witten, “Superstring Theory. Vol. 1: Introduction,” Cambridge, Uk: Univ. Pr. ( 1987) 469 P. ( Cambridge Monographs On Mathematical Physics)
- [6] M. B. Green, J. H. Schwarz and E. Witten, “Superstring Theory. Vol. 2: Loop Amplitudes, Anomalies And Phenomenology,” Cambridge, Uk: Univ. Pr. ( 1987) 596 P. ( Cambridge Monographs On Mathematical Physics)
- [7] J. Polchinski, “Superstring Theory,” Annals N. Y. Acad. Sci. **571** (1989) 9.
- [8] J. Polchinski, “String theory. Vol. 2: Superstring theory and beyond,” Cambridge, UK: Univ. Pr. (1998) 531 p
- [9] B. R. Greene, “String theory on Calabi-Yau manifolds,” hep-th/9702155.
- [10] E. Witten, “String theory dynamics in various dimensions,” Nucl. Phys. B **443** (1995) 85 [hep-th/9503124].
- [11] C. Vafa, “Evidence for F theory,” Nucl. Phys. B **469** (1996) 403 [hep-th/9602022].
- [12] D. J. Gross, J. A. Harvey, E. J. Martinec and R. Rohm, “The Heterotic String,” Phys. Rev. Lett. **54** (1985) 502.
- [13] D. J. Gross, J. A. Harvey, E. J. Martinec and R. Rohm, “Heterotic String Theory. 1. The Free Heterotic String,” Nucl. Phys. B **256** (1985) 253.

## Bibliography

- [14] L. J. Dixon, J. A. Harvey, C. Vafa and E. Witten, “Strings on Orbifolds,” Nucl. Phys. B **261** (1985) 678.
- [15] L. J. Dixon, J. A. Harvey, C. Vafa and E. Witten, “Strings on Orbifolds. 2.,” Nucl. Phys. B **274** (1986) 285.
- [16] L. E. Ibanez, H. P. Nilles and F. Quevedo, “Orbifolds and Wilson Lines,” Phys. Lett. B **187** (1987) 25.
- [17] W. Fulton, *Introduction to Toric Varieties*, Princeton University Press, 1993.
- [18] K. Hori, S. Katz, A. Klemm, R. Pandharipande, R. Thomas, C. Vafa, R. Vakil and E. Zaslow, “Mirror symmetry,” (Clay mathematics monographs. 1)
- [19] E. Witten, “Phases of N=2 theories in two-dimensions,” Nucl. Phys. B **403** (1993) 159 [hep-th/9301042].
- [20] D. R. Morrison and M. R. Plesser, “Summing the instantons: Quantum cohomology and mirror symmetry in toric varieties,” Nucl. Phys. B **440** (1995) 279 [hep-th/9412236].
- [21] J. Erler and A. Klemm, “Comment on the generation number in orbifold compactifications,” Commun. Math. Phys. **153** (1993) 579 [hep-th/9207111].
- [22] M. B. Green and J. H. Schwarz, “Anomaly Cancellation in Supersymmetric D=10 Gauge Theory and Superstring Theory,” Phys. Lett. B **149** (1984) 117.
- [23] A. Font, L. E. Ibanez, H. P. Nilles and F. Quevedo, “Degenerate Orbifolds,” Nucl. Phys. B **307** (1988) 109 [Erratum-ibid. B **310** (1988) 764].
- [24] F. Ploger, S. Ramos-Sanchez, M. Ratz and P. K. S. Vaudrevange, “Mirage Torsion,” JHEP **0704** (2007) 063 [hep-th/0702176].
- [25] L. E. Ibanez, J. E. Kim, H. P. Nilles and F. Quevedo, “Orbifold Compactifications with Three Families of SU(3) x SU(2) x U(1)\*\*n,” Phys. Lett. B **191** (1987) 282.
- [26] J. A. Casas and C. Munoz, “Three Generation SU(3) x SU(2) x U(1)-Y Models from Orbifolds,” Phys. Lett. B **214** (1988) 63.
- [27] J. A. Casas, A. de la Macorra, M. Mondragon and C. Munoz, “Z(7) phenomenology,” Phys. Lett. B **247** (1990) 50.



- [28] J. E. Kim, J. -H. Kim and B. Kyae, “Superstring standard model from  $Z(12-I)$  orbifold compactification with and without exotics, and effective R-parity,” *JHEP* **0706** (2007) 034 [hep-ph/0702278 [HEP-PH]].
- [29] W. Buchmuller, K. Hamaguchi, O. Lebedev and M. Ratz, “Supersymmetric standard model from the heterotic string,” *Phys. Rev. Lett.* **96** (2006) 121602 [hep-ph/0511035].
- [30] W. Buchmuller, K. Hamaguchi, O. Lebedev and M. Ratz, “Supersymmetric Standard Model from the Heterotic String (II),” *Nucl. Phys. B* **785** (2007) 149 [hep-th/0606187].
- [31] O. Lebedev, H. P. Nilles, S. Raby, S. Ramos-Sanchez, M. Ratz, P. K. S. Vaudrevange and A. Wingerter, “A Mini-landscape of exact MSSM spectra in heterotic orbifolds,” *Phys. Lett. B* **645** (2007) 88 [hep-th/0611095].
- [32] O. Lebedev, H. P. Nilles, S. Ramos-Sanchez, M. Ratz and P. K. S. Vaudrevange, “Heterotic mini-landscape. (II). Completing the search for MSSM vacua in a  $Z(6)$  orbifold,” *Phys. Lett. B* **668** (2008) 331 [arXiv:0807.4384 [hep-th]].
- [33] M. Ratz, “Notes on Local Grand Unification,” arXiv:0711.1582 [hep-ph].
- [34] H. P. Nilles, S. Ramos-Sanchez, P. K. S. Vaudrevange and A. Wingerter, “The Orbifolder: A Tool to study the Low Energy Effective Theory of Heterotic Orbifolds,” *Comput. Phys. Commun.* **183** (2012) 1363 [arXiv:1110.5229 [hep-th]].
- [35] S. Groot Nibbelink, M. Trapletti and M. Walter, “Resolutions of  $C^{**n}/Z(n)$  Orbifolds, their  $U(1)$  Bundles, and Applications to String Model Building,” *JHEP* **0703** (2007) 035 [hep-th/0701227].
- [36] S. Groot Nibbelink, H. P. Nilles and M. Trapletti, “Multiple anomalous  $U(1)$ s in heterotic blow-ups,” *Phys. Lett. B* **652** (2007) 124 [hep-th/0703211 [HEP-TH]].
- [37] S. Nibbelink Groot, T. -W. Ha and M. Trapletti, “Toric Resolutions of Heterotic Orbifolds,” *Phys. Rev. D* **77** (2008) 026002 [arXiv:0707.1597 [hep-th]].
- [38] S. Nibbelink Groot, D. Klevers, F. Ploger, M. Trapletti and P. K. S. Vaudrevange, “Compact heterotic orbifolds in blow-up,” *JHEP* **0804** (2008) 060 [arXiv:0802.2809 [hep-th]].
- [39] S. Nibbelink Groot, J. Held, F. Ruehle, M. Trapletti and P. K. S. Vaudrevange, “Heterotic  $Z(6-II)$  MSSM Orbifolds in Blowup,” *JHEP* **0903** (2009) 005 [arXiv:0901.3059 [hep-th]].

## Bibliography

- [40] M. Blaszczyk, S. Nibbelink Groot, M. Ratz, F. Ruehle, M. Trapletti and P. K. S. Vaudrevange, “A  $Z_2 \times Z_2$  standard model,” *Phys. Lett. B* **683** (2010) 340 [arXiv:0911.4905 [hep-th]].
- [41] M. Blaszczyk, S. Nibbelink Groot, F. Ruehle, M. Trapletti and P. K. S. Vaudrevange, “Heterotic MSSM on a Resolved Orbifold,” *JHEP* **1009** (2010) 065 [arXiv:1007.0203 [hep-th]].
- [42] M. Blaszczyk, S. Nibbelink Groot and F. Ruehle, “Green-Schwarz Mechanism in Heterotic (2,0) Gauged Linear Sigma Models: Torsion and NS5 Branes,” *JHEP* **1108** (2011) 083 [arXiv:1107.0320 [hep-th]].
- [43] C. Quigley and S. Sethi, “Linear Sigma Models with Torsion,” *JHEP* **1111** (2011) 034 [arXiv:1107.0714 [hep-th]].
- [44] S. Nibbelink Groot, “Heterotic orbifold resolutions as (2,0) gauged linear sigma models,” *Fortsch. Phys.* **59** (2011) 454 [arXiv:1012.3350 [hep-th]].
- [45] M. Blaszczyk, N. G. Cabo Bizet, H. P. Nilles and F. Ruehle, “A perfect match of MSSM-like orbifold and resolution models via anomalies,” *JHEP* **1110** (2011) 117 [arXiv:1108.0667 [hep-th]].
- [46] M. Blaszczyk, S. Groot Nibbelink and F. Ruehle, “Gauged Linear Sigma Models for toroidal orbifold resolutions,” *JHEP* **1205** (2012) 053 [arXiv:1111.5852 [hep-th]].
- [47] D. Lust, S. Reffert, E. Scheidegger and S. Stieberger, “Resolved Toroidal Orbifolds and their Orientifolds,” *Adv. Theor. Math. Phys.* **12** (2008) 67 [hep-th/0609014].
- [48] A. Adams, M. Ernebjerg and J. M. Lapan, “Linear models for flux vacua,” *Adv. Theor. Math. Phys.* **12** (2008) 817 [hep-th/0611084].
- [49] S. Hamidi and C. Vafa, “Interactions on Orbifolds,” *Nucl. Phys. B* **279** (1987) 465.
- [50] E. J. Chun, J. Mas, J. Lauer and H. P. Nilles, “Duality And Landau-ginzburg Models,” *Phys. Lett. B* **233** (1989) 141.
- [51] P. S. Aspinwall and M. R. Plesser, “Elusive Worldsheet Instantons in Heterotic String Compactifications,” arXiv:1106.2998 [hep-th].
- [52] V. Bouchard and R. Donagi, “An  $SU(5)$  heterotic standard model,” *Phys. Lett. B* **633** (2006) 783 [hep-th/0512149].
- [53] J. J. Atick, L. J. Dixon and A. Sen, “String Calculation of Fayet-Iliopoulos Terms in Arbitrary Supersymmetric Compactifications,” *Nucl. Phys. B* **292** (1987) 10

- [54] R. Blumenhagen, B. Jurke, T. Rahn and H. Roschy, “Cohomology of Line Bundles: A Computational Algorithm,” *J. Math. Phys.* **51** (2010) 103525 [arXiv:1003.5217 [hep-th]].
- [55] E. Zaslow, “Topological orbifold models and quantum cohomology rings,” *Commun. Math. Phys.* **156** (1993) 301 [hep-th/9211119].